# VORTEX ENERGY DISSIPATOR FOR SAN DIEGO OCEAN OUTFALL - LABORATORY INVESTIGATIONS

Norman H. Brooks
and
William H. Blackmer

W. M. Keck Laboratory of Hydraulics and Water Resources
Division of Engineering
CALIFORNIA INSTITUTE OF TECHNOLOGY
Pasadena, California

Report No. KH-R-5 December 1962

# VORTEX ENERGY DISSIPATOR FOR SAN DIEGO OCEAN OUTFALL - LABORATORY INVESTIGATIONS

by
Norman H. Brooks
Professor of Civil Engineering

and

William H. Blackmer
Civil Engineer
(James M. Montgomery, Consulting Engineers, Inc.)

Final Report to
Holmes and Narver-Montgomery
828 South Figueroa Street
Los Angeles, California

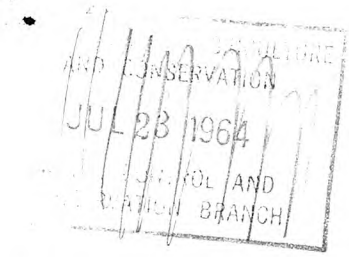


W. M. Keck Laboratory of Hydraulics and Water Resources
Division of Engineering
California Institute of Technology
Pasadena, California

Report No. KH-R-5 December 1962

# TABLE OF CONTENTS

# LIST OF FIGURES

# LIST OF TABLES

# SUMMARY AND RECOMMENDATIONS

## The Problem

The sewage effluent from the new sewage treatment plant for the City of San Diego, located on a bluff 95 feet above sea level on Point Loma, is discharged to the ocean through a long submarine outfall pipe. Under almost all conditions of flow, the hydraulic head at the treatment plant exceeds that required for flow through the outfall. Therefore, the excess energy must be dissipated in a special hydraulic drop structure located on the shoreline between the treatment plant and the ocean outfall.

The laboratory model investigation described herein basically sought to find a method for dissipating this excess energy safely without heavy entrainment of air into the flow in the ocean outfall. Such air entrainment could cause unsteady conditions of the pipe flow, and possibly bubbling at the point of discharge in the ocean, both of which must be avoided. The responsibility of this laboratory was to develop the hydraulic principles and a recommended hydraulic configuration which would provide assurance that the prototype to be designed by the sponsors (Holmes and Narver-Montgomery) would give satisfactory hydraulic performance.

## Investigations

From a study of the literature and engineering restrictions for the installation, it was concluded that the most satisfactory configuration would consist of basically a chute and stilling basin for the upper half of the drop, followed by a vortex tube structure with a tangential inlet for the lower half of the drop. First, five small scale models (28.5 : 1 prototype to model) were constructed and tested with various dimensions for the vortex tube and its inlet, and finally, one larger scale one (18 : 1) was built for testing the final recommended geometry (see Figs. 1 and 2). A simple pipe model (27 : 1) was also built for comparison. Models were operated in accordance with Froude's Law.

For the prototype the maximum allowable air entrainment rate in the outfall flow was estimated to be 1 per cent of the discharge (by volume at

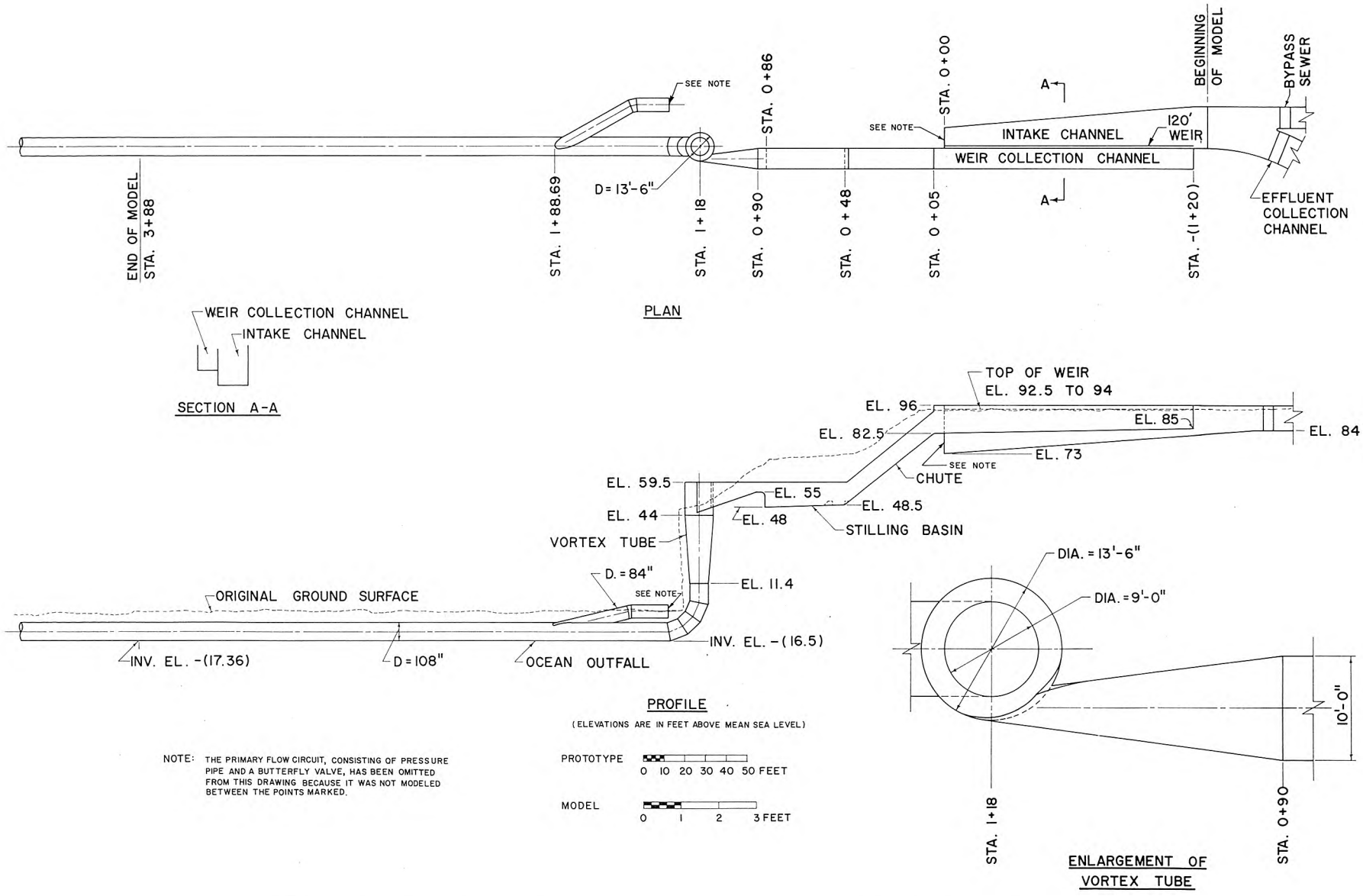


Fig. 1. Drawing of recommended design for vortex drop structure.

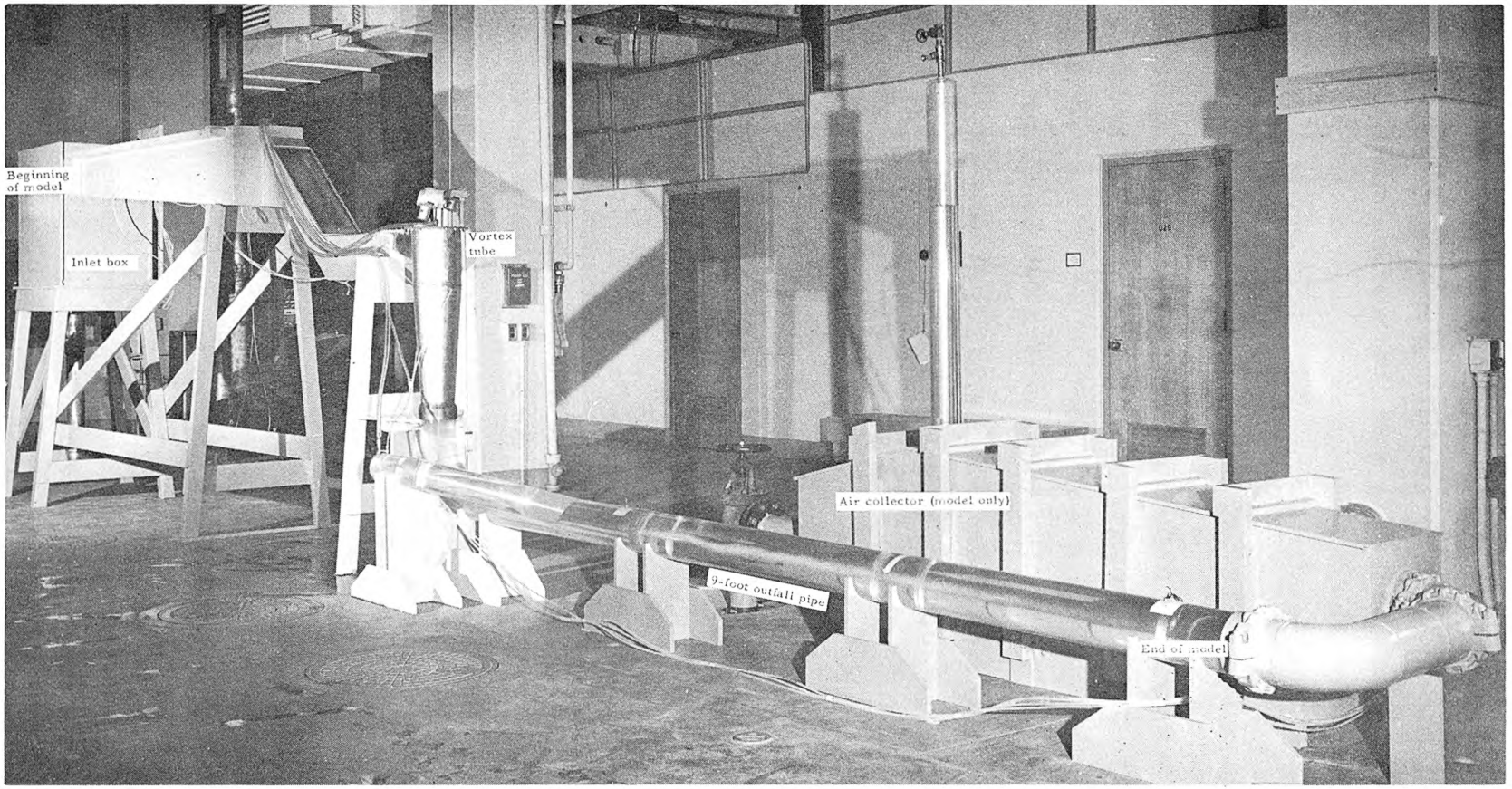


Fig. 2. Overall view of 18 : 1 scale hydraulic model of San Diego drop structure. (Upstream valve and venturi meter are hidden from view.)

atmospheric pressure). Since a scaling factor of 10 between model and prototype was judged reasonably safe, the maximum allowable air entrainment concentration in the model was set at only 0.1 per cent or 1000 ppm by volume.

Results

The performance of the final recommended hydraulic design (Fig. 1) was found to be satisfactory. The maximum air entrainment in the range of expected operations was only 0.02 per cent by volume in the model, well within the 0.1 per cent criterion. (For full results see Fig. 35.)

Visual observation and comparison of measured air entrainment rates in the various models demonstrated: (a) that the vortex is very effective in reducing air entrainment compared to a free fall because of the "air chimney" maintained in the eye of the vortex for release of air, and (b) that remarkable reductions in air entrainment were achieved by what appeared to be minor adjustments of the geometry of the vortex chamber and its inlet channel from the first model to the final one. These results could not have been obtained in any way other than by hydraulic model testing.

Measurements were also made to determine the approximate capacity required for the two pipe vents in the system: one at the top of the vortex structure, and the other in the 7-foot diameter branching pipe downstream of the butterfly valve (in the alternative flow circuit). Full results of model air flows from these points are given in Figs. 37 and 38. These vents must be open at all times.

One of the most interesting fluid flow phenomena observed was the reverse flow in the core of the swirling flow in the beginning of the outfall pipe downstream of the vortex tube. This reverse flow zone was important in driving air collected in the "eye" of the vortex back to the vortex tube for release to the atmosphere. (See Appendix A for velocity and pressure distribution measurements made as an adjunct to the model study.)

Chapter 6, "Summary of Results and Conclusions," gives a more detailed account of the results.

Recommendations

1. The drop structure should be built according to the hydraulic design shown in Fig. 1. (See also Fig. 12 for further geometric details of vortex tube and inlet.)

2. Air vent piping should be installed to discharge up to 100 cfs of air (at atmospheric pressure) from the top of the vortex chamber and from the 7-foot branch pipe. Since the large air flows are from either one or the other place, a common vent pipe is satisfactory. The rise in pressure in the drop structure necessary to drive the air through the vent system should not exceed 1 to 2 feet of water.

3. A suitable program of testing of the prototype operation should be undertaken at an appropriate time in order to ascertain how well the model predicts the prototype performance. Because of the scarcity of model-prototype comparisons for this type of structure, this information is not only of vital interest to the City of San Diego, but also to the hydraulic engineering profession. Results should be published in a technical paper.

# CHAPTER 1
# INTRODUCTION

## 1.01 Total Sewerage Project

The City of San Diego, California, and surrounding communities have experienced a rapid expansion in recent years which overtaxed the existing sewerage facilities — particularly the old sewage treatment plant located adjacent to San Diego Bay. In order to alleviate this situation, Holmes and Narver-Montgomery, a joint venture consisting of Holmes and Narver, Inc., Los Angeles, California, sponsor, and James M. Montgomery, Consulting Engineers, Inc., Pasadena, California, was retained by the City of San Diego to prepare a basic plan of sewage disposal for this metropolitan area (Holmes and Narver-Montgomery, 1958*). The joint venture was subsequently authorized to do the necessary design work to implement the plan recommended in the report. The new sewerage works, consisting of interceptors, force mains, pumping stations, sewage treatment plant, and outfall, will have a total construction cost of about $45,000,000. The major components, as finally designed, are shown in Fig. 3. It is anticipated that construction of these facilities will be completed by the summer of 1963.

## 1.02 Outfall

Unusual design problems were encountered with the outfall, which carries the effluent from the treatment plant approximately two miles out to sea for final discharge through a multiple-port diffuser. A large part of these design problems were associated with the land portion of this outfall, generally referred to as the land outfall. As can be seen in Fig. 1, the treatment plant is located on a bluff 95 feet above sea level. The land outfall must transport the plant effluent from this bluff to the ocean outfall located 12 feet below sea level, a total drop of over 100 feet, in a horizontal distance of 240 feet. To complicate matters further, the natural bluff line rises almost vertically from the ocean floor for a height of about 50 feet before sloping upward away from the ocean more gradually to the

---

* See list of references at end of report.

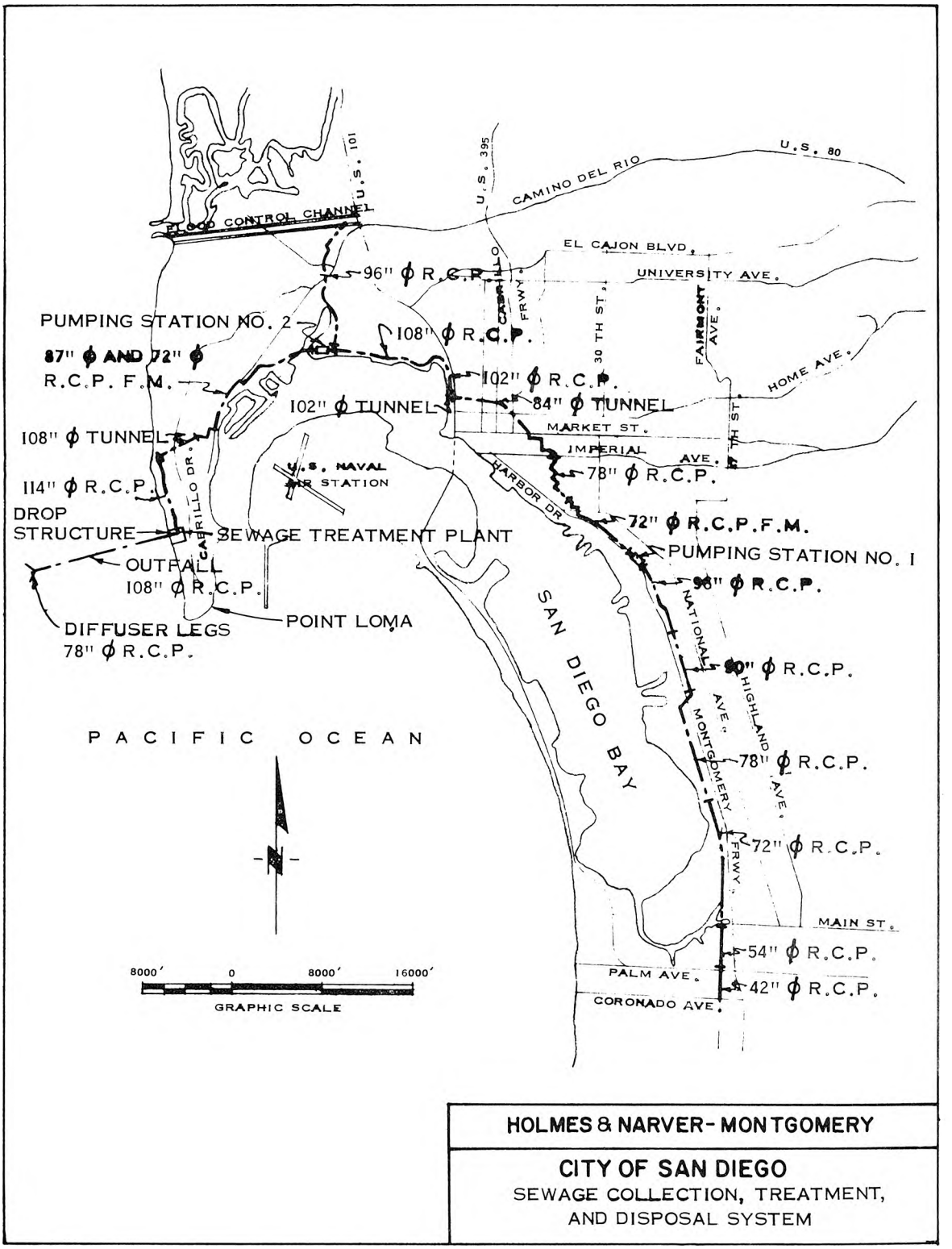


Fig. 3. City of San Diego sewage collection, treatment, and disposal system.

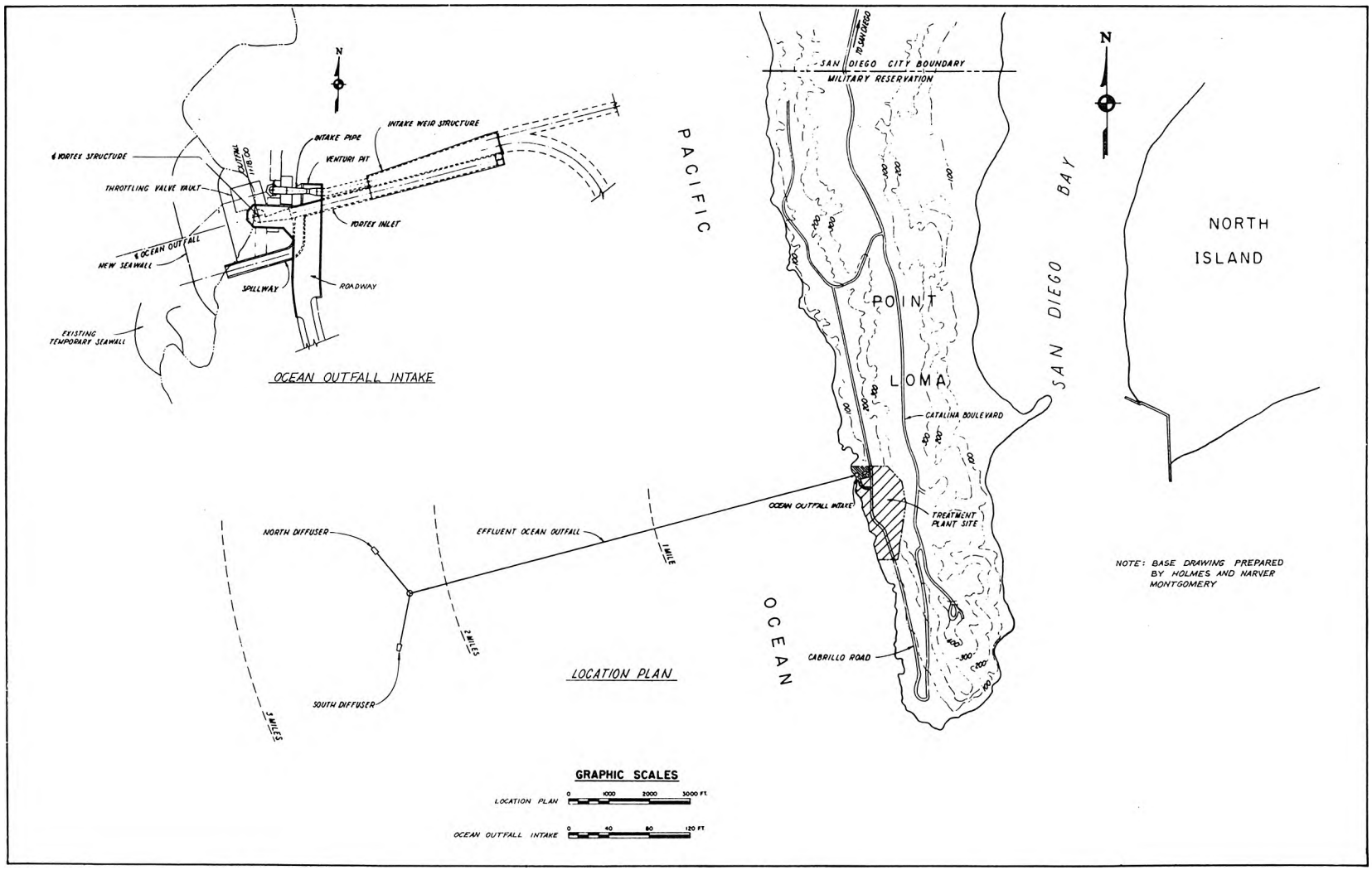


Fig. 4. Location plan for San Diego ocean outfall.

treatment plant site. A plan of the sewage treatment plant, ocean outfall intake, and outfall is shown in Fig. 4.

Only a small portion of the available head is needed during periods of low and moderate flows to overcome losses in the 108-inch ocean outfall and diffusers. In fact, the total available head is needed only when the maximum design flow is being carried and the losses are at their maximum possible.

The design of the land outfall has to provide economical means for:

1. Safe dissipation of the excess energy.
2. Upstream water surface control in the sewage treatment plant.
3. Restriction or elimination of air entrainment.
4. Odor control.
5. Control of foam from alkyl benzene sulfonate (ABS).
6. Ingress for an outfall cleaning device.

Furthermore, two independent systems have to be provided to insure continuous service.

## 1.03 Designs Selected for the Land Outfall

After considering the various possibilities, the design engineers elected to use an 84-inch pipeline with a submerged butterfly valve for the portion of the land outfall used most of the time, i.e., the primary system. The pipeline will be laid so that it essentially follows the ground profile. The butterfly valve will be located at the lower end of the pipe for complete submergence at all flows. The valve will be automatically throttled to keep a constant water surface in the treatment plant effluent collection channel. This design is standard enough so that reliable hydraulic computations may be made without benefit of a model study.

Since the primary system has mechanical and electrical components, it will be subject to periodic maintenance, repair, and malfunction. No storage has been provided anywhere in the sewerage system under construction; therefore, when the primary system for the land outfall is to be shut down, an alternative system must be immediately available to carry the flow to the ocean outfall.

The alternative system chosen for model study and shown schematically in Fig. 1 consists of the following:

1. A long weir over which the effluent will pass when rejected by the butterfly-valve circuit. This weir is located just downstream from the treatment plant.
2. An overflow channel to collect the flow coming over the weir.
3. A steep chute following the ground profile.
4. A stilling basin in which a hydraulic jump is formed.
5. A vertical vortex tube in which vortex flow is induced by means of a tangential entry.
6. An elbow connecting the bottom of the vortex tube to the ocean outfall.

The primary and alternative systems for the land outfall were chosen in preference to the other possible systems for several reasons as follows:

1. Completely independent systems — one is mechanical and electrical, while the other is entirely hydraulic with no moving parts.
2. These systems best conform to the topography.
3. These systems most completely meet all of the design requirements while remaining economically feasible.

Some of the components of the alternative system are well known and lend themselves to conventional hydraulic calculations. However, this particular combination of components and the vortex flow in the vortex tube are not so well known. Therefore, it was decided to verify the hydraulic calculations with a model study of all the components, with particular emphasis directed toward the vortex tube.

## 1.04 Preliminary Model Study

A preliminary-type model study was made on a portion of the alternative system in March 1961 (N. H. Brooks and J. F. Kennedy, 1961), but time limitations precluded a detailed study at that time. This study showed that the system was feasible and would perform essentially as anticipated for emergency use only, but would probably entrain fairly large quantities of air. This was not considered to be too important at that time, however, as two primary systems (including remotely controlled valves)

were to be constructed and the alternative system was to be used strictly as an emergency system.

A later change in criteria which discarded the second primary system and promoted the emergency system to an alternative system dictated that a more thorough model study be instigated, with particular attention to reducing air entrainment.

1.05 Contract between Joint Venture and California Institute of Technology

A contract covering the work included in this report was entered into by Holmes and Narver-Montgomery and California Institute of Technology on September 26, 1961. This contract called for a review of the literature on air entrainment and vortex devices, laboratory experiments on collection of air at vertical bends in a pipeline, and laboratory experiments on model energy dissipators. After the contract was executed and laboratory tests were made on energy dissipators, it was found that the air entrainment quantities could be kept low enough not to cause troubles in the outfall. Therefore, the experiments on collection of air at vertical bends were deleted from the program of work.

This report is the final one on the work performed under the above-mentioned contract.

# CHAPTER 2
# HYDRAULIC DESIGN

## 2.01 Hydraulic Design Criteria

This section will present in detail the objectives and restrictions to be met in the design of the hydraulic energy dissipator (hereafter referred to simply as the drop structure).

2.01.1 Energy to be dissipated. Fig. 5 shows the system head-discharge curves which determine the total head to be dissipated in the drop structure. Upstream from the drop structure the water level in the effluent channel from the sewage treatment plant is maintained at approximately 94 feet above mean sea level by a 120-foot long side channel weir with low velocity of approach. (Actually, the head on the weir does vary with flow and weir setting, but the variations are neglected, as they are only of the order of one foot or less.) At the downstream end of the energy dissipator, the energy gradeline elevation (hereafter called "tailwater head") is the summation of (a) the friction loss in the 11,300 feet of outfall pipe, (b) the friction loss in the diffuser pipes, (c) the head required for discharge through the diffuser ports*, (d) the head required to overcome the density difference between sewage and sea water for depth of discharge at about 210 feet, plus (e) the level of the tide. From experience on other outfalls, the design engineers decided that the maximum roughness factor would be a Manning n of 0.017 and the minimum possible, such as for brand new pipe, of 0.011. If the friction factor ever rises higher than the value 0.017, it is anticipated that the outfall would be cleaned by a cleaning device if necessary to restore adequate hydraulic capacity.

Thus, the amount of energy to be dissipated may be represented by the difference between 94 feet and the anticipated tailwater level for any given discharge. The design capacity of the outfall is set by the design engineers at 612 cfs; however, during the first years of operation, flows as low as 40 cfs are anticipated. Because of the decreasing head loss required

---

* Since the port arrangement will be changed from the "initial" stage to an "ultimate" stage at some future date, there are two sets of curves in Fig. 5.

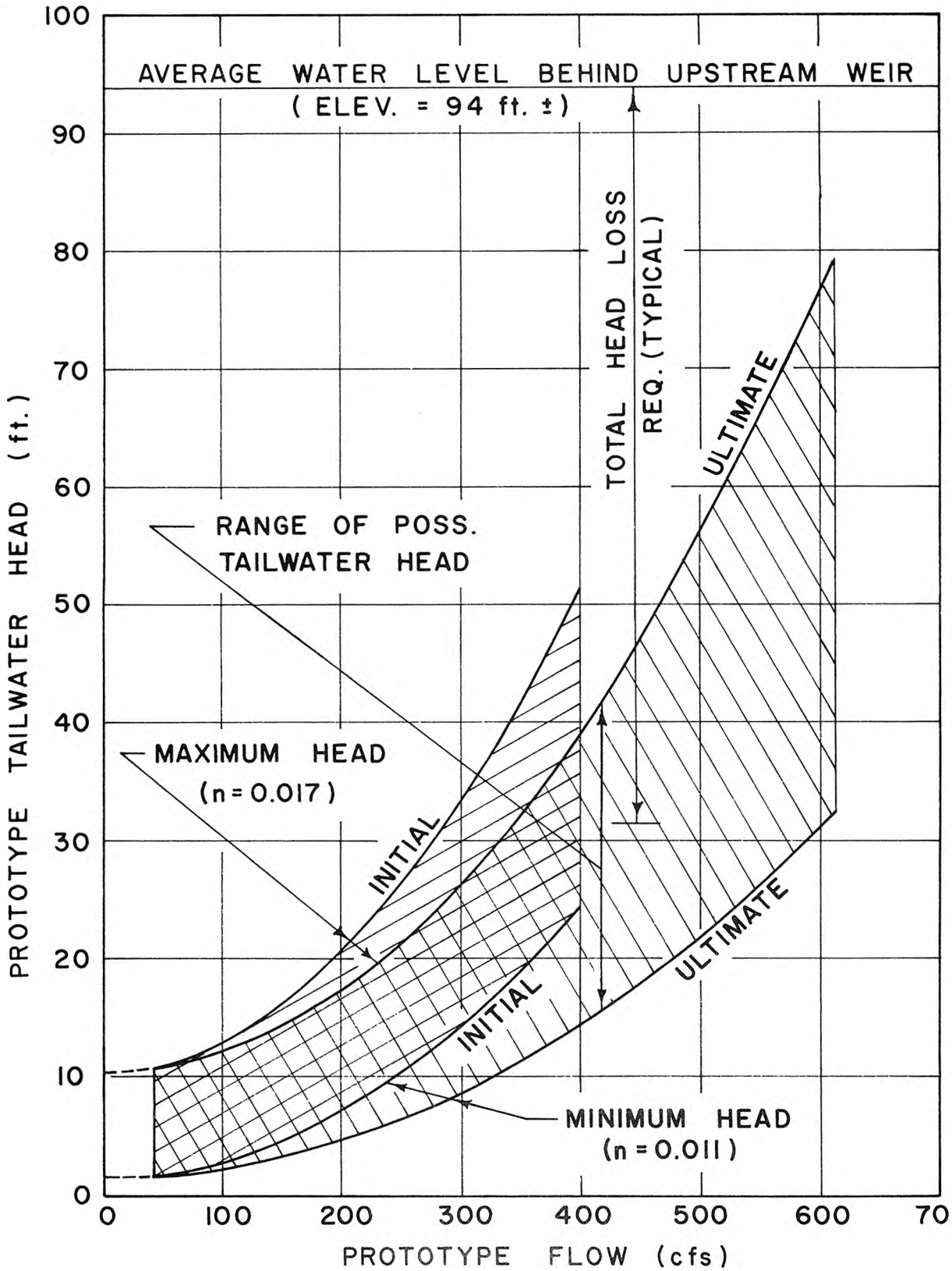


Fig. 5. Hydraulic head to be dissipated, shown as difference between calculated upstream and downstream heads. (Note: Small variations in upstream head due to weir setting and flow variations are neglected.)

with increasing flow, it is easy to see that any kind of fixed throttling device, such as a simple orifice, is completely unsuitable for this situation.

2.01.2 Hydraulic stability. Not only must the structure dissipate the required amount of energy, but it must also be hydraulically stable and free from excessive surges and vibrations. The prediction of resonance phenomena in complex hydraulic structures is very difficult, but may be easily checked in Froude models. Hydraulic models, of course, do not give proper structural modeling, but it is safe to presume that if any appreciable uncontrolled surge is observed in the model, then a similar prototype flow would be potentially dangerous.

2.01.3 Air entrainment. For this ocean outfall, the City of San Diego, through its Technical Advisory Committee, specified that the air entrainment should be kept very low in order to avoid bubbling of air from the end of the outfall. This rising air would possibly create a foam and odor problem on the surface of the ocean, constituting a public nuisance.

Furthermore, from a hydraulic point of view, it is absolutely essential that air entrainment be limited to prevent formation of large air pockets in the outfall at places where there are vertical downward curves. These air pockets can cause restriction in the outfall flow capacity and can blow back in huge surges, endangering both personnel and structures at the shore. It is worthy to note that the outfall has slopes varying from zero to approximately eight per cent downward as it follows the ocean bottom offshore to a depth of 210 feet in a distance of 11,300 feet (an average slope of approximately two per cent).

On the other hand, air which is entrained in the outfall may be dissolved, given sufficient time and dispersion of bubbles. Since oxygen is consumed in biochemical oxidation, large quantities can be dissolved; consequently, nitrogen solubility will limit how much air can be completely dissolved. As the sewage effluent travels to over 200 feet depth, the total pressure rises to more than seven atmospheres. Calculations were made of the maximum amount of air that could be taken into solution as a function of depth, using the perfect gas law and Henry's Law, giving results shown on

Fig. 6 *. Near the end of the outfall the hydraulic head for diffuser operation becomes relatively small compared to hydrostatic head, and thus is neglected. On Fig. 6 the maximum volume of air which can be dissolved is shown in per cent by volume at atmospheric pressure and 20° C rather than in the usual way of ppm by weight of the liquid. This graph shows that 10.0 per cent air by volume could be completely dissolved at 200 feet depth.

However, it is highly unlikely that that much air could be transported out through the outfall for gradual progressive solution along the way; rather, it would undoubtedly collect in large bubbles at grade breakpoints along the way. It was assumed that at least 1.0 per cent by volume of entrained air at atmospheric pressure could be dissolved in the outfall; this figure is equivalent to complete saturation of water with air at 20 feet additional pressure head, or only 1/10 of possible dissolution of air at full 200 feet (see Fig. 6 ). Since the rate at which air goes into solution is dependent on the contact area between air and water, large air pockets might persist relatively long times, while small bubbles well diffused in the liquid would dissolve quickly. Due to the turbulence generated in the drop structure itself, the air bubbles are likely to be small and well distributed at the beginning of the ocean outfall, and would only collect in large pockets after the effluent flows some distance downstream. Thus for all conditions for which the tailwater level is more than +12.5 feet MSL (soffit of beginning of outfall pipe being -7.5 feet MSL) the 20-foot increase in pressure head is sufficient to dissolve 1 per cent of air rapidly, probably before the air bubbles collect at the top of the pipe to form pockets of air.

In order to allow for scaling up, the maximum air entrainment concentration allowed for the model was set at one-tenth of the prototype value or 0.1 per cent, or 1000 ppm by volume (see Chap. 3).

2.01.4 No release of odors. It was specified by the City of San

---

*Henry's Law is $C_s = \beta p_g$, where $C_s$ = solubility or volume of gas (reduced) to 0° C and 760 mm mercury) absorbed by one volume of water at stated temperature when partial pressure of the gas is 760 mm mercury; $p_g$ is partial pressure of gas, in multiples of 760 mm mercury; and $\beta$ is Brunsen's coefficient, taken as 0.155 for nitrogen at 20° C. Air was assumed to be 80 per cent $N_2$, with $N_2$ solubility limiting.

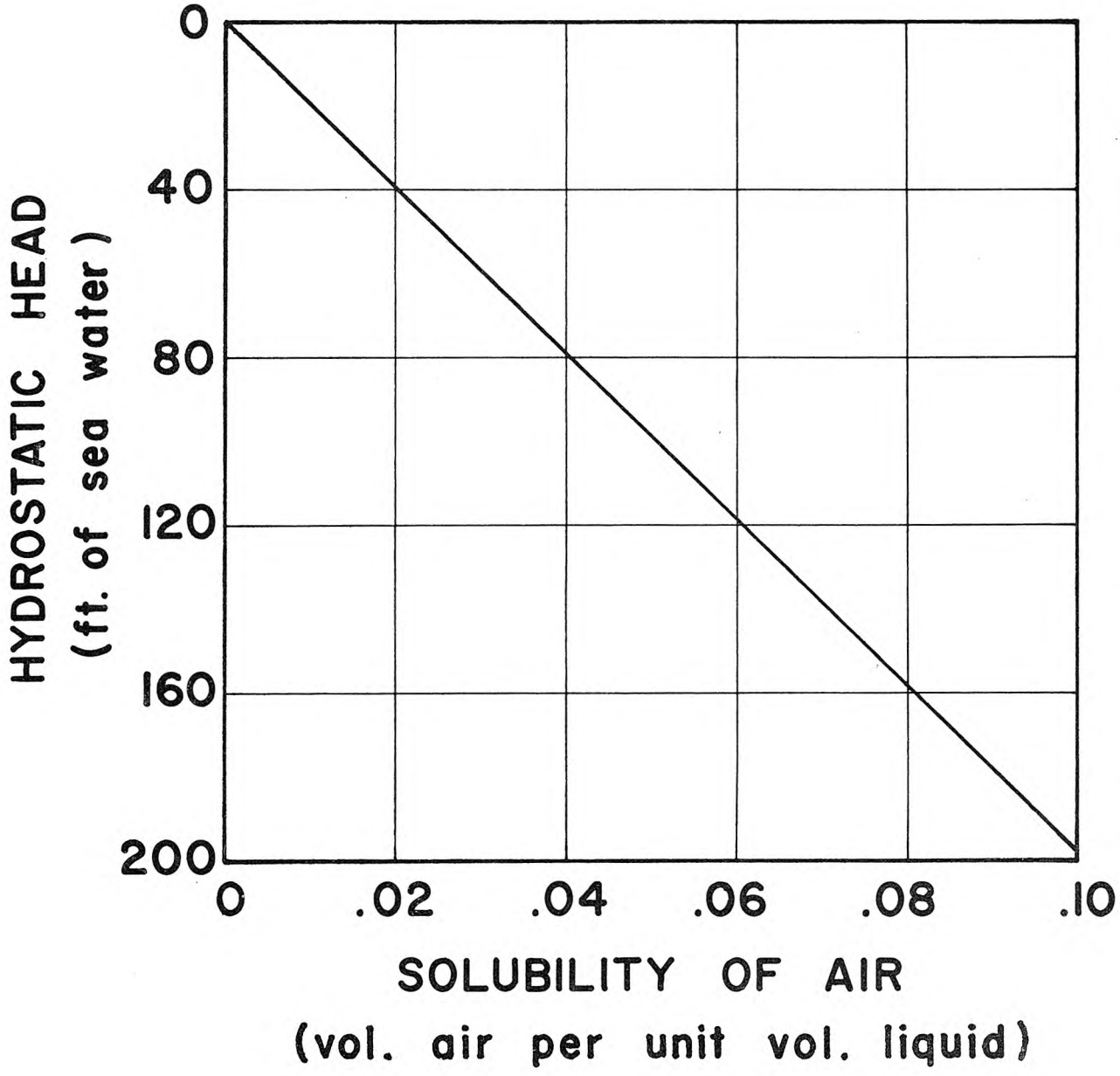


Fig. 6. Solubility of air in fresh water expressed as relative volume of air at atmospheric pressure and 20° C. (Nitrogen, 80% of air, is limiting constituent.)

Diego that the operation of the drop structure itself should not generate odors which would be released to the atmosphere. Therefore, it was necessary to make the system completely enclosed, including the discharge of air from vent pipes back into the air space above the free surface in the effluent channel. However, it was not necessary to include in the laboratory model the covers over the effluent channel and overflow weir structures of the prototype because the air space there in the prototype is maintained at practically atmospheric pressure.

2.01.5 Control of the generation of foam. Because of the presence of alkyl benzene sulfonate (ABS) in the sewage effluent, the entrainment of air and the presence of turbulence may lead to severe foaming. The foaming can be effectively controlled by covering the entire structure, as will be done anyway for odor control, and also limiting the inflow of fresh air. When all of the available air space is filled with foam, no more foam can be generated without simultaneously destroying "old" foam. (Furthermore, the design engineers have decided to provide water sprays for foam control over the collection channel for the 120-foot long weir at the upstream end of the drop structure. Any foam, therefore, which comes back up the drop structure, will effectively be intercepted and beat down by the sprays before it can fill the air space in the effluent conduit and thus travel back to the weir building and the sewage treatment plant exhaust system.)

2.01.6 Local foundation conditions and topography. In order to be economical, the proposed drop structure had to be related to the local topography as shown in profile in Fig. 1, which shows a moderately steep ground slope down to about 50 feet, followed by a vertical or slightly overhanging sea cliff. Because the sandstone is only of medium strength with some sea caves, the design engineers decided against any structures which required extensive rock excavation or tunneling. Thus, efforts were made to devise a structure which would essentially be placed in a surface cut and protected at the toe by an adequate sea wall.

2.01.7 Provision for insertion of cleaning device. Such provisions were necessary for the contingency that the ocean outfall itself needs to be

cleaned out by a traveling device which scrapes or scrubs the interior walls of the outfall. This condition placed some severe restrictions on the arrangement of hydraulic components; for example, a free drop into a large circular caisson with efflux into the outfall horizontally at the bottom would be unacceptable because there would be no feasible way of guiding the cleaning tool into the outfall pipe opening. The inlet would always be submerged and the location would be too hazardous for diver operations. It was thus necessary to arrange for the insertion of a cleaning tool at a sufficiently high elevation that a removable cover could be taken off a part of the structure and that the cleaning tool could be lowered by crane to a point where it would be self-guiding under the influence of hydraulic forces into the mouth of the outfall. The vertical vortex tube which evolved satisfies this condition for inserting and guiding the cleaning device. The vortex tube has a diameter of 13.5 feet at a top elevation of 59.5 feet MSL, tapers down to the outfall diameter of 9 feet in a vertical alignment, and is followed by a 9-foot diameter elbow with a centerline radius of 18 feet.

2.01.8 Automatic operation. The hydraulic structure should be completely automatic in its operation with no moving parts in order that it can function in the absence of power or control by sewage treatment plant personnel. As explained in Chap. 1, this hydraulic system tested in the model is the alternative system for the butterfly throttling valve circuit and will go into operation during periods of maintenance or malfunction of the butterfly valve. However, because of the critical nature of the structure and the absolute necessity to provide 24-hour service every day of the year, every effort was made to design a structure which would perform fully as well as the butterfly-valve circuit and could be used interchangeably with it.

It may be noted that the design criteria in Secs. 2.01.1 through 2.01.6 apply also to the butterfly valve circuit, except that the upstream water level is controlled by the valve with variable setting rather than by the weir. Secs. 2.01.7 and 2.01.8 apply only to the drop structure.

## 2.02 Types of Energy Dissipators and Literature Review

The various types of energy dissipators may be broadly classified

according to their basic principles of operation into the five categories described below.

2.02.1 Submerged jet. It is well known that if a jet is discharged into a reservoir, the kinetic energy of the jet is dissipated in turbulence and ultimately into heat. Every valve in a pipeline utilizes this principle, and dissipates energy by generating submerged jets just downstream of the valve. When the discharge is into a pipe instead of into a reservoir, not all of the kinetic energy is lost, but some is converted back into pressure head, with the loss of energy being determined by the equations for conservation of momentum*.

Basically, this principle is employed in the butterfly-valve circuit, which is not the main subject of this report. Because the head to be dissipated decreases as the flow increases, it is necessary for any device of this type to have a varying valve setting which is remotely controlled by a water level sensing device in the forebay. For an automatic hydraulic energy dissipator with no moving parts, this type of device cannot be used.

2.02.2 Hydraulic jump. The hydraulic jump is closely related to the submerged jet, because the high speed shallow flow in effect becomes a submerged jet when it plunges into the jump generated by a sufficiently high tailwater. It has the advantage over a fixed submerged jet in that the position of the jump and the depth before and after will automatically adjust themselves to take care of the energy loss imposed on the system, provided, of course, that the components are arranged in such a way that the hydraulic jump is not pushed completely out of the structure.

There has been a great deal of experience with the hydraulic jump as a means for dissipating energy at the base of chutes and spillways in hydraulic structures on rivers and canals. In fact, as an aid to the designer, the U. S. Bureau of Reclamation has recently developed generalized design criteria for small and moderate drops (U.S.B.R., 1960; J. N. Bradley and A. J. Peterka, 1957).

On account of the topography in the present situation, it is not feasible

---

*See discussions of sudden expansion in a basic fluid mechanics text.

to use a hydraulic jump to dissipate the full amount of energy. To do so would require a long sloping tunnel of a very large size, say, 20 to 25 feet in diameter, permitting the jump to move up and down in response to the wide fluctuations in the anticipated tailwater level, which, it may be noted, are not encountered in the usual situation of river flow below a dam. The very large tunnel size is required in order that the large amounts of air entrapped by the hydraulic jump may be released back to the open channel section rather than be drawn down into the closed pipe section and out into the outfall.

However, in the final design a hydraulic jump was used for the upper portion of the drop only (see Sec. 2.03).

2.02.3 Free fall. Certainly an obvious way to dissipate energy is to permit a free fall of water, such as in a natural waterfall, or a drop over a vertical weir or free overfall in a manmade structure. In this case, a small portion of the energy may be dissipated by the air friction on the falling water (especially when the quantity is very small) but the major portion is dissipated after the falling water plunges into a pool at the bottom of the waterfall. In a sense this is again a submerged jet which ultimately dissipates its energy into turbulence and heat. Very large amounts of air are entrained by this process and stilling pools of very considerable size are required in order to allow the air bubbles to escape before water enters a closed conduit. To use this method in the present situation would require a very large vertical caisson, perhaps 30 to 40 feet in diameter, which would be infeasible because of cost and also because of the impossibility of getting a cleaning tool into the outfall entrance at the bottom of the caisson. Undoubtedly huge quantities of foam would be generated also.

In many other applications, notably drops into sewage interceptors, air entrainment is not a problem because the collecting tunnel will normally be flowing only partly full, allowing air to be easily and safely vented. On the other hand, for power installations, the tunnel or pipeline at the bottom of the drop is usually flowing full and entrained air is definitely a problem.

A good example of a sewer drop shaft with a free fall is the design developed for the City of St. Paul by S. H. Anderson (1961) with model tests

at University of Minnesota. The flow plunges down a straight vertical shaft (without swirl) into an "impact cup" (sometimes called "casserole"), then overflows into a chamber several times as large as the drop shaft. In the chamber, the air rises and escapes backward along the downward sloping soffit of the transition section joining the drop chamber to the tunnel section (see Fig. 7). Entrainment of air was not an essential consideration, provided quantities were moderate. In the model studies entrained air was considered a qualitative indicator of the degree to which the drop energy was dissipated in the structure. The impact cup definitely improves the performance of a free fall device by accelerating energy dissipation. It is interesting to note that one of the recommended designs is for a drop of 62 feet and a flow of 600 cfs (the same flow as the San Diego drop, but a greater drop at this flow). The design includes a drop shaft, 8 feet in diameter, an impact cup 9 feet in diameter (and perforated), a lower chamber 23 feet in diameter and 19 feet high, and a transition to the tunnel which is 46.5 feet long (Fig. 7 ). Although this is an excellent energy dissipator with small air entrainment it is nevertheless a very large structure, with severe dynamic forces on the impact cup and chamber walls.

A. A. Kalinske (1941) has studied the hydraulics of flow down vertical pipes under part-full conditions with free discharge at the bottom; air and water discharge were measured for pipe diameters in the range from 0.08 to 0.48 foot and length of vertical pipe from 3.6 to 17 feet. Generally the air entrainment was very high, with typical values of the order of 10 to 35 per cent of the water discharge (by volume). However, these results are not directly applicable because there is no tailwater or back-pressure, and the length to diameter ratio is larger than for the San Diego problem.

Following Kalinske, G. Marquenet (1953) made a more extensive experimental study of flow in vertical shafts including cases of submerged discharge and covering several different water-air flow regimes. The air entrainment was always so large that Marquenet proceeded to develop and test an excellent device which he called "siphon of maximum depression" to solve the air entrainment problem.

In the siphon of maximum depression, Marquenet avoids air entrainment basically by preventing air from entering the enclosed drop pipe. This

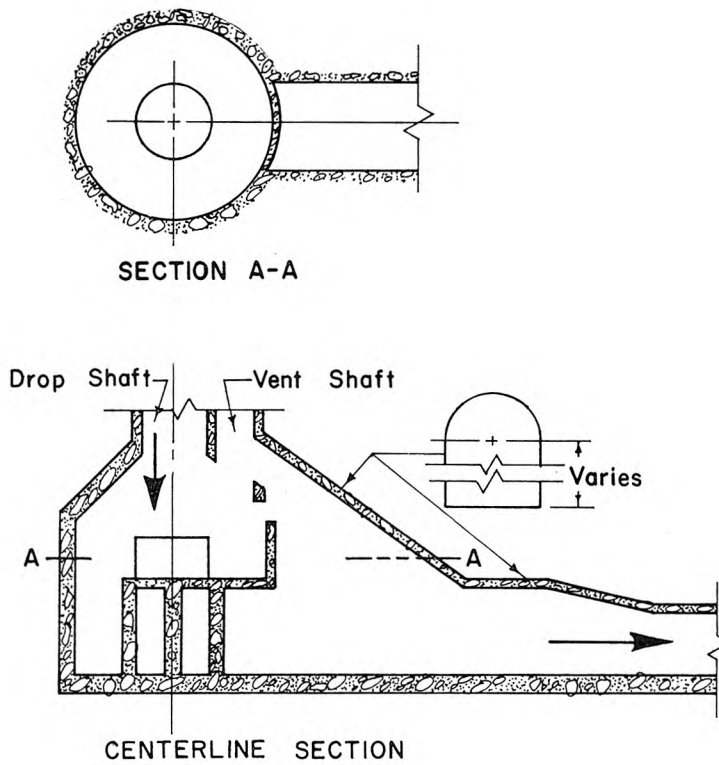


Fig. 7. "Casserole"-type drop structure (after Anderson).

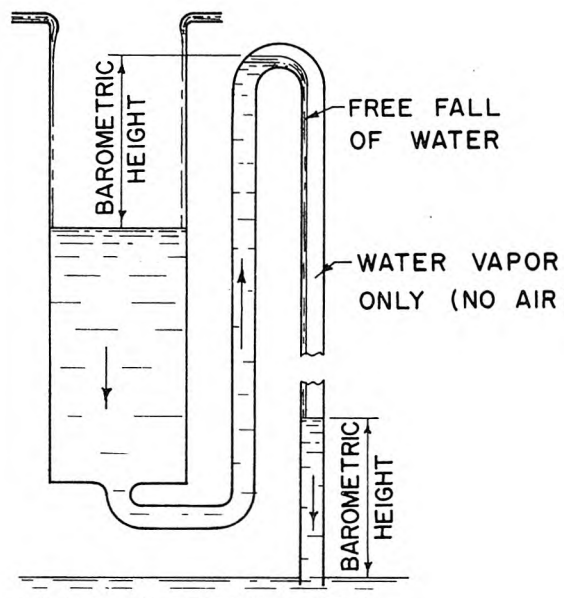


Fig. 8. Siphon of maximum depression (after Marquenet).

requires a siphon-type arrangement to limit the flow rate to the inflow rate and create a free fall in a near vacuum, or rather space filled with water vapor (see Fig. 8). This vapor is entrained at the base of the fall very much as air is but as soon as the system flows downward to higher hydrostatic pressure the vapor condenses back to water. R. A. Hill* has reported marked success of several small installations of siphons of maximum depression. This system was considered for application to the San Diego system, but because of the large flows, it is too costly to build the necessary structures, including a siphon of height of over 30 feet (i.e., one atmosphere less vapor pressure). Had the amount of drop been many times the equivalent of one atmosphere, this scheme might have been attractive.

Other types of free fall devices used for sewers and secondary water intakes for power tunnels are reviewed by Anderson (1961) and J. Cotillon (1959).

2.02.4 Spiral flows. Spiralling or vortex type flow can be used for drops with considerable improvement over a free fall (except of course the siphon of maximum depression). One basic idea is to make the falling water follow a helical path down the wall of a vertical cylinder or cone, thus leaving the center space open for release of air (much as a chimney). With low flows and low tailwater level the flow spirals around the circumference into a pool at the bottom. Much of the energy may be dissipated in the area of impact, but some of the energy persists in the helical motion downstream. Under other flow conditions, there may not be much free fall, but instead a large vortex flow filling the entire vortex tube except for a small but deep air hole. In this case, the required dissipation is less, and is accomplished almost entirely by the great increase in internal and wall shear.

Prior use of vortex-type drop structures has been limited to relatively small flows in large drops, whereas the present application is a relatively large flow (up to 612 cfs) with only medium to small drops (range about 90 to 15 feet total).

L. M. Laushey (1952; — and F. T. Mavis, 1953) has made laboratory

---

*Personal communication from Mr. Raymond A. Hill, Leeds, Hill and Jewett, Inc., Los Angeles, California.

investigations on vortex flow down vertical shafts for application to various sewer drops in 8- to 36-inch pipes down as much as 90 feet to interceptor sewers in Pittsburgh (Allegheny County Sanitary Authority). Model studies covered drops of up to 30 feet in a 5.59-inch diameter shaft. To generate the vortex, Laushey proposed a large tank of diameter 4 to 6 times the shaft diameter with a tangential inlet to generate the vortex; the bottom of the tank was flat with a sharp-edged inlet to the shaft in the center (see Fig. 9). Comparison of the spiral flow inlet with a simple radial flow inlet to the shaft showed its superiority for limiting air entrainment. The volume ratio of air discharge to water discharge was found to be dependent almost entirely on the actual drop distance to the hydraulic grade line from the top of the shaft.

Since air entrainment was large and could not be eliminated, vents in the horizontal interceptor pipe were tested and recommended for the prototype. Typical model values of the air-water volume discharge ratio were very large, ranging up to 30 per cent with a tailwater sufficient to form full pipe flow at the bottom of the shaft, and as high as 100 per cent with lower tailwater, allowing plunge directly into the interceptor (which may flow only partly full at low flows).

M. Viparelli (1961) has recently reported on experiments at Naples similar to those of Laushey. The flow was introduced into a long vertical drop shaft through the bottom of a small spiral inlet tank to make the flow spiral down the walls of the shaft. Both cases of free and submerged discharge were studied with variable pressure at the point of discharge. Using Laushey data, Viparelli derived some empirical equations for the volume of air discharge for various flow regimes. However, the amounts were always large (~ 10 to 30 per cent), and probably could not be tolerated in prototype down shafts to closed power tunnels. Although the writers believe that the intensity of the initial swirl is an important variable, neither Laushey nor Viparelli considered it to be.

Several other investigators (H.-C. Hsu, 1947; R. C. Kolf, 1956; J. C. Stevens and R. C. Kolf, 1959; and R. C. Kolf and P. B. Zielinski, 1959) discuss the effect of a vortex on discharge through horizontal orifices, showing that as the circulation increases the discharge coefficient decreases and the required head increases markedly for given flow. Owing to this fact,

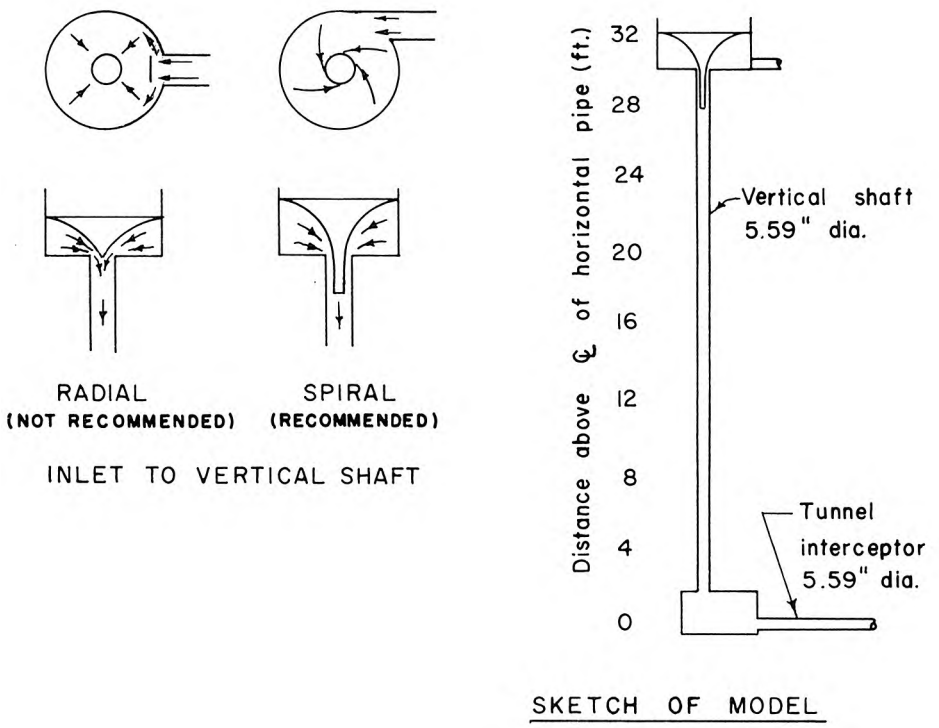


Fig. 9. Drop shaft with spiral-flow inlet (after Laushey).

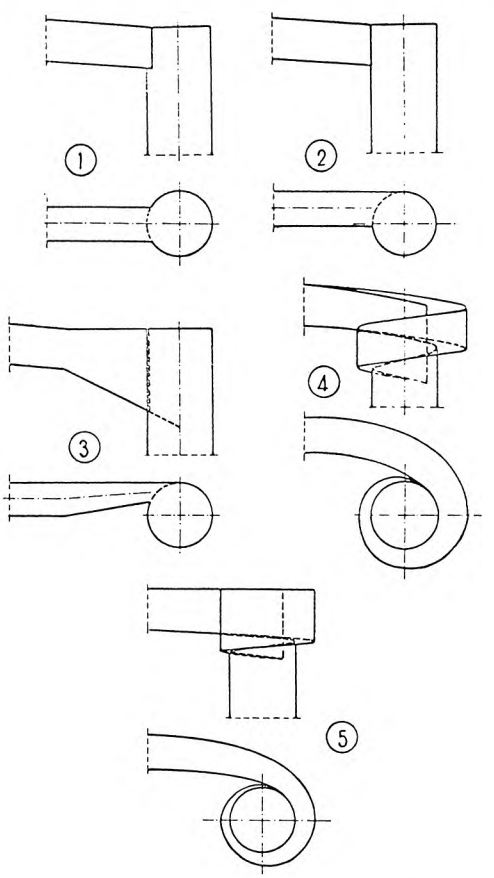


Fig. 10. Various drop shaft inlets tested by Jevdjevich and Levin.

an orifice (or sharp-edged inlet) at the bottom of a tank at the top of a drop shaft is not suitable for the San Diego drop structure.

For large flows it appears more feasible to introduce the water tangentially into the top of the drop shaft pipe rather than through an inlet tank. With this approach, V. Jevdjevich and L. Levin (1953) have made model tests for a secondary intake to a power tunnel, for which the vertical shaft was to be 2 meters in protoype and the design flow 1.5 $m^3$/sec (53 cfs). The drop height was not specified. The model was built on 15 : 1 scale with five different inlets directly into the top of the shaft (as shown in Fig. 10). Two of them were spiral (No. 4 and 5), two were tangential (No. 2 and 3), and one was simply axial (No. 1).

Comparing the inlets on the basis of air entrainment over a range of tailwater levels, the axial inlet 1 was by far the poorest of the five, with inlet 2 next, followed by inlet 4. Inlets 3 and 5 were judged equally good in spite of the much more complex forming of the channel for inlet 5. A typical value of the volume rate of air entrainment for inlet 3 was 0.3 per cent of the discharge, which authors imply should be a limiting value for the design flow. Since this value is much smaller than any obtained by Laushey or Viparelli, it is suspected that Jevdjevich and Levin had a stronger swirling motion.

2.02.5 Boundary layer or pipe friction. Another way to dissipate energy is by ordinary pipe or channel friction, but this is usually infeasible for large amounts of head to be dissipated in a relatively compact structure carrying large flows. To develop sufficient pipe friction would require feeding the water into a great many small tubes and arrangements would have to be made for operation of a variable number of different sizes to match the varying discharge. In fact, since friction loss tends to increase with the square of the velocity, the characteristic of any individual tube is opposite to that required for the structure as a whole, namely, that the amount of energy to be dissipated decreases as the discharge increases.

Nevertheless, ingenious multiple-siphon energy dissipators have been described by Jevdjevich and Levin (1953), N. O. Boughton (1959, 1960), and others, for use for secondary power intakes. At the laboratories of the

Snowy Mountains Hydro-Electric Authority in Australia, Boughton designed and tested such a device consisting of a battery of 20 self-priming siphons, which come into operation in sequence to match the required inflow. The discharges from the siphons direct the water in a spiralling motion into the tailwater pool at the bottom of the shaft, thus generating a vortex to reduce the entrainment of air. This device in prototype operation has successfully reduced air entrainment, but has not succeeded in completely eliminating it and the attendant difficulties of air accumulation in tunnels*.

W. Eastwood, G. A. Taylor, and J. Allen (1953) have tested a less desirable single siphon structure with a tangential jet into a vortex separator for a secondary power intake. Since it carries only a constant flow, its operation is intermittent with large slugs of air entering the system on each making and breaking of the prime.

## 2.03 Selection of Hydraulic Components

On the basis of the preceding considerations, the senior author** recommended the general arrangement of components shown in Fig. 1. Subsequently, model investigations undertaken by the California Institute of Technology demonstrated that this arrangement was hydraulically satisfactory. From numerous tests, suitable hydraulic dimensions for the various components were determined (or confirmed).

Before describing the laboratory investigations some comments will be presented below to explain some of the reasons for the choice of components.

2.03.1 Overflow weir and collection channel. The free fall concept is utilized in the present case for a small drop from the 120-foot long overflow weir into the weir collection channel at the upper end of the drop structure. The amount of the drop ranges from only about 1 foot at the upper end of the channel at peak flows to as much as about 10 feet at very low flows at the downstream end. Although this is not the optimum way to dissipate energy and keep control of odor release, foam generation, and limitation

*Personal communication from Mr. R. A. Hill.

** Serving as hydraulics consultant to Holmes and Narver-Montgomery (1960-62).

of air entrainment, it is unavoidable because of the necessity for the long overflow weir to maintain the correct water level in the effluent channel.

The idea of the free fall was not utilized for the main drop because it appeared from the literature that an adequate structure would be much bigger and more expensive than other possible solutions.

2.03.2 Chute and stilling basin. Because of the good features of the hydraulic jump, it was decided to dissipate the upper 30 feet by means of a chute running into a conventional stilling basin for a hydraulic jump. The stilling basin was laid out according to the above-mentioned design criteria (U.S.B.R., 1960, p. 296; or Bradley and Peterka, 1957, Paper 1403), except that the top of the channel was closed at an elevation just slightly lower than the expected free height of the jump. This was necessary not only for odor control, but also to allow a roadway above the structure for crane access to the opening for the cleaning device. Because of the typical nature of this stilling basin, which performed satisfactorily in the model, there will not be much further discussion of it in this report.

The stilling basin designed is set horizontally with an end sill having a crest elevation of 55 feet MSL to maintain a tailwater for the stilling basin adequate to generate a hydraulic jump when the tailwater for the system drops to lower values. From Fig. 5 it may be observed that the system tailwater level rarely rises above 60 feet and in those cases where it does it may be anticipated that the jump will be pushed back up into the closed rectangular chute (cross section 10 feet wide by 8 feet high)*.

The air which is entrained by the fixed hydraulic jump in the stilling basin (or in the chute) has a chance to be released from the air vent at the top of the vortex structure downstream from the stilling basin. Thus, the principal objection to the hydraulic jump for this application is overcome when it is used only for the first part of the drop structure because of the efficiency of the vortex structure in collecting and venting the air.

*Because of the inherent head loss in the vortex structure even when running full, the hydraulic jump is actually pushed back out of the stilling basin at tailwater levels as much as 15 feet below the 60 foot level for the maximum flows.

2.03.3 Vortex tube. Since the vortex tube was the most uncertain part of the preliminary hydraulic design, the details were evolved from the model studies as explained in following parts of the report. For vortex generation it was found that the use of a tank on top of a vertical shaft as suggested by Laushey (1952) was not feasible because of the large size required, both in diameter and depth. When Anderson (1961) noted that for 600 cfs the recommended diameter according to Laushey was 32 to 48 feet with depth of 18 to 28 feet, and also found experimentally that smaller tanks were completely inadequate in flow capacity, he completely abandoned the idea of a swirling flow.

Nevertheless, it is perfectly feasible to generate swirling flow simply by a tangential inlet, as commonly used for cyclone separators for removing particles from fluids. The inlet configuration finally developed for the San Diego drop structure is similar to inlet No. 3 of Fig. 10 (after Jevdjevich and Levin, 1953) although it was arrived at independently.

The velocity of flow into the vortex tube is controlled by the sill at the end of the stilling basin; the flow is critical at this point, except for cases of high hydraulic grade line downstream. Although the stilling basin flows completely full (for $Q > 290$ cfs), open channel flow starts just beyond the sill, which in effect is a broad-crested weir under slight pressure. The transition section, between the sill and the vertical vortex tube, decreases the width and increases the depth in a way to maintain approximately uniform cross sectional area for the flow at the design discharge (612 cfs). Thus, since the flow through the transition is maintained at near the critical velocity over the sill, highly supercritical flows are avoided and at the same time the transition itself produces no backwater. At flows lower than the design discharge, the velocity is supercritical because of the downward slope of the transition invert; for example, at very small flows, the velocity head may approach the total drop in the invert of the transition, namely $55 - 47.2 = 7.8$ feet or velocity = 22 fps. Therefore, the intensity of circulation is greater for the lower flows, a factor which is desirable because the head to be dissipated is most at the low flows.

2.03.4 Elbow and outfall pipe. The radius of the mitered elbow below the vortex tube (18 feet to centerline) was made sufficient to allow passage of the cleaning device, and was adequate hydraulically.

The elevation of the 9-foot diameter outfall pipe at the elbow was established by balancing increased cost of excavation for lowering it with the increased benefit in further reducing air entrainment as determined from the model. In the final design the centerline of pipe was set at -12.0 feet MSL at the elbow.

* * *

The following chapters pertain to the laboratory investigation. Model laws and scaling factors are covered in Chap. 3, experimental procedure and results are given in Chap. 4, and are discussed in Chap. 5. Summary of results and conclusions are presented in Chap. 6.

# CHAPTER 3
# MODEL LAWS AND LIMITATIONS

## 3.01 Description of Model Law

A model of this type is most strongly influenced by gravity forces and therefore is modeled by Froude's Law, that is,

$$F_m = F_p$$

where

$F$ = Froude number = $\frac{V}{\sqrt{gL}}$

$m$ = subscript for model

$p$ = subscript for prototype

$V$ = any characteristic velocity

$L$ = any characteristic length

$g$ = acceleration due to gravity

therefore

$$\frac{V_m}{\sqrt{gL_m}} = \frac{V_p}{\sqrt{gL_p}} \quad \text{or} \quad \frac{V_p}{V_m} = \left[\frac{L_p}{L_m}\right]^{\frac{1}{2}}$$

$$\text{or } V_r = L_r^{\frac{1}{2}}$$

where subscript r indicates prototype-model ratio.
Furthermore, the discharge ratio is

$$Q_r = V_r A_r = L_r^{\frac{1}{2}} L_r^{2} = L_r^{\frac{5}{2}}$$

and the time ratio is

$$T_r = \frac{L_r}{V_r} = L_r^{\frac{1}{2}}$$

Limitations of this model law for this problem are discussed in Sec. 3.03 below.

3.02 Model Scales

In selecting a model length scale, it is necessary to have the model large enough to get fully turbulent flow and be reasonably free of capillary effects (although not possible for air entrainment) and at the same time make it fit the laboratory space and available water supply without becoming unwieldy. Three length ratios were used during the model tests as follows:

1. Small models, except 5S, $L_r$ = 28.5 : 1
2. Small model, 5S only, $L_r$ = 27 : 1
3. Large model, $L_r$ = 18 : 1

The corresponding ratios of other quantities, according to the equations above, are given in Table 1.

TABLE 1

RATIOS OF PROTOTYPE TO MODEL QUANTITIES

| | | | |
|---|---|---|---|
| Length ratio, $L_r$ | 28.5 | 27.0 | 18.0 |
| Velocity ratio, $V_r$ | 5.34 | 5.20 | 4.24 |
| Discharge ratio, $Q_r$ | 4,330 | 3,791 | 1,374 |
| Time ratio, $T_r$ | 5.34 | 5.20 | 4.24 |
| Maximum model flow for maximum prototype flow of 612 cfs, in cfs | 0.141 | 0.161 | 0.445 |

These length ratios were chosen so that standard size transparent lucite tubing could be used to model the ocean outfall. In the case of the 28.5 : 1 models, a 4-inch lucite tube was used to model a 114-inch outfall. To simulate a 108-inch outfall, which was the size finally specified by the design engineers, a 4-inch lucite tube also was used in the 27 : 1 model and a 6-inch lucite tube was used in the 18 : 1 model.

The Reynolds numbers associated with the ocean outfall models at the chosen scale ratios are given in Table 2. Reynolds number = $Vd/\nu$ where V = mean forward velocity, d = pipe diameter, and $\nu$ = kinematic viscosity of flowing liquid ($1.059 \times 10^{-5}$ $ft^2$/sec for water at 70° F).

TABLE 2

REYNOLDS NUMBERS IN MODEL AT HIGH AND LOW FLOWS

| | | | |
|---|---|---|---|
| Length ratio | 28.5 : 1 | 27 : 1 | 18 : 1 |
| Outfall pipe diameter, model, ft | 0.333 | 0.333 | 0.50 |
| Kinematic viscosity, $\nu$, $ft^2/sec$ | $1.059 \times 10^{-5}$ | $1.059 \times 10^{-5}$ | $1.059 \times 10^{-5}$ |
| High flow (prototype flow = 612 cfs) | | | |
| Model flow, cfs | 0.141 | 0.161 | 0.445 |
| Model velocity, fps | 1.62 | 1.84 | 2.27 |
| Model Reynolds number, $N_R$ | 50,500 | 57,400 | 107,000 |
| Low flow (prototype flow = 100 cfs) | | | |
| Model flow, cfs | 0.023 | 0.026 | 0.073 |
| Model velocity, fps | 0.26 | 0.30 | 0.37 |
| Model Reynolds number, $N_R$ | 8100 | 9400 | 17,500 |

It should be noted that the Reynolds numbers in the model ranged from 8,100 to 107,000, definitely within the range of turbulent flow. The corresponding Reynolds numbers in the 108-inch prototype outfall would be 1,340,000 and 8,170,000.

3.03 Limitations of Model Law

It is mandatory to use Froude's Law to achieve the correct gross flow behavior under influence of gravity in the chute, stilling basin, and vortex tube, as implied in Sec. 3.01. However, this flow also depends strongly on viscosity (energy dissipation, rate of rise of air bubbles) and surface tension (air entrainment, foam generation). For correctly modeling viscous effects, one uses Reynolds number similarity ($N_R = \frac{Vd}{\nu}$) and for capillary or surface tension effects the Weber number,

$$W = \frac{V}{\sqrt{\sigma/\rho L}}$$

where $V$ = velocity

$\sigma$ = surface tension

$\rho$ = mass density

$L$ = characteristic length

It is impossible to model all three ways at once (or even any two), when water is used as the model fluid. In practice one model law is followed and empirical distortions or "scaling factors" are included to take account of variables not properly modeled.

3.03.1 Viscous effects. For proper modeling of the overall hydraulic resistance, it is necessary to have the Darcy's friction factor f the same in model and prototype, where f is defined by the equation

$$h_f = f \frac{L}{D} \frac{V^2}{2g}$$

where $h_f$ = head loss, L = length of pipe, D = pipe diameter, V = mean velocity, and g = gravitational acceleration. For the prototype-model ratio,

$$h_{f_r} = f_r \left(\frac{L}{D}\right)_r \frac{V_r^2}{g_r} = f_r V_r^2.$$

By Froude's Law

$$V_r^2 = L_r,$$

hence

$$h_{f_r} = f_r L_r,$$

and

$$\left(\frac{h_f}{L}\right)_r = f_r.$$

For an undistorted model, it is desired to have the head loss $h_f$ model like the geometric lengths, or in other words, the slope $h_f/L$ should be the same in model and prototype. Consequently,

$$f_r = 1 \quad \text{and} \quad f_m = f_p.$$

The predicted prototype Manning roughness value (n) for the outfall is between the limits 0.011 and 0.017, or assuming an average of 0.014, the corresponding friction factor for full pipe flow at 612 cfs is $f_p = 0.0174$ In the model where the outfall pipe is hydrodynamically smooth lucite and the Reynolds number $N_R$ is 107,000 (Table 2), the friction factor is $f_m = 0.0178$, very close to the required value. However, for the lower flows the model f-value increases as $N_R$ decreases (e.g., at $Q_p$ = 100 cfs, $N_R$ = 17,500, $f_m$ = 0.027). Therefore, in a gross sense, the hydraulic

resistance is of the correct order of magnitude in the model pipe, even though it is the downstream valve which regulates the total tailwater head anyway.

No adjustment was made for viscous effects in transferring model results to the prototype. Nonetheless, because of the larger Reynolds numbers in the prototype, the boundary layers in the vortex tube will not be as thick, and the wall shear will be relatively less; in the outfall pipe going downstream, the vortex motion will probably not decay as fast in the prototype as in the model.

3.03.2 Air entrainment. N. O. Boughton (1960) has given a careful discussion of required modeling laws for hydraulic structures with a vortex chamber involving air entrainment. He specifies three conditions:

1. Length scales must be undistorted.
2. Froude's Law is required for velocity modeling. (If water is used in both model and prototype, pressure gradients will thus be the same.)
3. Ratio of bubble velocities relative to water in a particular pressure gradient must be same as the velocity ratio by Froude's Law.

To satisfy the third condition, Boughton suggests using kerosene drops. These criteria will give a proper indication of the motion of bubbles once formed, but they still do not help solve the problem of how much air will be entrained, and what the bubble sizes will be. This model investigation followed (1) and (2) above, but no attempt was made to follow (3).

Scaling factors for air entrainment concentrations may best be determined from comparisons of model and prototype performance on completed structures of a similar nature. The closest such example found in the literature is the morning glory spillway for Heart Butte Dam (Peterka, 1954, 1956). When the total drop in water level through Heart Butte Dam was about 70 feet at the near-maximum observed flow of 3600 cfs, the air demand in the prototype was 7.7 per cent of the discharge (by volume), whereas in the 21.5 : 1 scale model at U.S. Bureau of Reclamation

it was only 1.9 per cent. At a lower flow of 1000 cfs, the prototype and model values were respectively 20.5 and 5.5 per cent. Thus at both flows the prototype entrained about four times as much air as the model, on a percentage by volume basis.

Another prototype-model comparison of air entrainment has been presented by F. B. Campbell and B. Guyton (1953) and reproduced by U. S. Corps of Engineers (1961) in Hydraulic Design Criteria. They measured air demand behind partially open gates in outlet tunnels from dams and compared the results with laboratory air entrainment by a hydraulic jump in a 6-inch pipe measured by A. A. Kalinske and J. M. Robertson (1943). The air demand for the large scale structures ($Q_{air}/Q_{water}$) was found to be approximately 1 to 3 times as much as expected from the laboratory experiments, depending on the Froude number. Although these flow situations are only remotely similar to the present one, still the order of magnitude of the scaling factor (approximately 1 to 3) is of interest.

General bibliographies on air entrainment, mainly for open channel flow, may be found in O. P. Lamb (1949) and ASCE (1961).

No explicit prototype information on air entrainment in vortex-type drop structures was found in the literature. Nonetheless, J. F. Laboon (1960, 1961) has stated that the numerous drop shafts with vortex inlets built for the Pittsburgh sewerage system following Laushey's model studies (1952, 1953) have been operating satisfactorily, but no details were given.

In consideration of previous knowledge of air entrainment in models and prototypes, it was decided that it would be safe to use a scaling factor of 10 for air entrainment (expressed as the discharge ratio $Q_{air}/Q_{water}$). Hence, to meet the 1.0 per cent by volume limit set for the prototype, the model must transport air into the outfall at a rate less than 0.1 per cent (or 1000 ppm) of the flow of water.

# CHAPTER 4
# EXPERIMENTAL RESULTS

## 4.01 Description of Models

The various models that were tested can be divided into two categories. The earlier models were small preliminary models (28.5 : 1 and 27 : 1 scales) and were connected to a portable constant head tank. The final model was a larger one (18 : 1 scale) and was connected to the permanent constant head tank in the laboratory. They were all assembled from various components made of marine plywood, lucite, and sheet metal by skilled mechanics to tolerances of $\pm \frac{1}{32}$ inch. Elevations of the key points of the large model were set with the aid of a surveyor's level to nearest 0.005 ft.

Models on which tests were made are listed in Table 3, and the details of each vortex tube, the essential feature under study, are shown on Fig. 11 (see Fig. 1 for overall system). Photographs of various model setups and flow conditions make up Figs. 2, 13-24, and 27-32 (see list in Table 3); for the best overall view of a small model, see Fig. 17 and for the large model, see Fig. 2. The preliminary or small models were not exact models in all details upstream and downstream of the vortex tube itself (such as the elbow geometry and stilling basin width) because their purpose was primarily to establish the principal desirable features of the vortex tube. With the experience gained in the small models, where changes could be made cheaply and quickly, it was then possible to build a successful larger model on the first trial with all details correctly reproduced. Model 5S, which was an obviously unsatisfactory solution consisting of a simple conduit following the ground profile, was built only as a demonstration and basis for comparison.

Some changes between successive models were due to adjustments in requirements of the design engineers, namely, raising the centerline of the outfall and adding a straight section above the elbow for guidance of the cleaning device (see 3S and 4S in Fig. 11). Other changes were made by

TABLE 3

MODELS TESTED

| Model Number * | Scale | Drawings in Figs. | Photos in Figs. | No. of Flow Conditions for Which Air Entrainment Was Measured | Remarks |
|---|---|---|---|---|---|
| Preliminary | | | | | |
| SDDS-1S | 28.5:1 | 11,41 | – | 4 each | e,f,g |
| SDDS-1SI | 28.5:1 | 11,42 | 13 | 13 each | a,e,f,g |
| SDDS-2S | 28.5:1 | 11,43 | 14 | 17 | f,g |
| SDDS-3S | 28.5:1 | 11,44 | 15 | 27 | f,g |
| SDDS-3SI | 28.5:1 | 11,45 | – | 9 | a,f,g, |
| SDDS-4S | 28.5:1 | 11,46 | 16 | 14 | f,g |
| SDDS-5S | 27:1 | 47 | 19 | 12 | c,e,g |
| SDDS-6S | 28.5:1 | 11,48 | 17,18a,c | 12 | f,g |
| SDDS-6SM | 28.5:1 | 11,49 | 18b,d | 17 each | b,e,f,g |
| Final | | | | | |
| SDDS-1L | 18:1 | 1,11,50 | 2,20,21,22,23 | 20 | – |
| SDDS-1LM-1 | 18:1 | 1,11 | 2,20,21,22 | 0 | b |
| SDDS-1LM-2 | 18:1 | 1,11 | 2,20,21,22, | 0 | b |
| SDDS-1LM-3 | 18:1 | 1,11,12,51 | 2,20,21,22 23,24,27-32 | 25 | b,d |

a - added insert in vortex tube inlet

b - change in vortex tube inlet only

c - no vortex or hydraulic jump, simple pipe only

d - recommended for final design

e - air entrainment measurements made with open 1/2-in. vent (model) on top of outfall pipe at prototype Sta. 1+98

f - air entrainment measurements made with no vent or closed vent

g - 7-ft branch pipe not modeled

* All models have the same first part to their designation - namely, SDDS, which stands for San Diego Drop Structure. This designation is followed by a dash and then a number, and at least one letter. The number (1 through 6) indicates the chronological order of the model and the letter (S or L) indicates whether the model is small or large. Thus, SDDS-4S means that this model was the fourth small model to be built. A further designation of I (for insert) or M (for modified) is used to differentiate a slightly modified later version of a model from the original model.

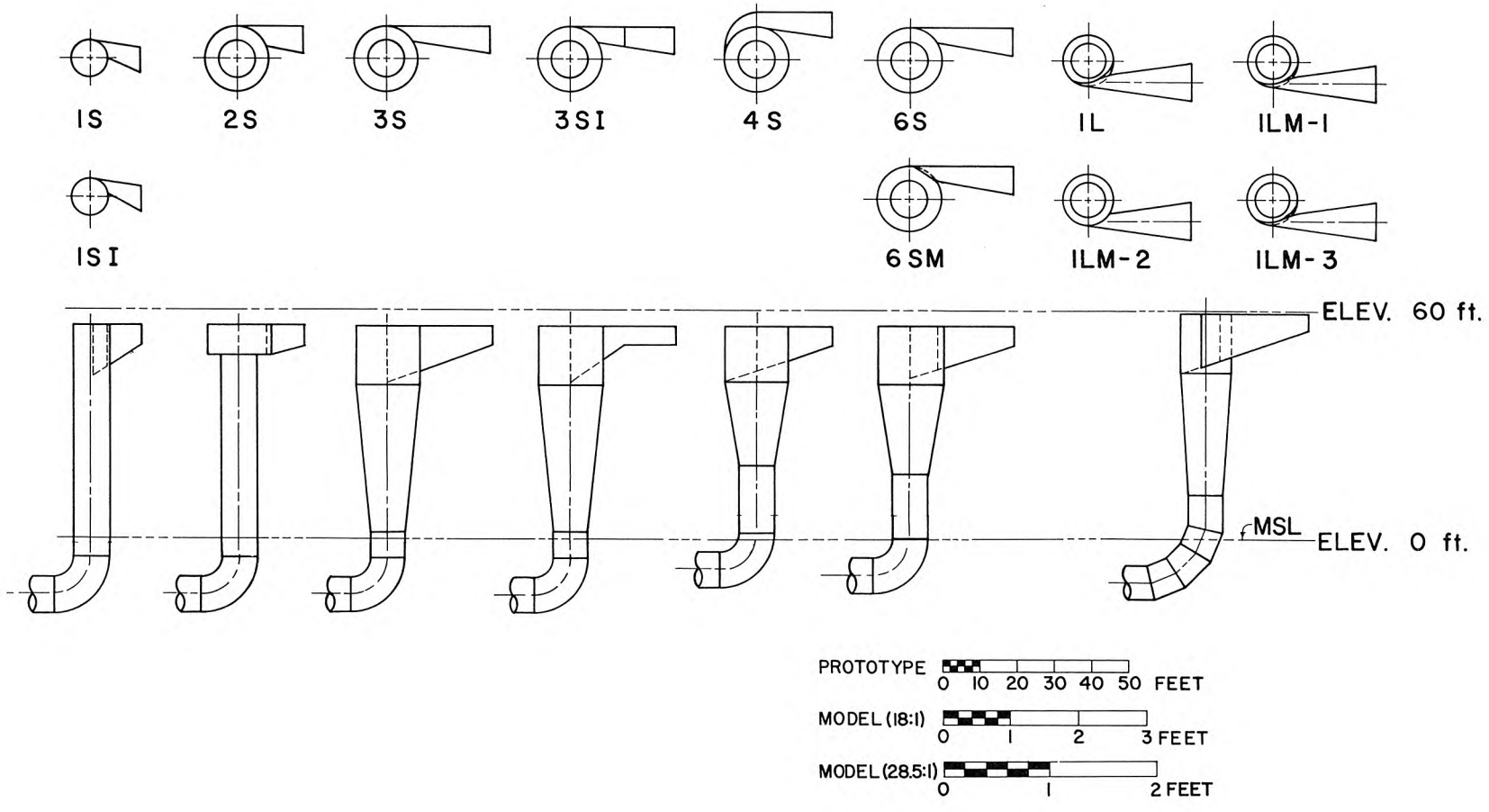


Fig. 11. Vortex tubes and inlets tested. Final design is based on 1LM-3.

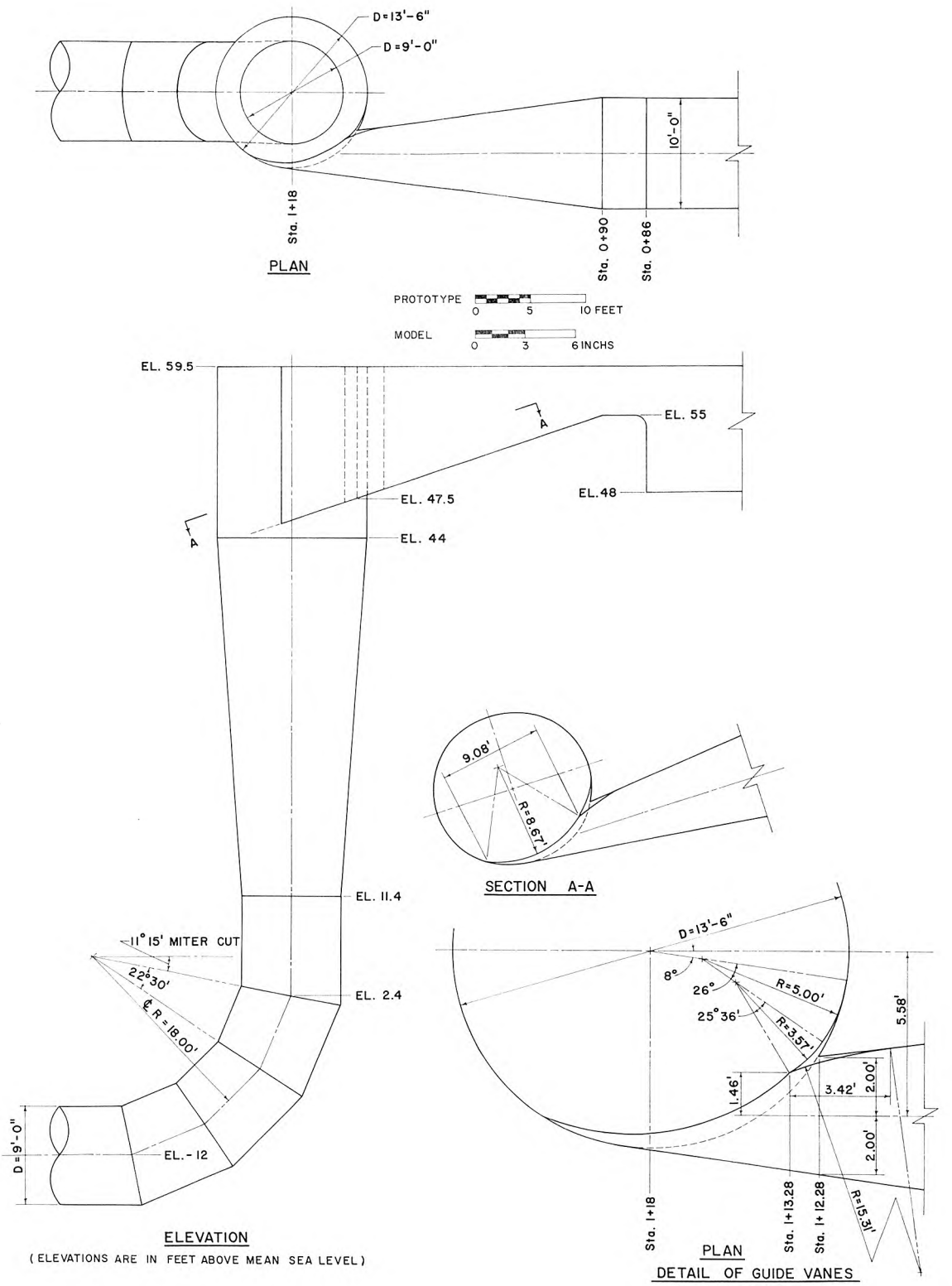


Fig. 12. Details of vortex tube and guide vanes for 1LM-3.

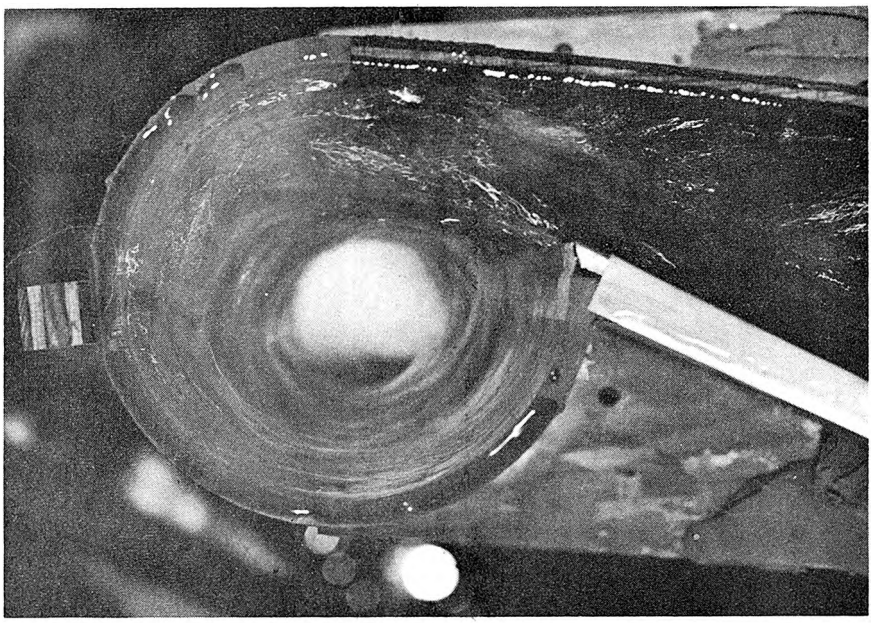

a) Top view. Flow was improved by making inlet symmetrical in Model 1L. $Q_p$ = 612 cfs, TW = 49.5 ft.

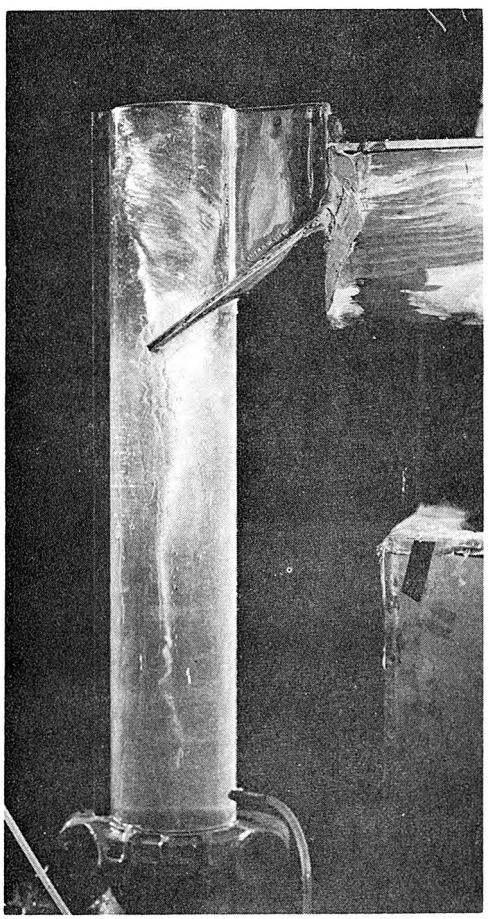

b) Elevation. Flow was improved by tapering vortex tube in later models. $Q_p$ = 612 cfs, TW = 49.5 ft.

Fig. 13. Model 1SI, vortex tube only. See Fig. 17 for full layout of apparatus.

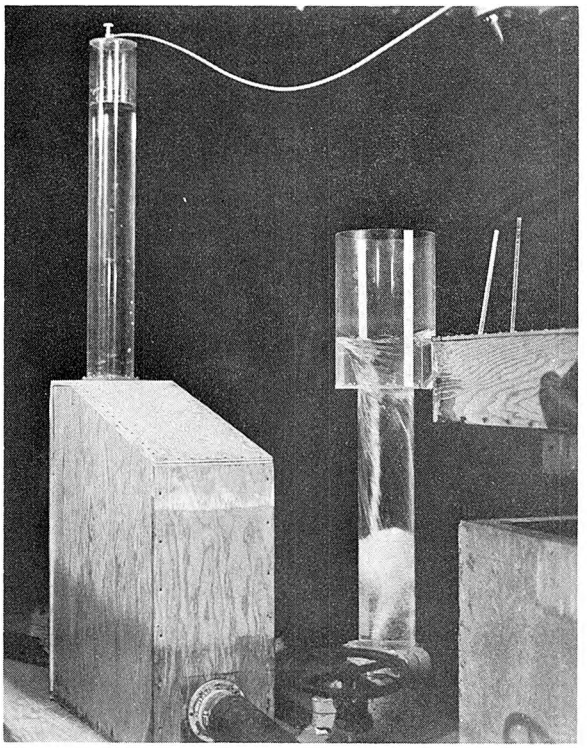

a) $Q_p$ = 350 cfs, TW = 20 ft.

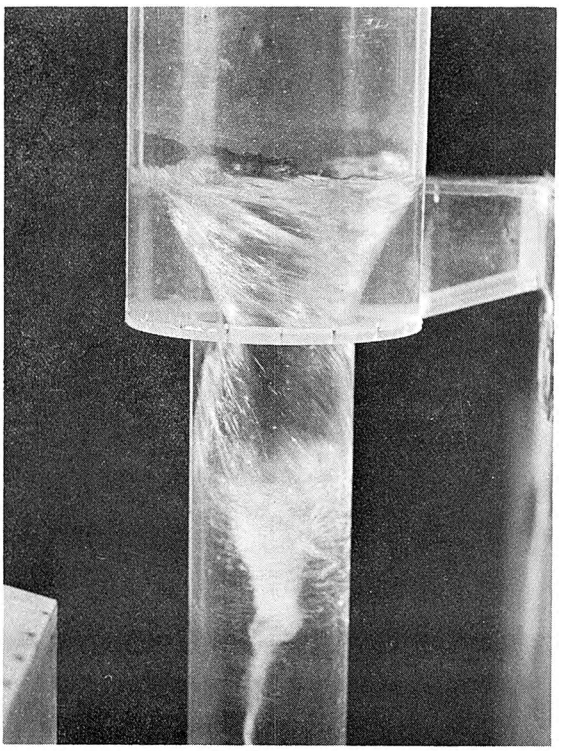

b) $Q_p$ = 350 cfs, TW = 40 ft.

Fig. 14. Model 2S. This model had insufficient discharge capacity due to sharp-edged inlet to vortex tube.

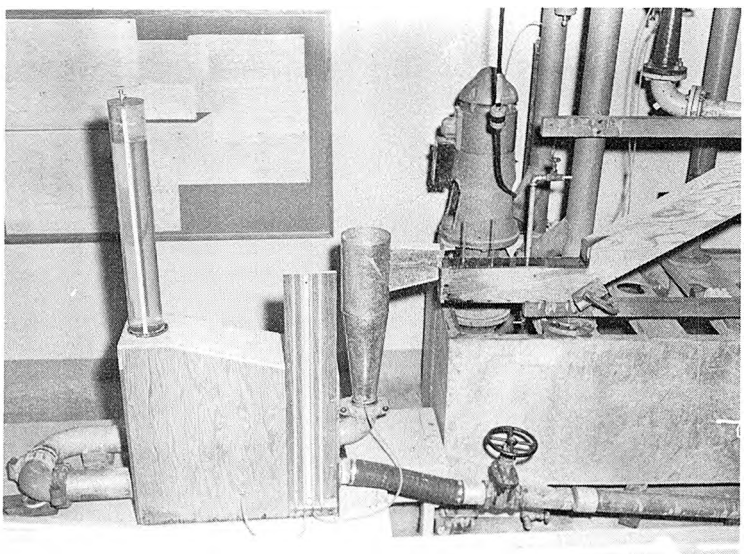

Fig. 15. Model 3S. This model showed that tapered vortex tube produced a good vortex without restricting flow capacity as did Model 2S.

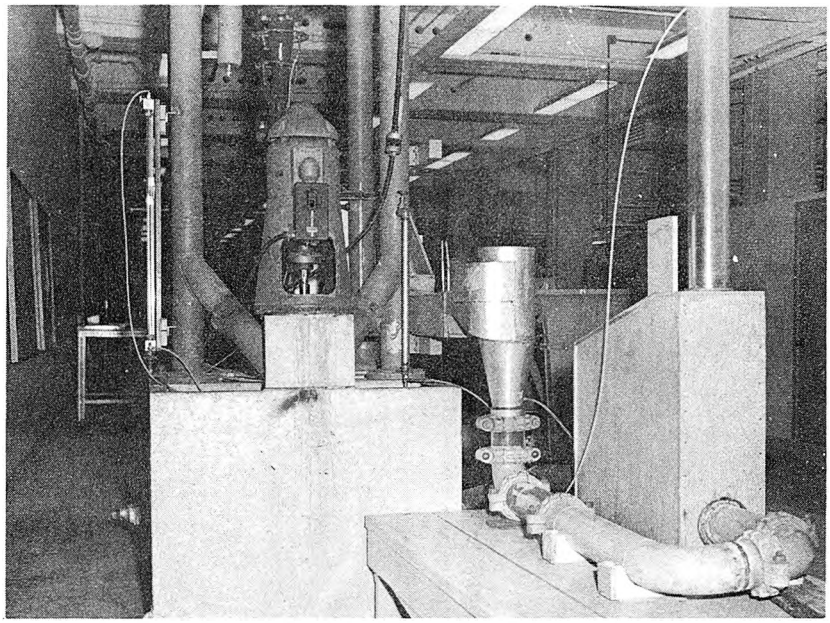

Fig. 16. Model 4S. Scroll case inlet was unsatisfactory because of surface waves. Pump is below motor, and manometer (far left) is for venturi meter (behind motor).

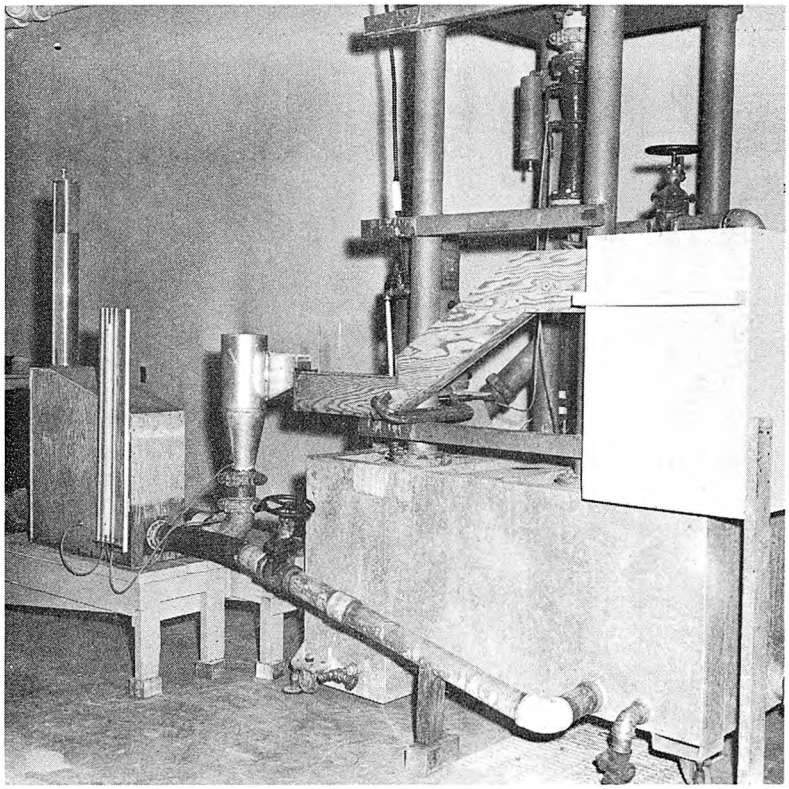

Fig. 17. Model 6S, showing also general arrangement of apparatus for all small models. Small constant head tank is only partially in view at top. Final vortex tube (Model 1L) was similar to this one, but with less taper.

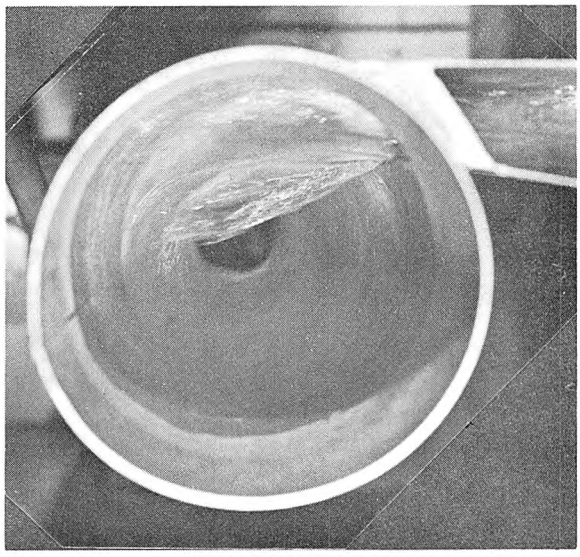

a) $Q_p$ = 450 cfs, TW = 21 ft.

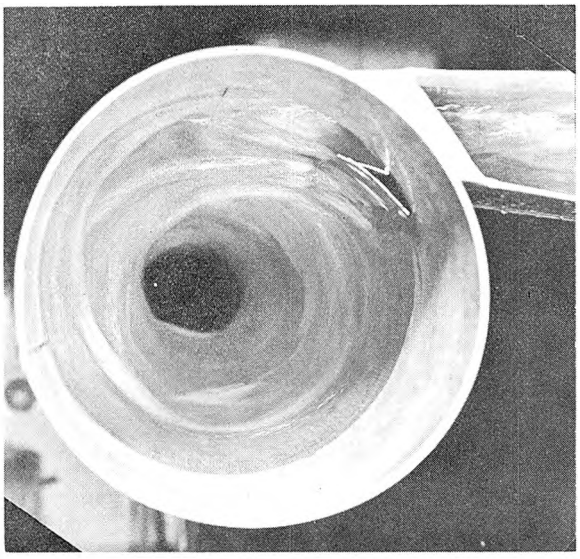

b) $Q_p$ = 450 cfs, TW = 21 ft.

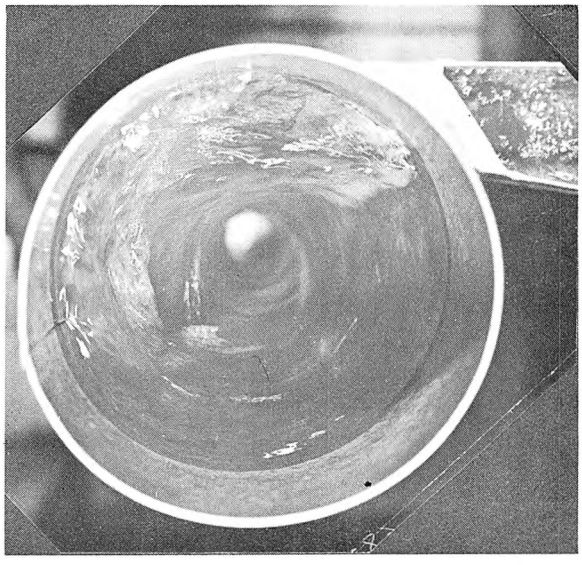

c) $Q_p$ = 612 cfs, TW = 42 ft.

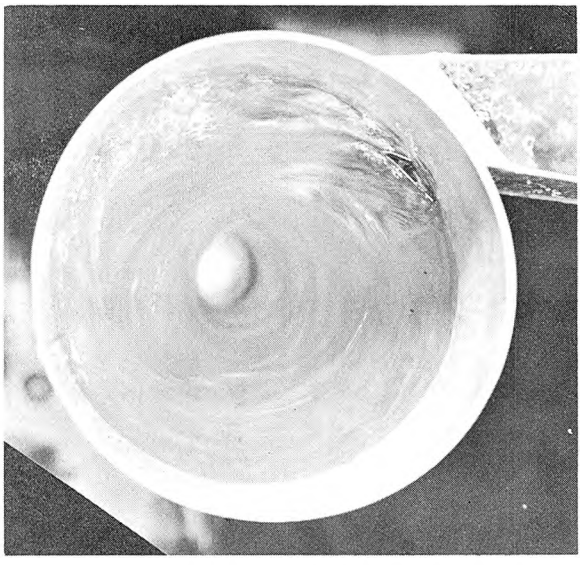

d) $Q_p$ = 612 cfs, TW = 36 ft.

Fig. 18. Comparative top views of 6S (a, c) and 6SM (b, d) showing improvement in vortex flow due to guide vanes at inlet at two flow conditions. For higher tailwater (as in c and d) the change is less pronounced than cases of lower tailwater.

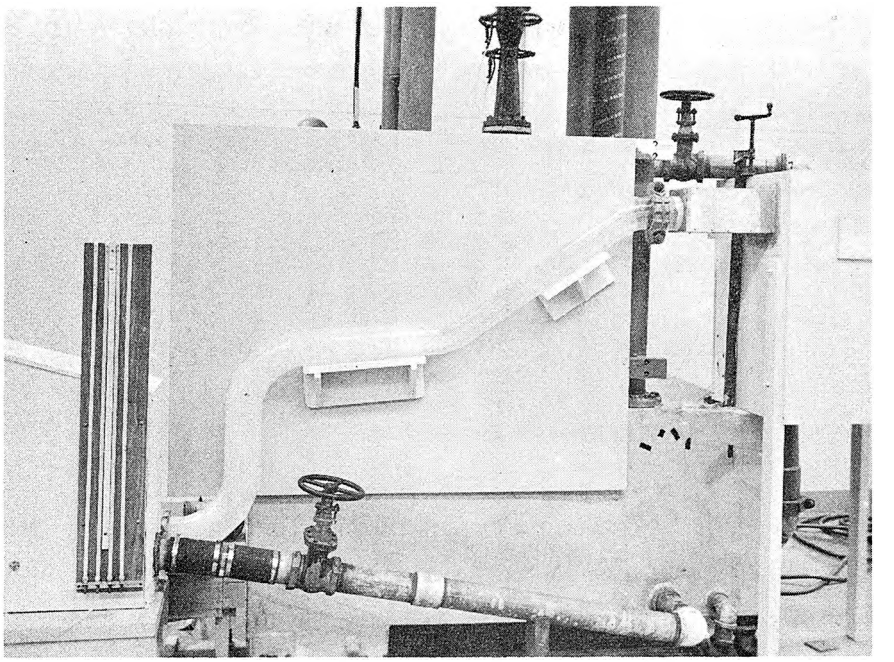

a) Overall view. (Not shown is horizontal portion of ocean outfall and return loop hidden behind air collector at extreme left.)

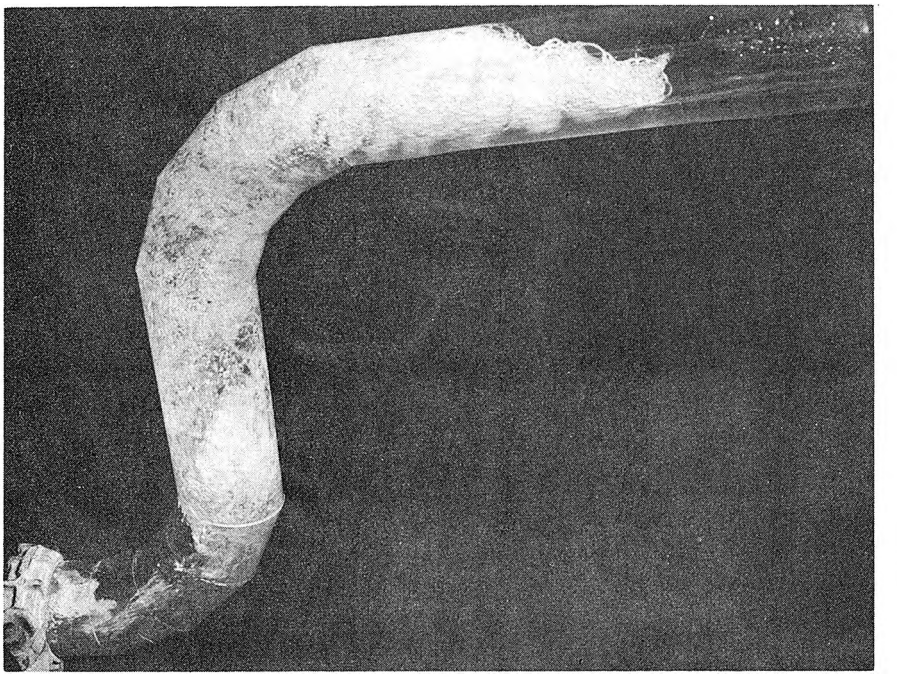

b) Closeup of vertical drop. Note large air bubble about to rise from elbow. $Q_p$ = 612 cfs, TW = 37 ft.

Fig. 19. Model 5S, a simple pipeline following contour of ground. Not recommended because of heavy air entrainment and instability.

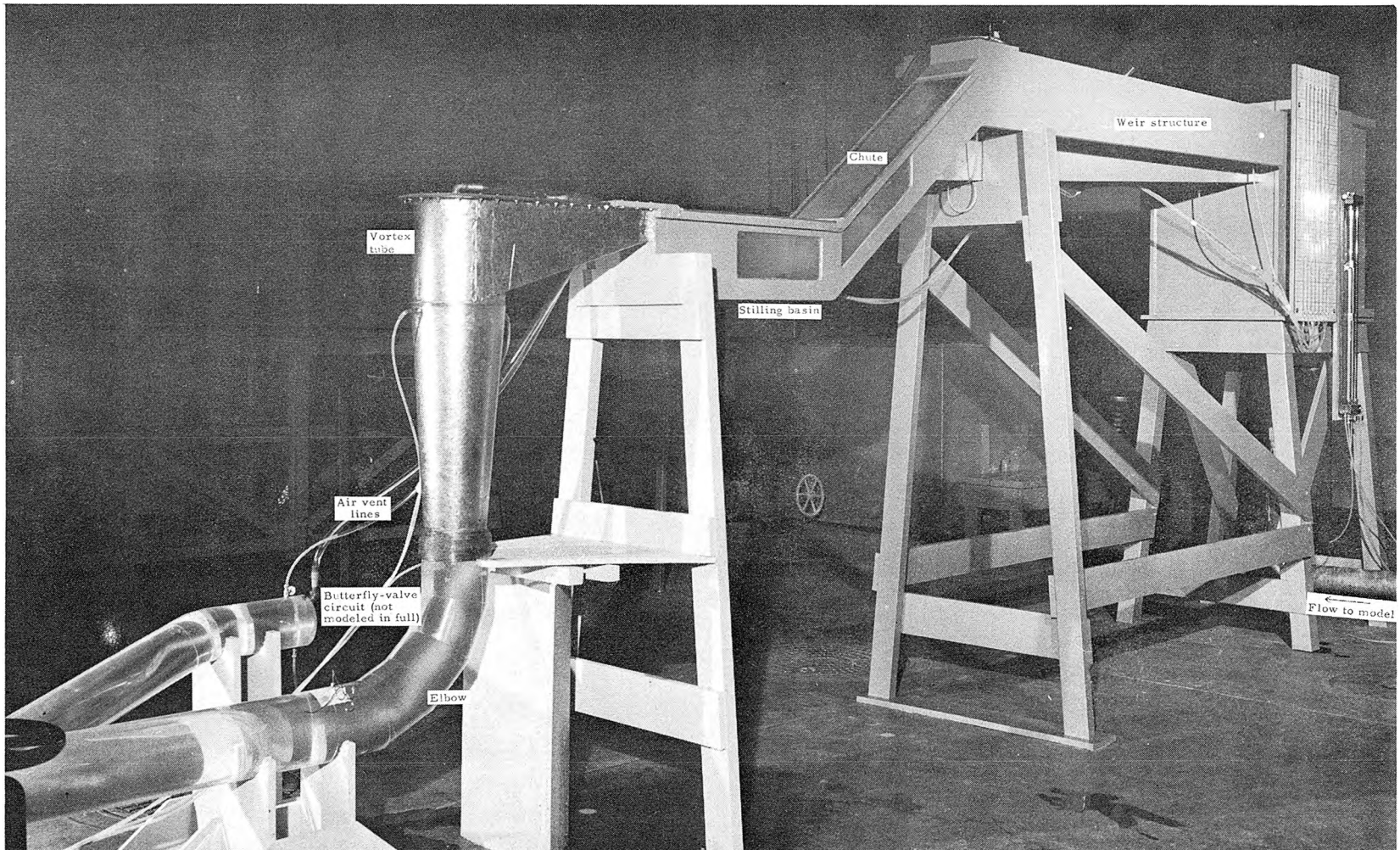


Fig. 20. View of upstream portion of hydraulic model of San Diego drop structure (Model 1L, 18 : 1 scale).

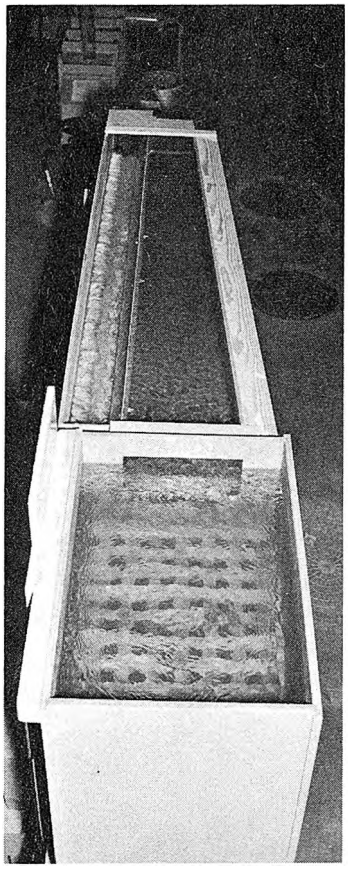

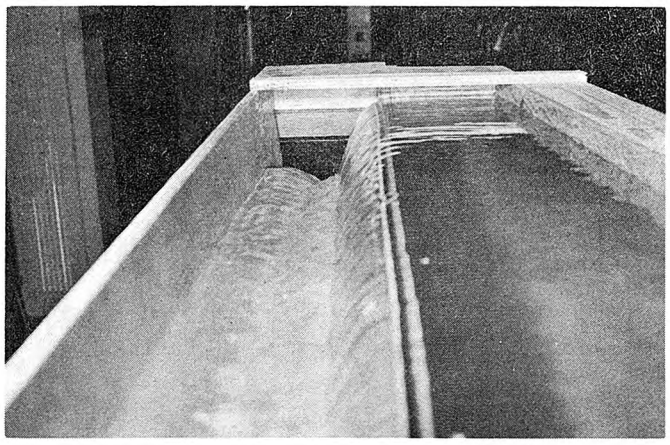

b) Part of weir and collection channel which conducts flow into chute at far end. ($Q_p$ = 612 cfs.)

a) General overhead view. ($Q_p$ = 400 cfs).

Fig. 21. Inlet box (flow up through bottom), side channel weir and collection channel.

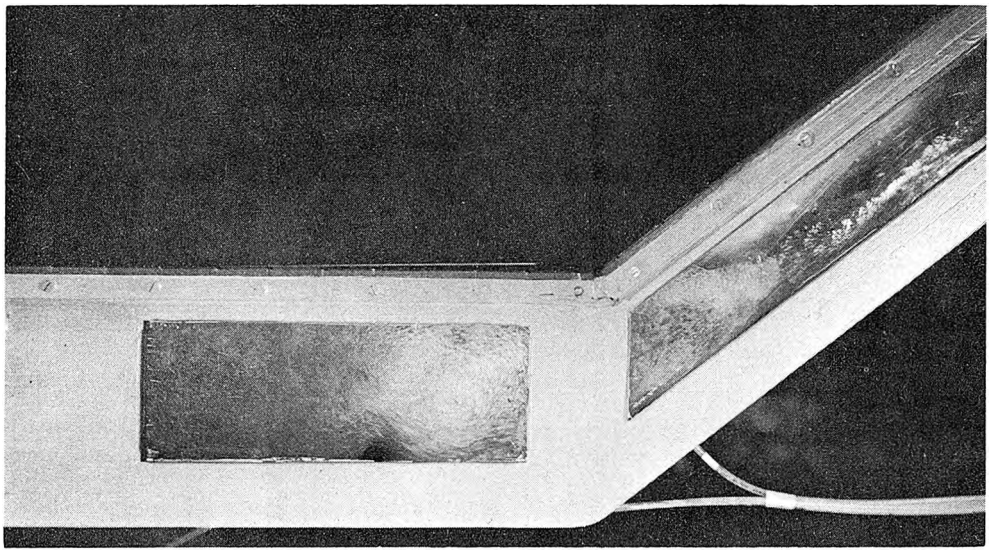

Fig. 22. Streaks of air bubbles show strong roller of hydraulic jump in forward part of stilling basin. Note baffle blocks; chute blocks at base of chute are not visible. $Q_p$ = 612 cfs, TW = 40 ft.

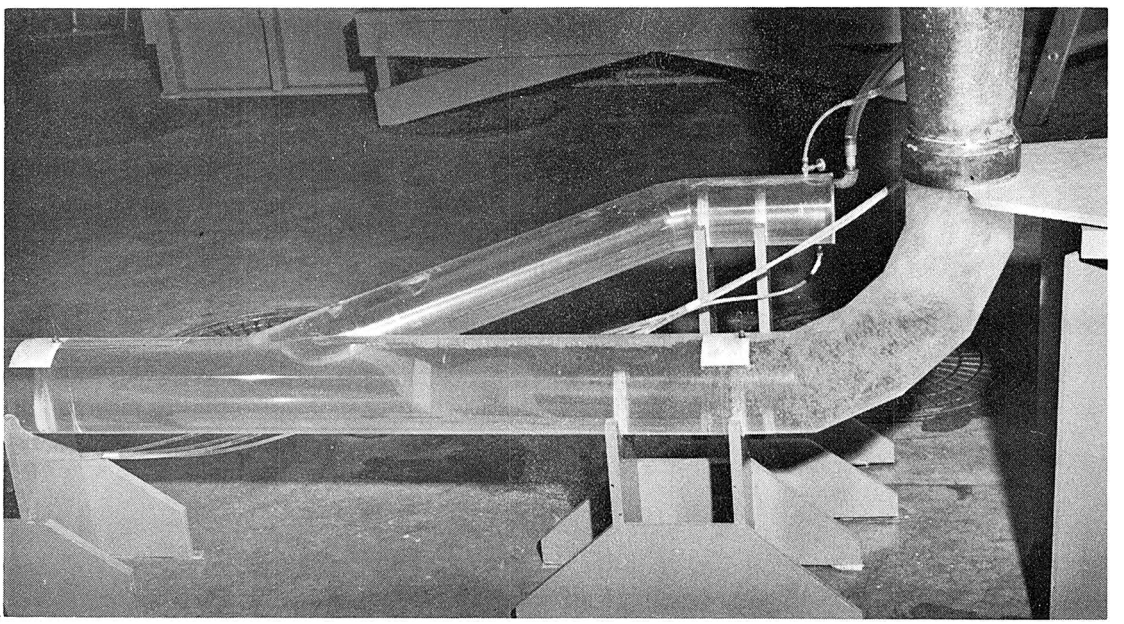

Fig. 23. For low flows air is swept down into elbow below the vortex tube, then collects on top of pipe, which is vented downstream of shut butterfly valve (latter not included in model). $Q_p$ = 100 cfs, TW = 10 ft. $Q_a/Q$ from vent = 6590 ppm.

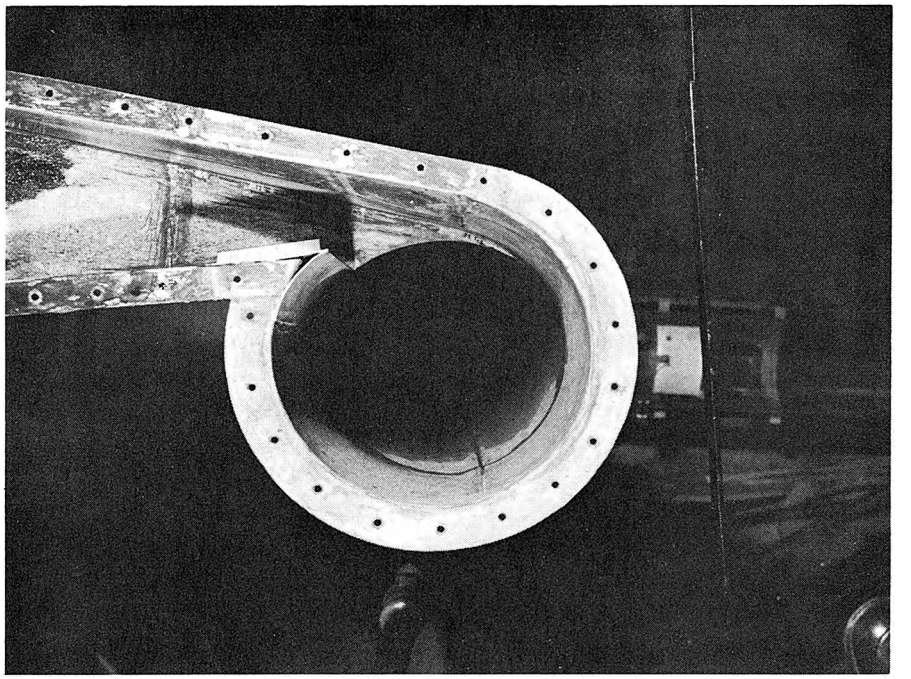

a) Top view.

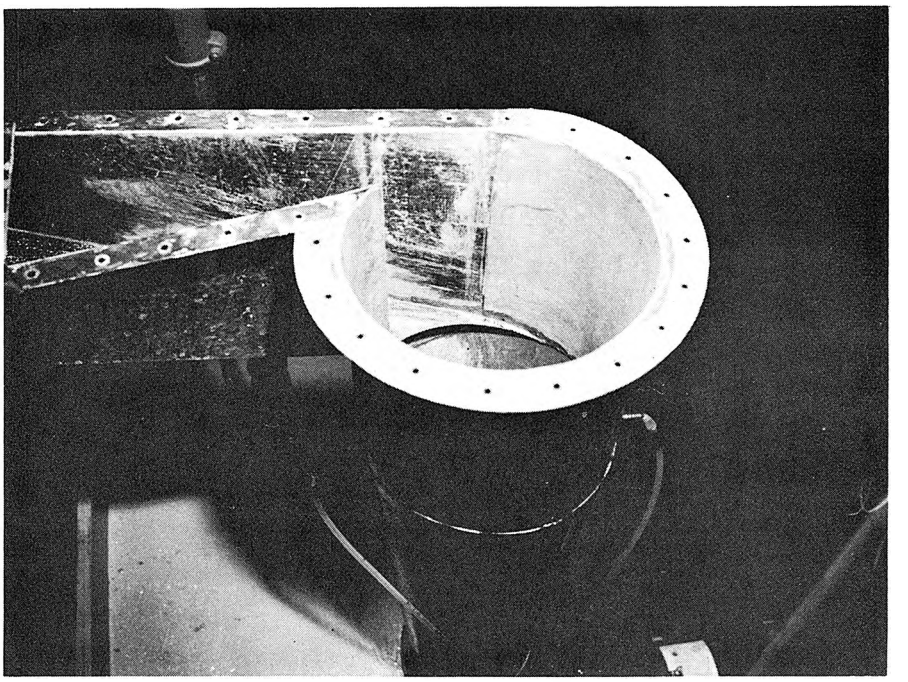

b) Oblique view.

Fig. 24. Details of vortex tube inlet. In (a) note the vertical vanes (two curved pieces) to guide the flow at the intersection of inlet channel and the vortex tube, and in (b) note the curved bottom extension to reduce interference below.

the investigators to achieve improved flow conditions between successive trials.

Dimensions of the vortex tube and inlet channel finally recommended for design are shown in Fig. 12 (for Model 1LM-3); the reader is also referred to Fig. 24 for closeup photographs showing the top of the vortex tube in the model.

Various details of the flow patterns illustrated by the photographs will be discussed under appropriate headings below. No attempt will be made to give a chronology of the evolution of the hydraulic design, inasmuch as the discussion of the salient features of the recommended design (large model) reveals the shortcomings of the various preliminary designs (small models).

In the figures and discussion which follows, the discharge is always given in prototype values ($Q_p$) and the downstream head in prototype feet above mean sea level (TW for tailwater).

## 4.02 Testing Procedure

Operation of the model simply required the setting of two valves: one upstream of the model for regulation of the discharge and one downstream for regulation of tailwater head (abscissa and ordinate respectively of Fig. 5). Most tests were conducted at valve settings representing possible ultimate prototype operating conditions, as shown in Fig. 5.

Data recorded for various models included: (a) discharge (by venturi meter); (b) downstream head (or tailwater, TW) by piezometers; (c) visual observations of flow configuration, especially in the vortex tube and pipe downstream; (d) rate of air entrainment into outfall pipe; (e) piezometric heads at various points; (f) strength of rotation in horizontal outfall pipe, as indicated by direction of dye streaks injected near the wall. All were by routine procedures except for air entrainment described below.

The discharge of entrained air was measured volumetrically in a transparent vertical column mounted on top of an air collector box (see Figs. 1 and 17). Backflow of air was prevented by having the outlet of

the model piping (below the downstream valve) completely submerged. The two air collector boxes used were essentially settling tanks where bubbles rose to the top and were funneled into the column or stack. The tank overflow rates* were 0.083 and 0.054 fps respectively for the small and large models. Thus, for example air bubbles with a rate of rise of 0.054 fps would ideally all be trapped in the air collector for the large model; because of an inlet baffle and favorable length-to-height ratio, the efficiency of the large air collector was believed to be very good. Hence, the smallest diameter of bubbles expected to be practically all removed is 0.1 mm, corresponding to a rise velocity of 0.054 fps, according to W. L. Haberman and R. K. Morton (1956).

At the beginning of the run the water surface in the air measuring column was raised to near the top (above the hydraulic gradeline) by an aspirator which evacuated the air. Air which was carried down the model outfall became trapped in the column and displaced the water; from the observed drop in the water level in the column in a measured time interval, the air discharge was easily computed. Observations were always repeated several times to ensure that steady conditions and representative time averages of the entrainment rate were determined for each flow setting.

Theoretically, a slight negative correction in air volumes and discharges should have been made because volumes were measured at pressures up to 3 feet of water below atmosphere; for adiabatic expansion of rising air bubbles, the correction would be -6 per cent at most, or for isothermal conditions -9 per cent. However, this correction was not made because of comparable errors probably still present, namely less than 100 per cent efficiency of air-trapping and uncertainties about model-prototype relations. Air going into solution in the model, a further source of error, was believed negligible because vigorous agitation in the main reservoir by overflow from the constant head tank undoubtedly kept the model flow fully saturated with air.

The measurement of the tailwater in the model presented minor

---

* Overflow rate = maximum discharge/plan area

problems because the hydraulic head in the pipe downstream from the elbow was not uniform owing to the residual swirling motion; the result was that the head at the wall was higher than at the center. To overcome this problem, the tailwater in the small models was taken as the piezometric head in the air collector plus a small correction based on a computed normal pipe friction loss back to the elbow below the vortex tube. In the large model, the tailwater was taken as the piezometric head at the wall at prototype Sta. 3+70 (in model 14.0 ft downstream of centerline of vortex tube, prototype Sta. 1+18). Hence, the tailwater head may not be considered more accurate than a few feet at high flows because the definition itself is blurred by the propagation of swirling motion for long distances downstream from the vortex tube. Also, no adjustments were made for the difference between hydraulic grade line and energy grade line (1.4 feet at maximum flow, 612 cfs).

## 4.03 Characteristics of Flow

4.03.1 Stilling basin. The stilling basin, although rather short and closed on top, produced a satisfactory hydraulic jump at all flow conditions. The baffle blocks produced a strong roller, as shown in Fig. 22, and gave stability. In the final model (1L), for observed flows of less than 290 cfs (prot.), the flow did not seal at the top of the basin, leaving an air space connecting the vortex tube to the chute; but for flows of 290 cfs or more, the basin was sealed, due to the backwater from the sill at the downstream end of the basin. (One-dimensional analysis, assuming critical depth over the sill, predicts sealing at 305 cfs; the actual value is somewhat less, due to boundary layer effects.)

Under the sealed condition at the soffit of the stilling basin, air bubbles collecting there were swept downstream into the top of the vortex tube for escape through the open vent at the top of the vortex tube; on the other hand, some air was swept back upstream by the roller when it collected upstream of the stagnation point at the soffit. Should the vent on the vortex tube be closed, there would be a dangerous accumulation of air in the vortex tube, gradually increasing in pressure and depressing the water level in the vortex tube. Ultimately, the accumulated air would blow back, or at least cause an

increase in entrainment into the outfall to balance the flux from the hydraulic jump. Quantitative data on air release are presented in Sec. 4.04.

As long as the sill remained the hydraulic control, the maximum piezometric head at the downstream end of the stilling basin (measured at bottom) was only 62 feet MSL or a surcharge of only 2.5 feet at the maximum flow of 612 cfs. But when the tailwater rose to high levels at high flows (e.g., above 40 feet for 612 cfs), the end sill ceased to be the hydraulic control for the flow in the stilling basin. The jump was progressively backed up the chute to the top, as the downstream head increased to its highest possible level.

4.03.2 Inlet channel to the vortex tube. The small scale models quickly showed how sensitive the flow in the vortex tube is to the geometry of the inlet transition. The evolution of the design is clearly indicated in Fig. 11. The transition design had to meet the following restrictions:

1. Surface waves should not be generated in the transition as they disturb vortex flow.
2. The hydraulic control must always be at the sill and not in the transition.
3. For economy of construction, the shortest possible length was preferred.
4. For maximizing the strength of the swirl, the flow should enter the vortex tube with streamlines nearly perpendicular to the axis of the vortex tube, rather than dipping down steeply.

To satisfy restriction (1), the plan was made symmetrical (as in 1L) with respect to the centerline of the stilling basin in order to make two equal angles (8°2') in the side walls rather than having a discontinuity of double the angle on one side only (as in other models). Because of critical flow in the channel at these angle points, oblique surface waves are generated, with height increasing with angle of discontinuity. Waves in final design were very small and the flow appeared satisfactorily smooth and regular (see Figs. 27-30).

The scroll case attempted in model 4S (see Figs. 11 and 16) was poor because of the large free surface waves generated in the scroll. A straight tangential entrance gave less disturbed flow in the vortex tube.

Backwater was avoided by allowing the cross-sectional area of the transition to be approximately equal at the two ends for the same water level at peak flow. At the inlet end, which is essentially over the broad-crested sill (elevation 55.0 feet MSL), the critical depth is 4.88 ft (for 612 cfs), but the flow depth is limited to 4.50 ft by the soffit at 59.50 ft MSL, yielding a cross-sectional area of 45.0 $ft^2$. At the downstream end the area for the same elevation at the tip of the guide vane is (59.5'-47.16') x 3.33'width = 41.1 $ft^2$, or only about 9 per cent less than at the sill. Nevertheless, it was observed that the sill remains the control until flooded by the vortex itself at high tailwater.

The tank type of inlet (such as used by Laushey, 1952, and others) was tried in Model 2S but found unacceptable because of grossly inadequate flow capacity and accompanying backwater into the stilling basin.

A reasonable compromise between restrictions on overall length and angle of invert of the transition was obtained with an angle of 18°36' resulting from a chosen length of 28 feet from the beginning of the transition to the centerline of the vortex tube.

4.03.3 Guide vanes* at end of inlet channel. The exact detail of the end of the transition channel where it discharges into the vortex tube has a significant effect on the smoothness of the vortex flow. Two details are important: (a) two vertical guide vanes for the blending of the entering flow with the vortex flow at the inside wall intersection, and (b) an extension of the invert of the inlet channel to make a smoother spiral for low tailwater levels. These vanes are detailed for final design in Fig. 12 and are illustrated in Fig. 24.

Fig. 18 for Models 6S and 6SM gives a clear indication of the flow improvement due to a simple bending and extension of the walls of the

---

* Called "insert" in laboratory notes.

circular tube and of the inlet channel to termination in a nearly tangential intersection, producing a sharp trailing edge. (Models were built with hand-worked sheet metal inserts.) The final configuration shown in Fig. 12 resulted from a number of qualitative trials of various shaped insert pieces. A further benefit of the curved guide vane was a final flip of the flow toward the outside wall of the vortex tube ensuring that the flow adheres to the cylinder walls even for low flow-low tailwater conditions (see Fig. 30).

The other vane, extending the channel floor, was crescent-shaped and prevented the flow near the outside lower corner of the inlet channel from dropping suddenly down, due to its low velocity and increased pressure of the main stream above, as it starts the turn in the vortex tube. If this downward squirt were not controlled, there would be a significant splash disturbance where it would hit the main flow on the second turn on the downward spiral at low tailwater levels. By trial and error and visual observation the inclined crescent-shaped extension (or guide vane) was developed.

Disturbances could by no means be completely eliminated because different remedies are required for the widely different flow conditions. The proposed solutions correct the worst difficulties, and remaining disturbances at some particular conditions are unavoidable but believed tolerable.

4.03.4 Types of flow in vortex tube. Because of the wide range of discharges and downstream heads, there is a variety of flow conditions in the vortex tube. These may be approximately classified, as shown schematically in Fig. 25, into types which occur as a function of discharge and tailwater as shown in Fig. 26, and are illustrated by typical photographs for the final model (1LM-3) in Figs. 27-30. The types are as follows:

Type A: The vortex flow is developed up to a high level in the vortex tube, so there is no free fall into a foam pool. The air core extends down to a considerable depth, sometimes nearly to the elbow. Due to the entry of flow on one side, the air core is usually displaced slightly off-center away from the inlet. Flows in

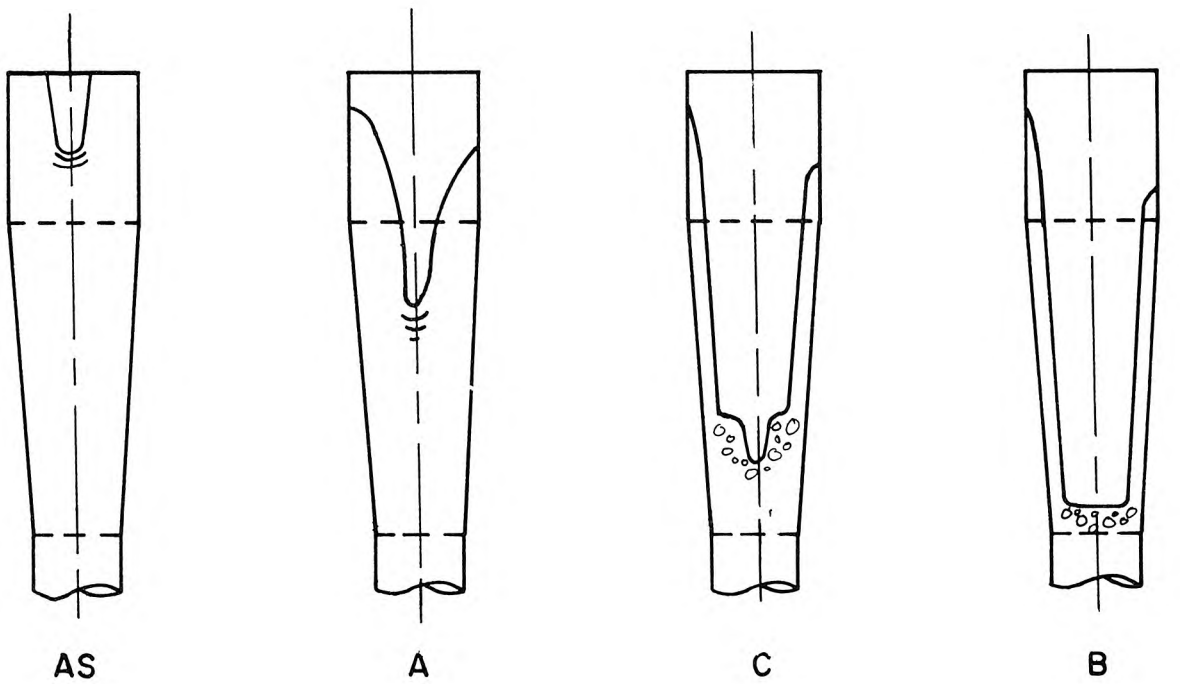


Fig. 25. Classification of flow regimes in vortex tube: AS, fully developed vortex, partially sealed against top; A, fully developed vortex; C, intermediate case with spiral flow against wall jumping into full vortex; B, spiral flow against wall plunging into pool.

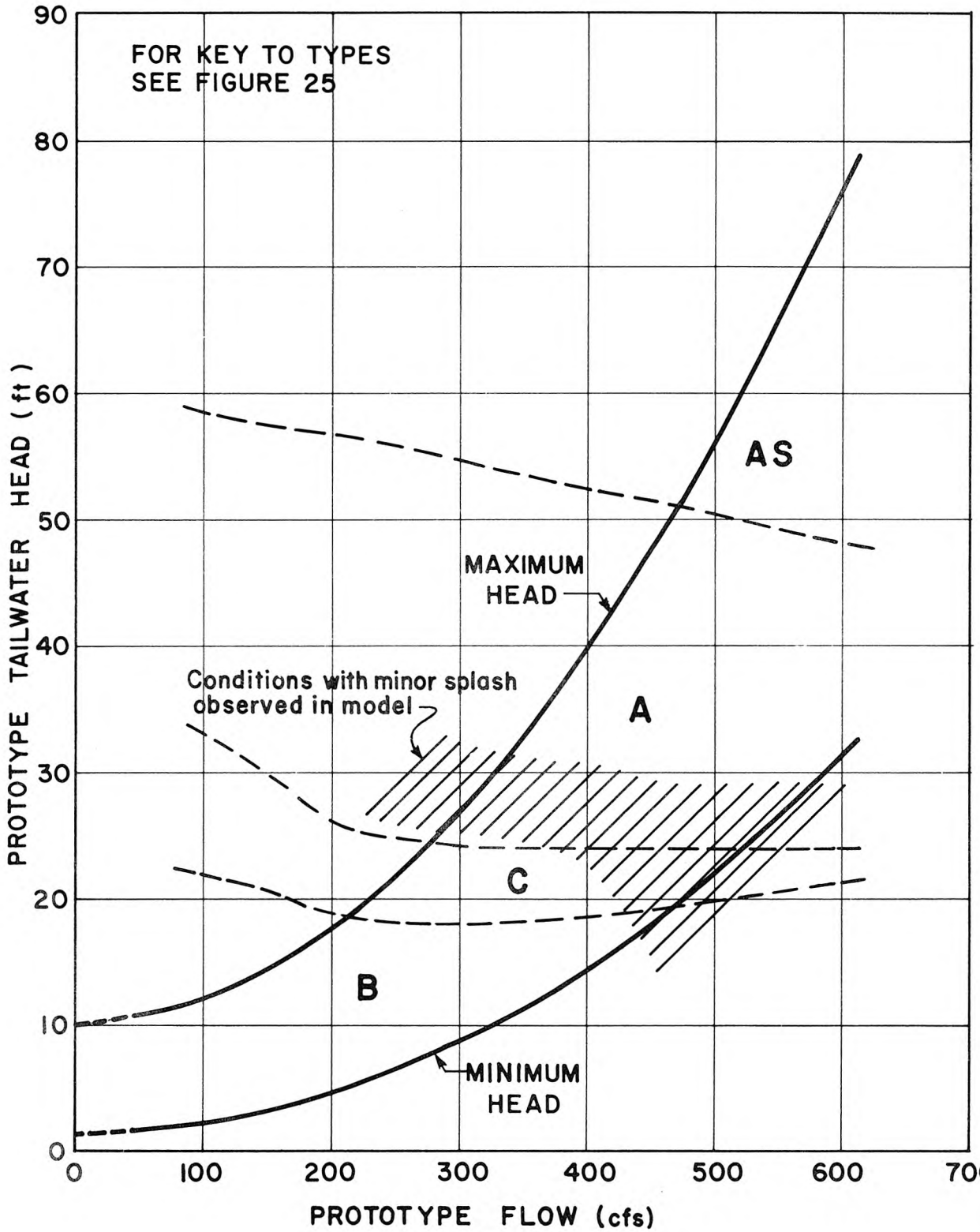


Fig. 26. Flow types in vortex tube drop structure as function of flow condition.

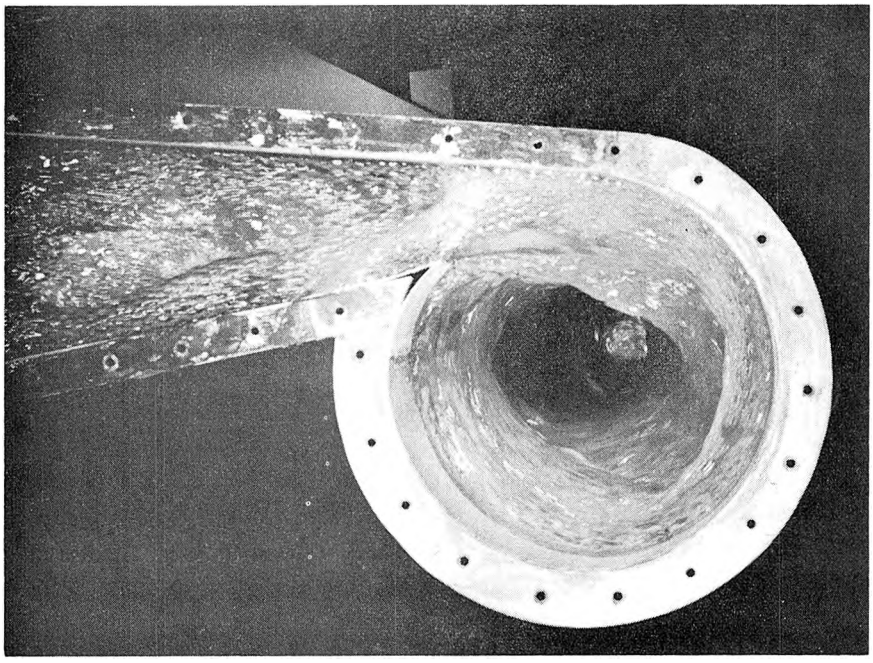

a) $Q_p$ = 612 cfs, TW = 37 ft.

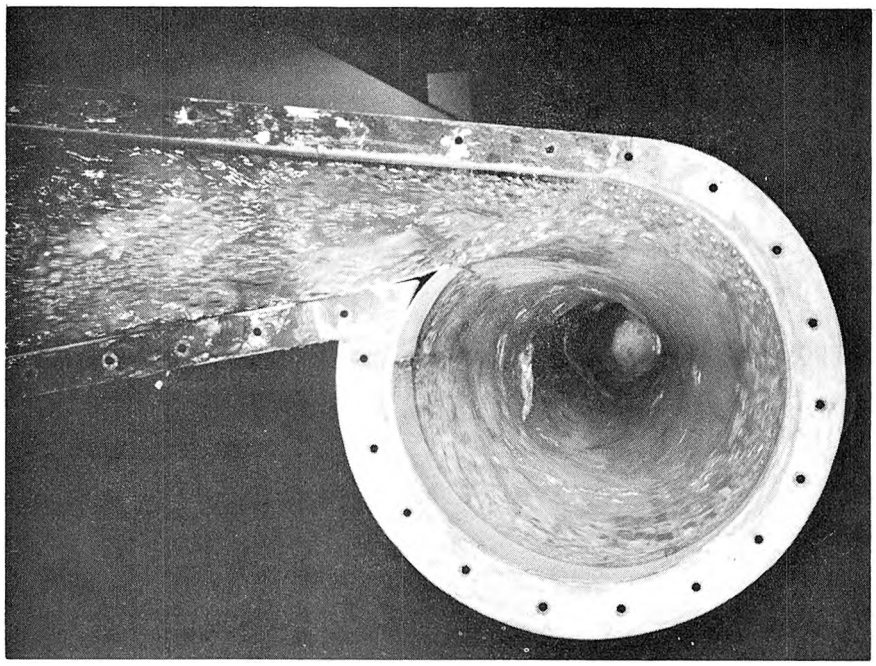

b) $Q_p$ = 500 cfs, TW = 40 ft.

Fig. 27. Type A flow in vortex tube: one large continuous vortex with relatively smooth flow throughout.

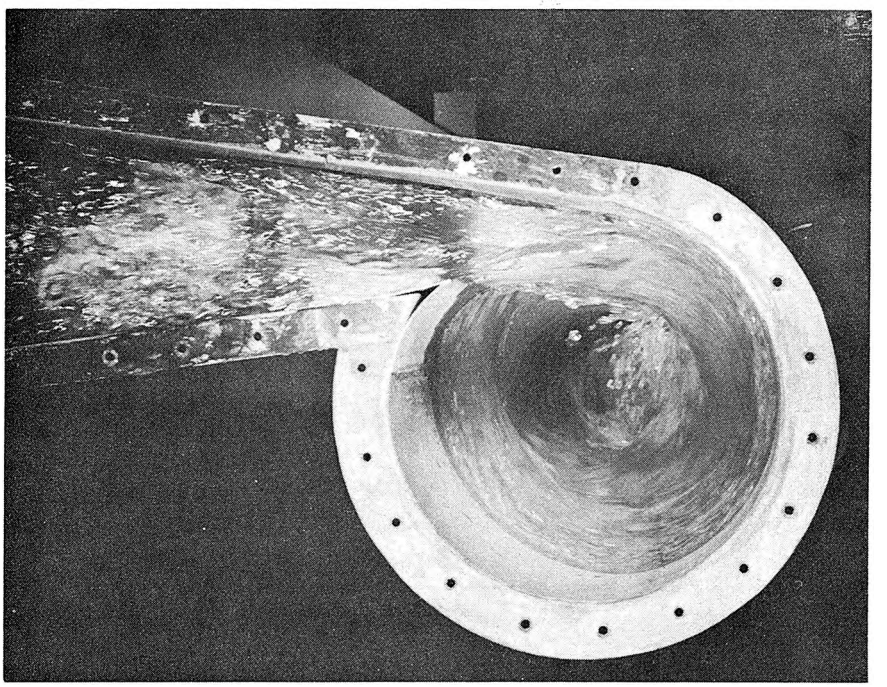

a) Top view.

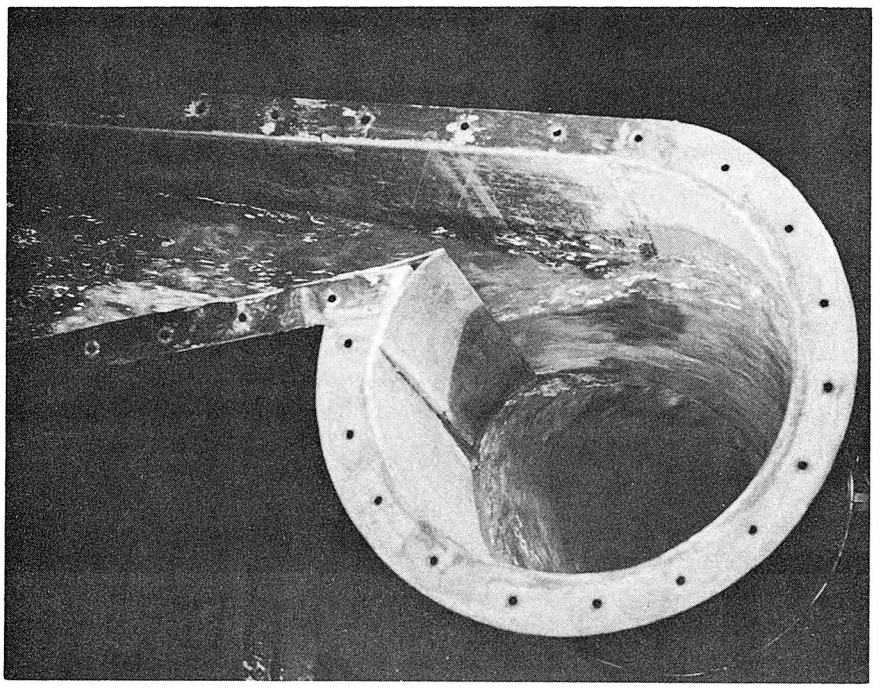

b) Oblique view.

Fig. 28. Type A flow in vortex tube near transition. $Q_p$ = 400 cfs, TW = 30 ft. Current of water after one revolution almost clears bottom of initial jet, but there is some observable interference which cannot be avoided at particular conditions like this one.

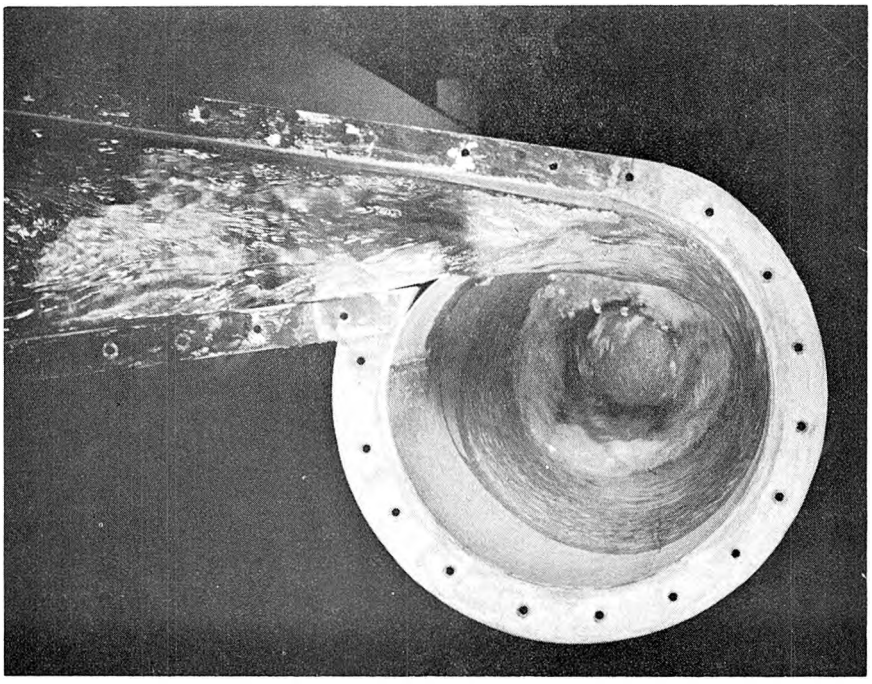

Fig. 29. Type C flow in vortex tube. $Q_p$ = 300 cfs, TW = 22 ft. "Circular" hydraulic jump forms above level where pipe becomes full.

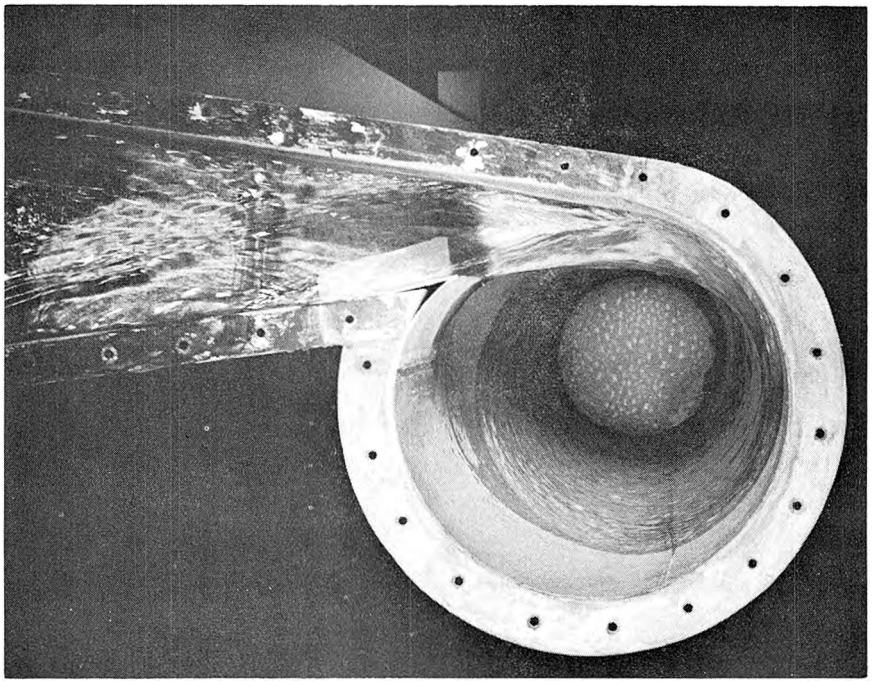

Fig. 30. Type B flow in vortex tube. $Q_p$ = 200 cfs, TW = 10 ft. Water flows down walls with plunge into pool at bottom; bubbles are caused by release of air from center.

this configuration were usually stable, and free from splash as long as the vertical inlet guide vanes were in place (see previous section). Type A is typical for the higher tailwater levels; see Fig. 27 for illustration.

As the tailwater decreases, the free surface of the flow at the wall of the tube drops progressively until the flow starting the second turn just slices under the inlet. At this point, there is some mild instability and splash, as shown in Fig. 28. This is about the lower limit of Type A flow.

Type AS: As a slight modification of Type A for the highest tailwater levels the flow partially seals against the closed top of the vortex tube (elev. 59.5 ft MSL), but with an air core persisting near the center, collecting air (if any) from the hydraulic jump and allowing it to be exhausted through the vent in the center of the cover of the vortex tube. Even at the highest tailwater level tested (73 ft at 612 cfs), a small air core remained, about 3/4 inch in diameter and 2 inches deep in the model. At the peak flow, Fig. 26 shows that the transition between Type AS and Type A is at approximately 48 ft tailwater -- i.e., when the free surface extends to the walls and no part of the top is sealed.

Type C: The flow spirals down the wall into a circular hydraulic jump. There the thickness of the flow against the wall suddenly increases, with accompanying turbulence and energy loss. The air core penetrates to a still lower level, as much as 10-12 inches (model) below the hydraulic jump (illustration Fig. 29). As shown in Fig. 26, Type C occurs only for a limited range of intermediate tailwaters between those for Types A and B.

Type B: At low tailwater conditions, the flow spirals down the wall of the vortex tube and plunges into the periphery of the pool at the bottom. Much air is entrained but is then released from the center of the pool, due to circulation in the core upward toward the surface, helping air bubbles to escape. For illustration see Fig. 30,

and for range of flow conditions see Fig. 26.

This type of flow induces the largest air entrainment because of the long fall, braked only by skin friction on the walls of the tube. For the lowest flows and tailwater heads (5 ft MSL) the fall is approximately 50 ft from the sill to the pool, giving a specific energy of 50 ft less only the dissipation. Thus, velocities of the order of 50 to 55 fps may be anticipated at the point of impact.

However, this situation occurs only at the lower flows when the pipe itself is more nearly adequate as a stilling basin and entrained air may more readily rise to the surface for escape, either in the vortex tube or from the 7-foot pipe downstream. Furthermore, the spreading of the downward current around the periphery is as favorble as possible for undisturbed escape of air because of the unobstructed "air chimney." It was very easy to see that without the spiral motion the air entrainment would have been intolerably high (see for comparison Model 5S, without swirl, pictured in Fig. 19).

Observed disturbances in the flow in the vortex tube were of two types: oscillations of the water surface, and generation of spray and splash which would fall freely in the air core. Adjustment of the entrance guide vanes (as previously described) reduced disturbances to satisfactory proportions but did not completely eliminate them. In the final model 1LM-3 the vertical surge at the wall never exceeded 3/4 inch in model (1.1 foot in prototype) at about 1/2 sec period (2+ sec in prototype), a condition easily tolerated. Lateral oscillation of the air core was negligible, but there were small waves (of no consequence) spiralling down the air-water interface in the core.

Splash was usually associated with flow interference between the incoming flow and the flow beginning the second turn on the helix, as illustrated in Fig. 28 for Q = 400 cfs, TW = 30 ft. Although the drops which break away may fall freely and entrain air on impact in the pool, the effect on the meaured air entrainment in the final model was nil because the observed amounts of splash were relatively small (as seen in Fig. 28, one of the worst splash cases). Nonetheless, this is a type of behavior which cannot be reliably scaled from the model to the prototype, and there is a chance that this splash

will contribute significantly to foaming and air entrainment in the prototype.

4.03.5 Flow in pipe downstream — reverse flow in core. Considerable circulation of the flow persists past the bottom of the vortex tube and into the elbow and downstream pipe (horizontal, then sloping slightly downward). Although the vortex was initially conceived simply as a means for providing a "chimney" for the escape of entrained air in the vortex tube, it was soon apparent that there were two other powerful favorable factors: (a) swirl imposed on flow in a pipe greatly increases the loss due to friction, and (b) there is a substantial core of fluid along the pipe axis which actually flows backward with respect to the mean flow for most flow conditions.

Since the swirl increases the loss in the pipe, the intensity of energy dissipation in the drop structure itself is reduced. Crude measurements of the intensity of the swirling motion in the pipe were made by measuring the angle $\phi$ between the pipe axis and a small stream of dye injected at the wall of the pipe (as in Fig. 32a). This angle was observed visually at the top of the pipe for the full range of discharge and tailwater at three stations -- just beyond the elbow (prototype Sta. 1+38), beyond 7-foot pipe junction (Sta. 2+08), and about 1 foot (model) from the end of the straight run in the model (Sta. 3+60). (The first of these points is visible in Fig. 20, and the other two in Fig. 2.) Because of fluctuations in the flow, $\phi$ could only be read to the nearest 5°. The values of $\phi$ are tabulated in Fig. 33. Although decay (such as from angle of 55° to 45°) is apparent in the 12.3-foot model length of pipe, some circular motion will undoubtedly persist for hundreds of feet in the prototype outfall pipe.

The reverse flow in the core is illustrated by the dye in the photographs of Fig. 32. The zone of reverse flow occupies approximately 1/5 of the diameter or 1/25 of the cross-sectional area, and backward axial velocities were observed by bits of paper and air bubbles to be frequently as much as 60 per cent of the mean forward velocity. Since the air bubbles collect along the eye of the vortex (see Fig. 31), due to the reverse centrifuge effect, the backward flow of the core is highly beneficial because it

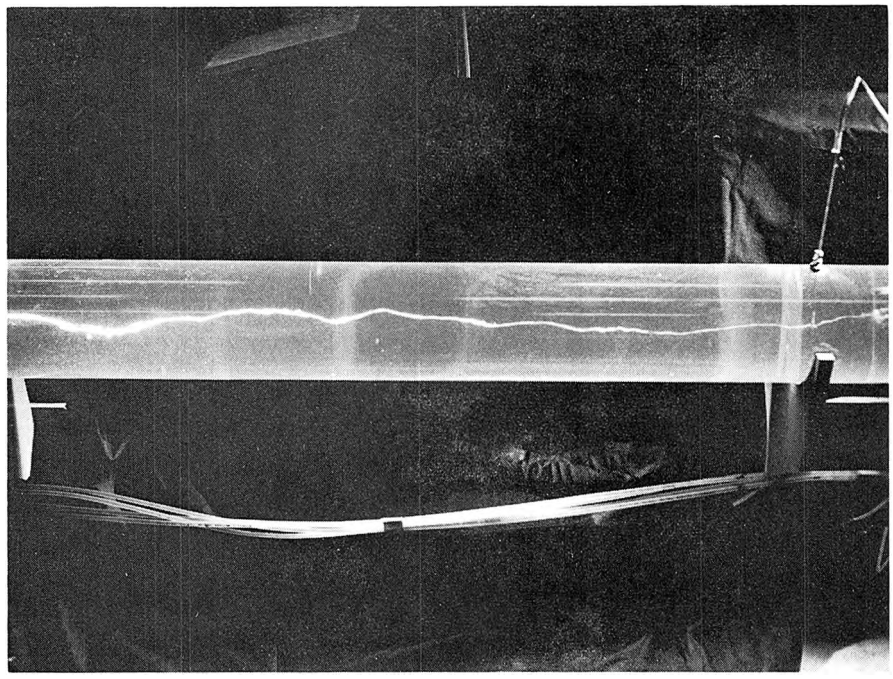

Fig. 31. Collection of air in center of horizontal outfall pipe due to rotation of flow; view shows prototype stations 2+20 to 2+90. This is typical of all except the very low flows. $Q_p$ = 400 cfs, TW = 30 ft (same as Fig. 28).

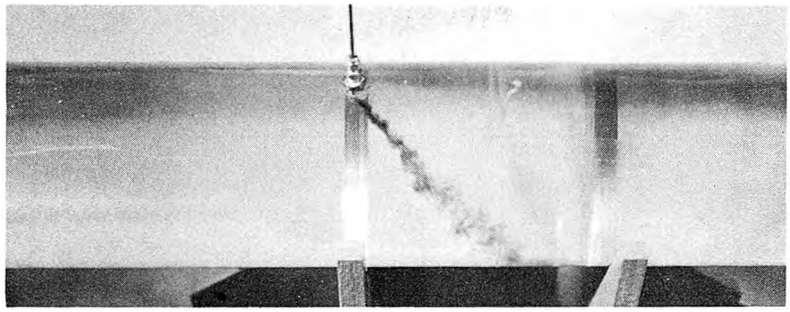

a) Injection of dye at wall (r/R = 1).

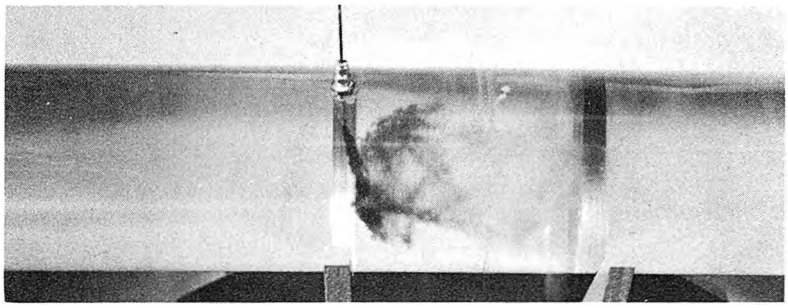

b) Injection at r/R = 2/3.

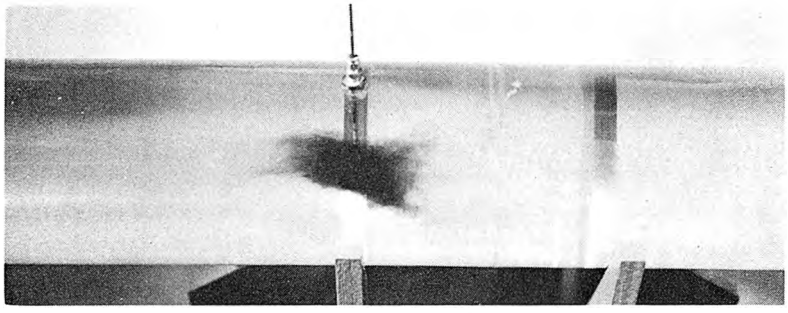

c) Injection at r/R = 1/3

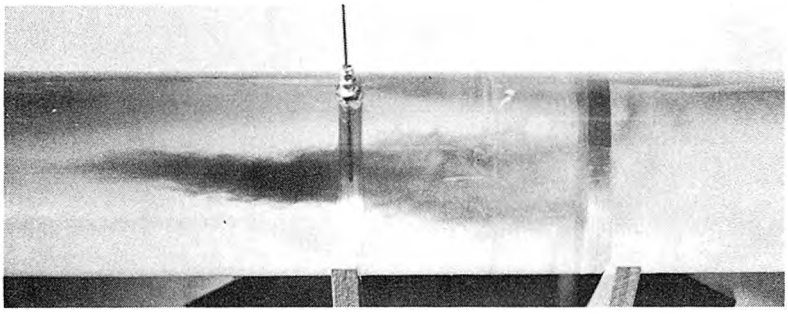

d) Injection at centerline (r/R = 0)

Fig. 32. Reverse flow in core of swirling flow in horizontal pipe illustrated by dye. Q = 400 cfs, tw = 40 ft, injection at prototype station 2+87. Thus, air shown in Fig. 31 usually travels upstream.

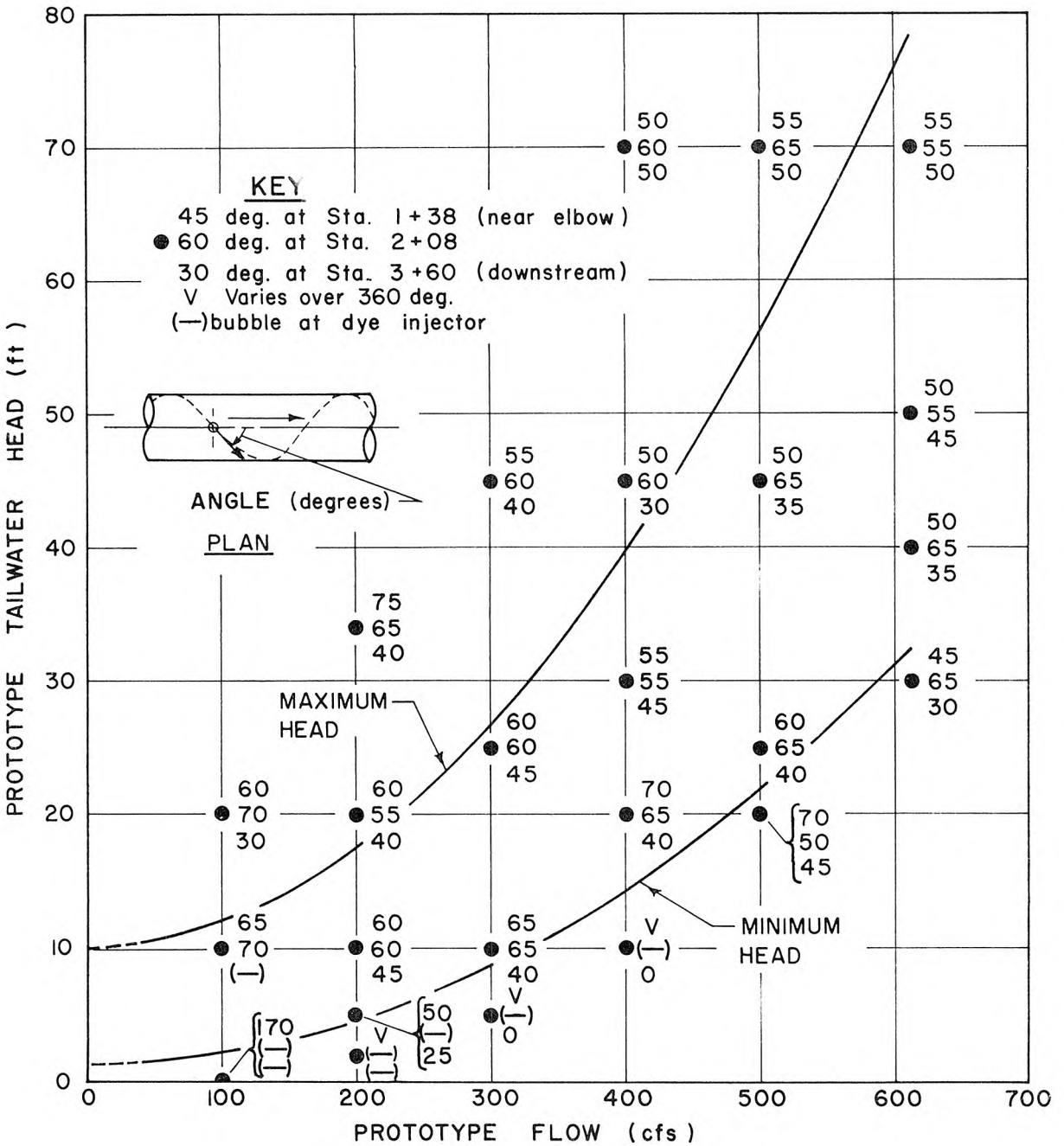


Fig. 33. Dye streak angles vs. flow condition.

tends to move collected air back to the free surface for escape. Thus, the presence of air may be quite prominent, whereas the transport downstream is nil; for example, for Q = 400 cfs, TW = 30 ft (see Fig. 31), the measured air discharge in the outfall is only 5 ppm by volume.

At high tailwater (see Fig. 32), there may be no visible air filament at the center of the vortex because air is not being entrained in the vortex tube. At intermediate tailwater heads the air filament gives a vivid indication of the vortex axis, which oscillates considerably (roughly $\pm$ 1/2 inch from centerline). At low tailwater levels (approximately 10 feet and lower), the vortex becomes relatively weak and a large quantity of entrained air collects on top of the pipe rather than in the core (see Fig. 23), and is released through the 7-foot branch pipe.

Some further detailed observations of the distribution of velocity and head within the swirling flow in the pipe are presented in Appendix A.

4.03.6 Air flow patterns. The drop structure problem involves not only the patterns for the liquid flow, but also for the air flow. Although the essential features have been described in various sections above, the complete flow air cycle is summarized in Fig. 34 and described below.

Starting at the top of the chute, air enters the drop structure in the air space over the flow (or possibly already entrained by flow over the weir in prototype). Slight additional entrainment or release may occur in the chute flow in prototype. Next the hydraulic jump, being the cause of the air flow in the chute, entrains all the air flow, unless the stilling basin is not sealed at the top. The entrained air is then mostly released from the jump either back to the front of jump or downstream to the air space in the vortex chamber. Thence the air may be discharged through the vent pipe at the top of the vortex tube, or it may be entrained again at the bottom of the vortex tube and carried into the outfall. From there it may be (a) returned to the vortex tube by the reverse flow in the core, (b) discharged through the 7-foot pipe for the butterfly-valve circuit, which is equipped with a vent downstream from the valve, or (c) transported down the outfall.

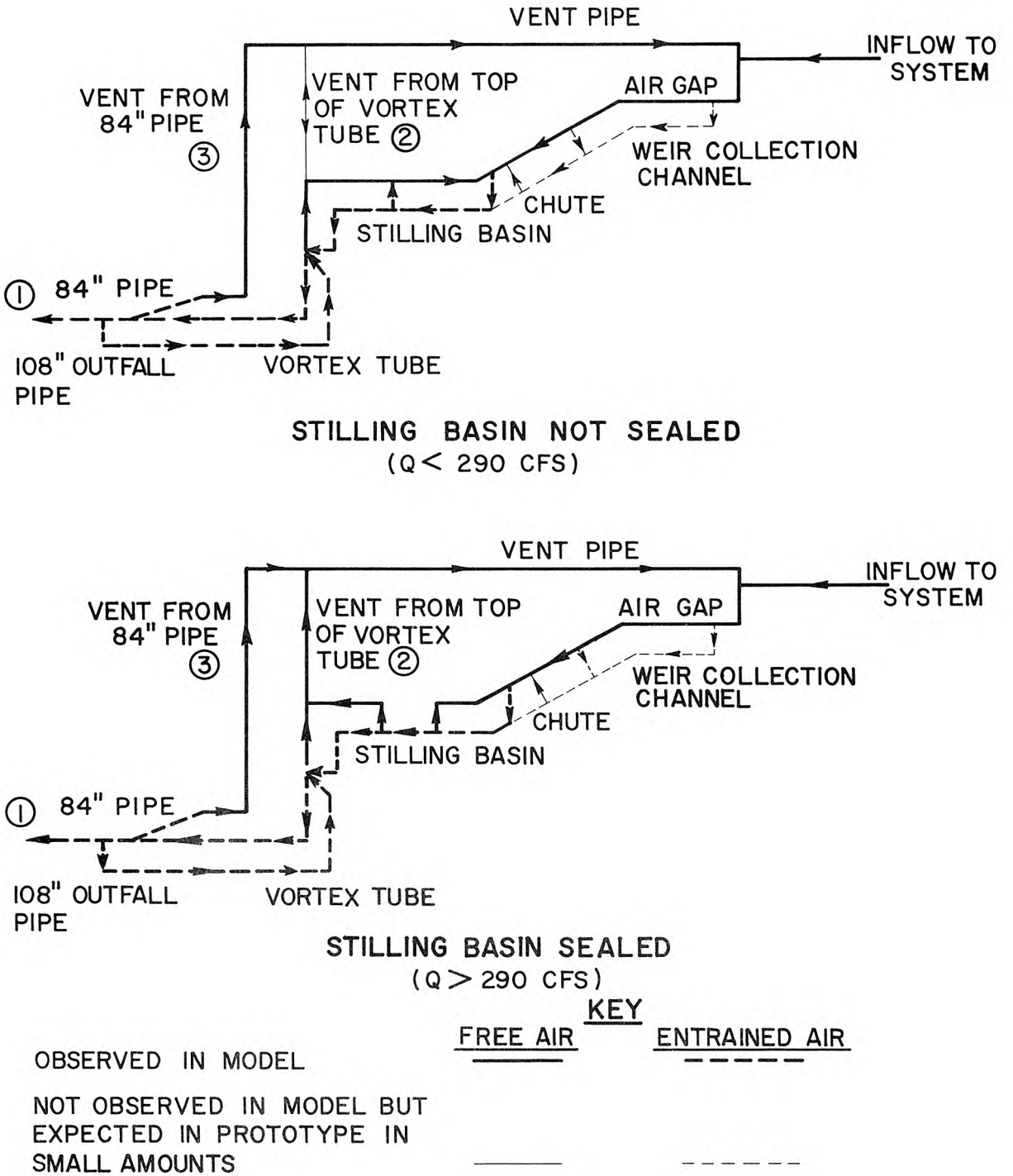


Fig. 34. Schematic air flow cycle showing all possibilities. Quantitative air flow measurements were made in model for flow paths 1, 2, 3 shown above. (See Figs. 35, 37, and 38, respectively.)

The vented air is returned to the enclosed weir structure for odor and foam control; thus, it is simply recycled, and the only additional air drawn into the system is that required to balance the net transport into the ocean outfall.

It is essential that all air spaces be maintained near atmospheric pressure to avoid changing the water levels and flow configurations. To accomplish this, large vents are required to transport maximum air flows (see next section) without a pressure rise of over a foot or two in the prototype. The vent on the vortex structure is also needed to permit entry or release of air to accommodate the changing volume of sewage in the vortex tube due to varying tailwater.

In the prototype, alkyl benzene sulfonate in the sewage may cause all the air spaces to become filled with foam. However, the basic cycle will remain the same, and foam will be recycled as described above -- i.e., destroyed and regenerated as it is entrained and released. Since the entire drop structure is closed, the amount of foam generated will be limited to the volume of air in the system.

### 4.04 Air Entrainment in Flow in Outfall Pipe

Of primary concern is keeping the air entrainment into the ocean outfall down to safe limits, as previously described in Sec. 2.01.3. The net amount of air entrainment in the flow in the model outfall pipe was measured as a volume rate of discharge into the air collector, and was expressed as a ratio to the water discharge in parts per million (ppm) by volume at atmospheric pressure. Since the independent variables were discharge and tailwater head in each test, the air entrainment has been plotted as a function of these two variables within the expected ultimate operating range taken from Fig. 5. The results for the final model (1LM-3) are shown in Fig. 35, and for all the earlier models in Figs. 41-50 in Appendix B. For the final model, highest value obtained within the operating range was 206 ppm (at Q = 200 cfs, TW = 5 ft) or well below the established goal of 1,000 ppm for the model (assuming a scaling factor of 10, and allowable prototype value of 1.0 per cent).

Comparative values of air entrainments for all the models for two

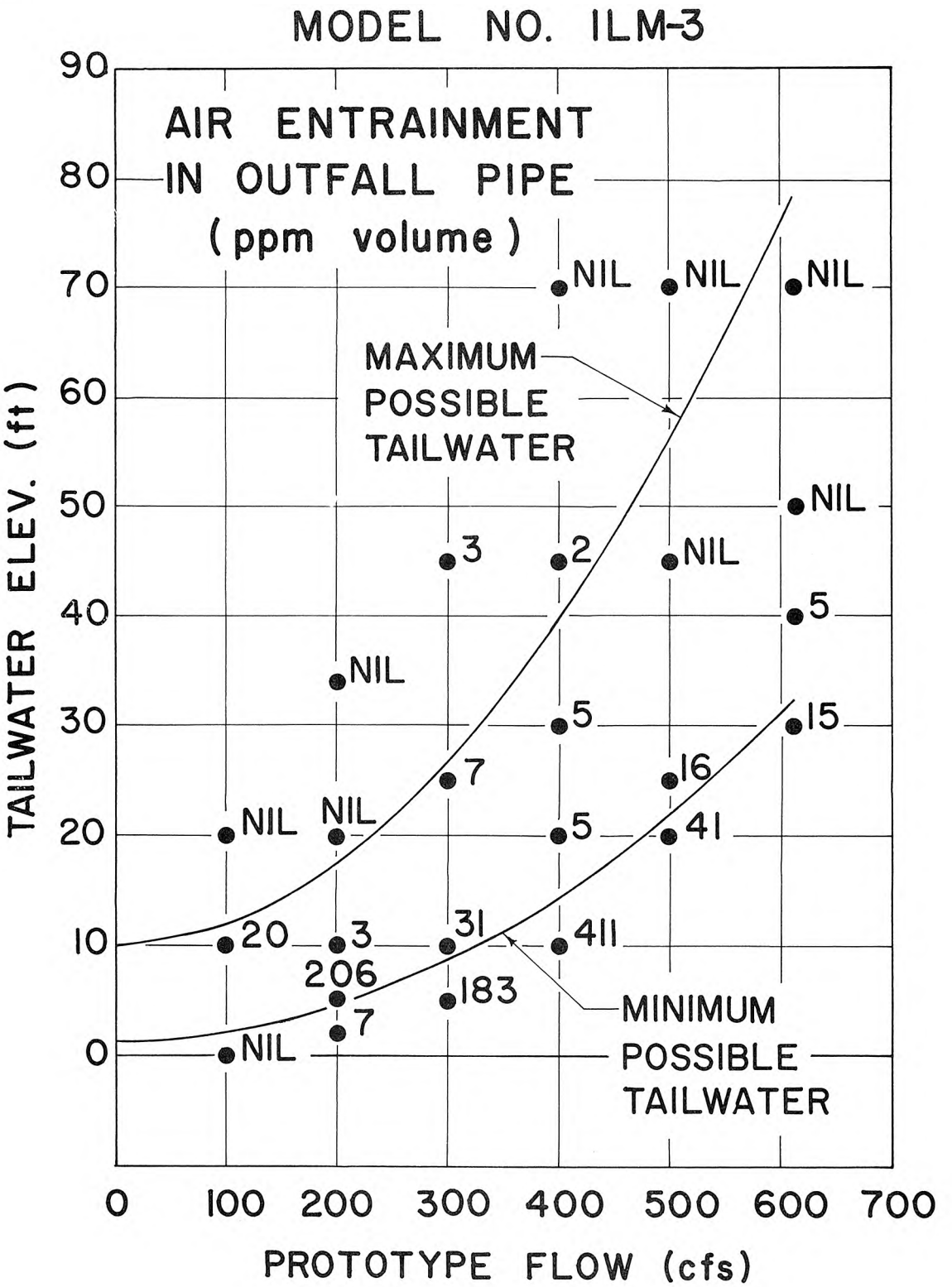


Fig. 35. Air entrainment in outfall pipe as function of flow condition for Model 1LM-3.

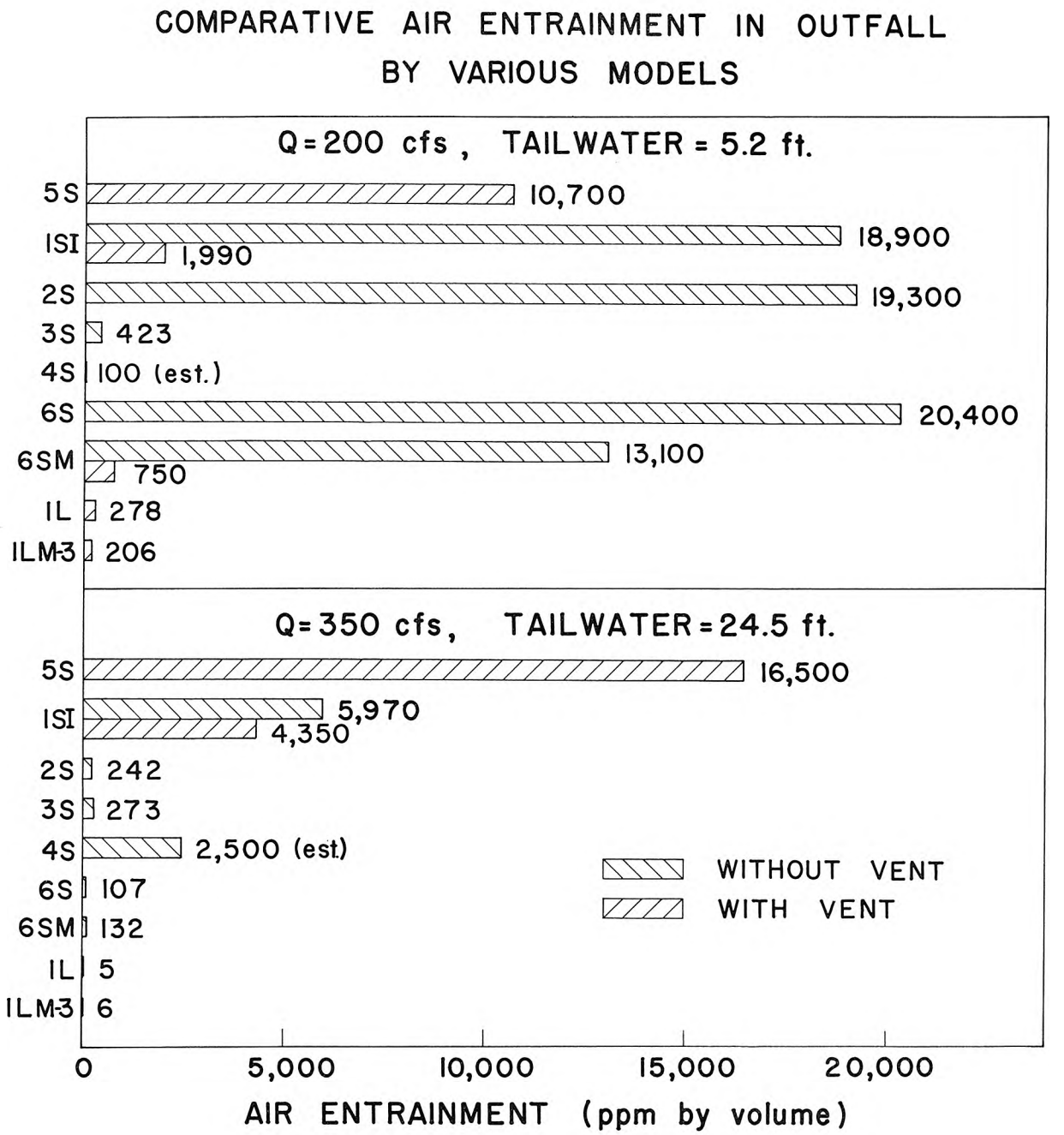


Fig. 36. Comparative air entrainment in outfall pipe for various models at two typical flow conditions.

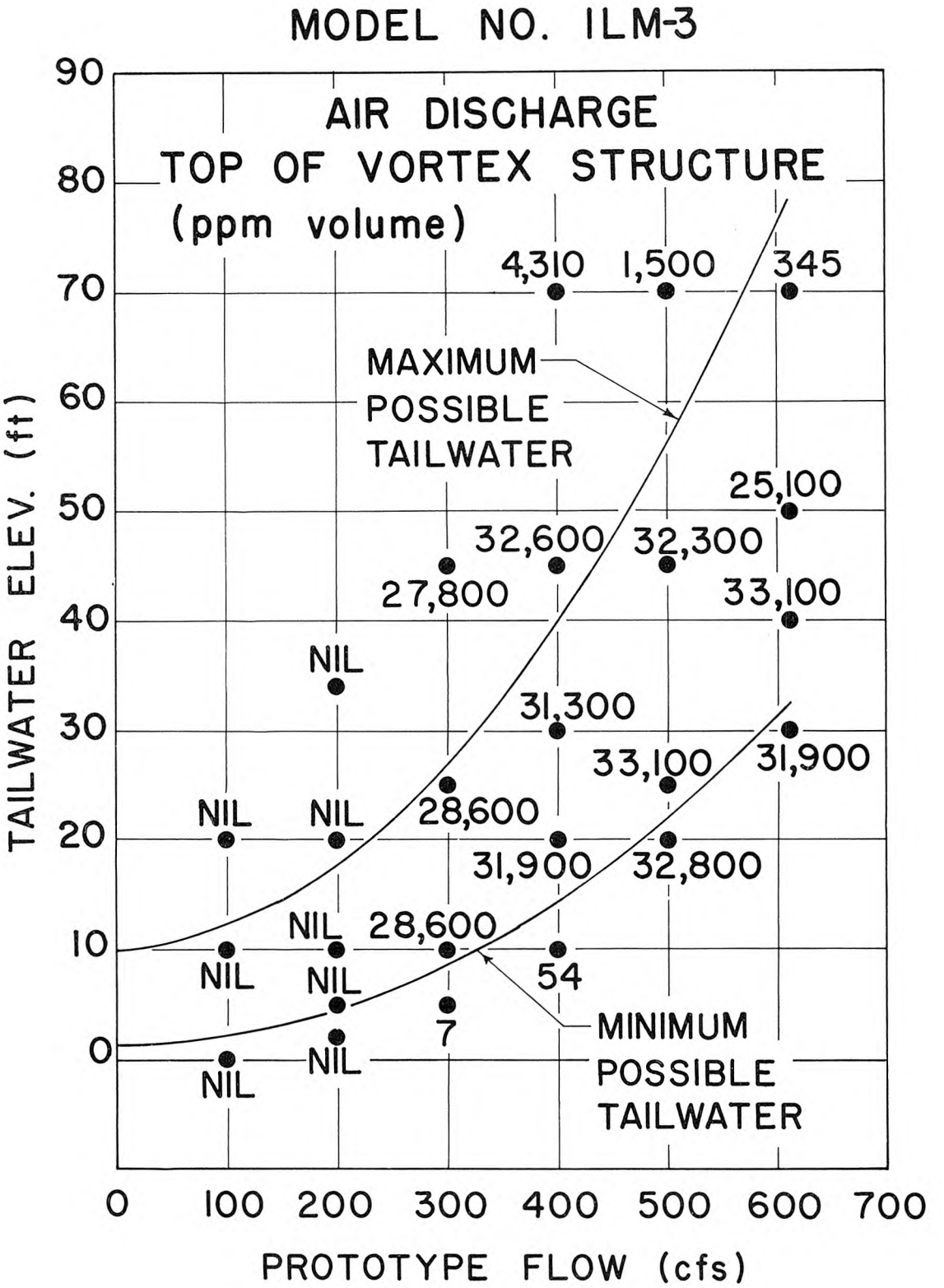


Fig. 37. Air discharge from top of vortex structure as a function of flow condition for Model 1LM-3.

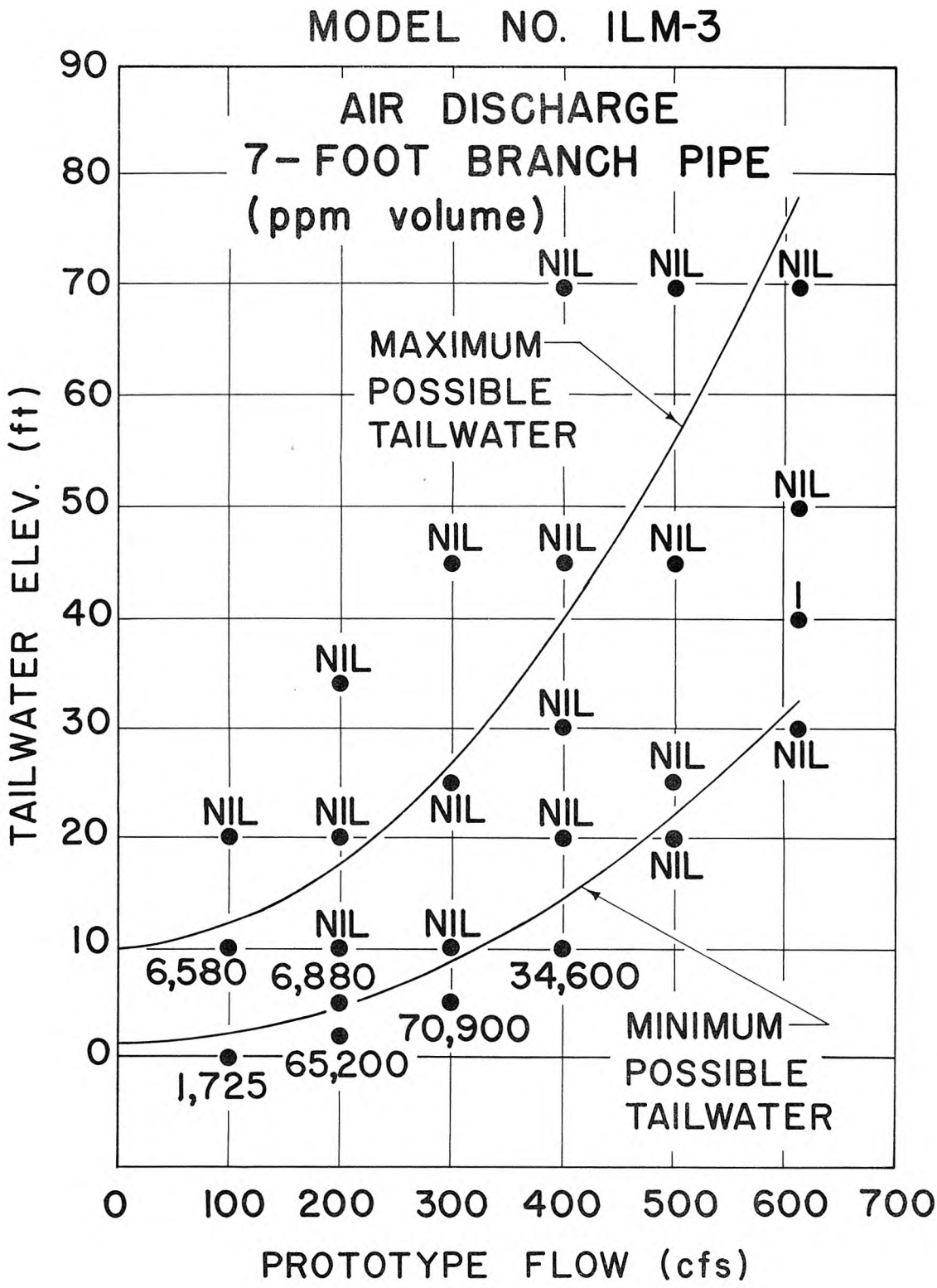


Fig. 38. Air discharge from vent on 7-foot branch pipe as a function of flow condition for Model 1LM-3.

selected flow conditions have been plotted in Fig. 36 in order to show the marked improvement in air entrainment achieved with the successive changes in the design of the vortex tube (cf. Fig. 11). Model 5S is listed first because it is the only model without a vortex tube, thereby indicating by comparison the relative benefit of the vortex principle.

4.05 Air Recirculation through Vent Pipes

The final model (1LM-3) showed that there was substantial flow of air within the structure and that large vents would be required to bleed air from the top of the vortex tube and from the 7-foot diameter branch pipe (part of butterfly valve circuit). The vortex tube receives air from the hydraulic jump at the higher flows; on the other hand, the branching pipe receives air at lower flows when the tailwater level is near the lower limit and the plunge point practically moves down to the elbow, large amounts of air being swept into the outfall pipe. (For further discussion of overall air flow patterns, see Sec. 4.03.6 and Fig. 34).

The air discharge from these two points was carefully measured, without allowing pressure rises greater than the order of 1 foot of water (prototype) in the air spaces being vented. The results, shown in Figs. 37 and 38, provide a basis for estimating needed venting capacities. For the top of the vortex structure, the air flow is expected not to exceed $33,100 \times 10^{-6} \times 612 \times 5 = 100$ cfs, allowing a scaling factor of 5, which is considered reasonable for such a large air flow. Similarly, the branch pipe maximum in an extreme case might be expected to be $70,900 \times 10^{-6} \times 300 \times 5 = 106$ cfs (for a point slightly below computed operating range of heads). Since Figs. 37 and 38 show that these large air flows cannot occur simultaneously, the vent pipes may be joined into a common line, which should have capacity for at least 100 cfs of air flow with pressure rise of only 1 to 2 ft of water. The provision of these vents, to be open at all times, is absolutely essential to safe operation.

From the air flow diagram (Fig. 34) it may be noted that for each flow condition the sum of the air entrainment in the outfall and the air discharges through the two vent pipes given by Figs. 35, 37, and 38, respectively, is equal to the air flow into the chute. For all flows of 300 cfs or

above, this air flow into the chute is of the order of 30,000 ppm or 3 per cent, and, except for one point, it is almost all discharged from the top of the vortex tube. In fact, for all tests in this flow range, more than 99.7 per cent of the total air demand is discharged through the vents and only 0.3 per cent or less is carried out the outfall pipe in the model. For flow tests at 100 and 200 cfs, there is no flow through the vent at the top of the vortex structure because the stilling basin is not sealed and the entrapped air may more easily move out through the air gap there than through the vent pipe. At these lower flows, the amount of air entrained at the base of the vortex tube is of the order of 10,000 ppm (1 per cent) or less; of this amount, at least 97 per cent is discharged into the 7-foot diameter pipe and the vent attached to it, and 3 per cent or less goes down the outfall in the model.

4.06 Observed Piezometric Heads

The piezometric heads were measured at 13 points in the final model 1LM-3 for all the runs. The readings were taken from two multitube manometer boards marked and set to read directly the prototype elevation in feet above sea level with tenths interpolated by eye. (One manometer is visible at far right of Fig. 20.) The locations of the piezometer taps are shown at the top of Fig. 39. Tailwater heads used throughout this report are readings of piezometer number 12.

The mean piezometer readings are plotted in Fig. 39 for flows of 612, 400, and 200 cfs at various tailwater heads. Two significant observations may be made, namely:

(1) The sill at the end of the stilling basin acts as a hydraulic control as intended, until flooded from downstream (for example at TW = 50 and 70 ft for Q = 612 cfs).

(2) The energy loss in the vortex tube and pipe under the completely submerged condition is of the order of 5 times the value computed for ordinary pipe friction. Table 4 shows that the observed loss in the model between the stilling basin (piezometer 6) and the end of the model pipe (piezometer 12) was 13 velocity heads. By conventional head loss calculations (swirl neglected) one obtains approximately 2 to 3 velocity heads, or only 1/5 as much. The

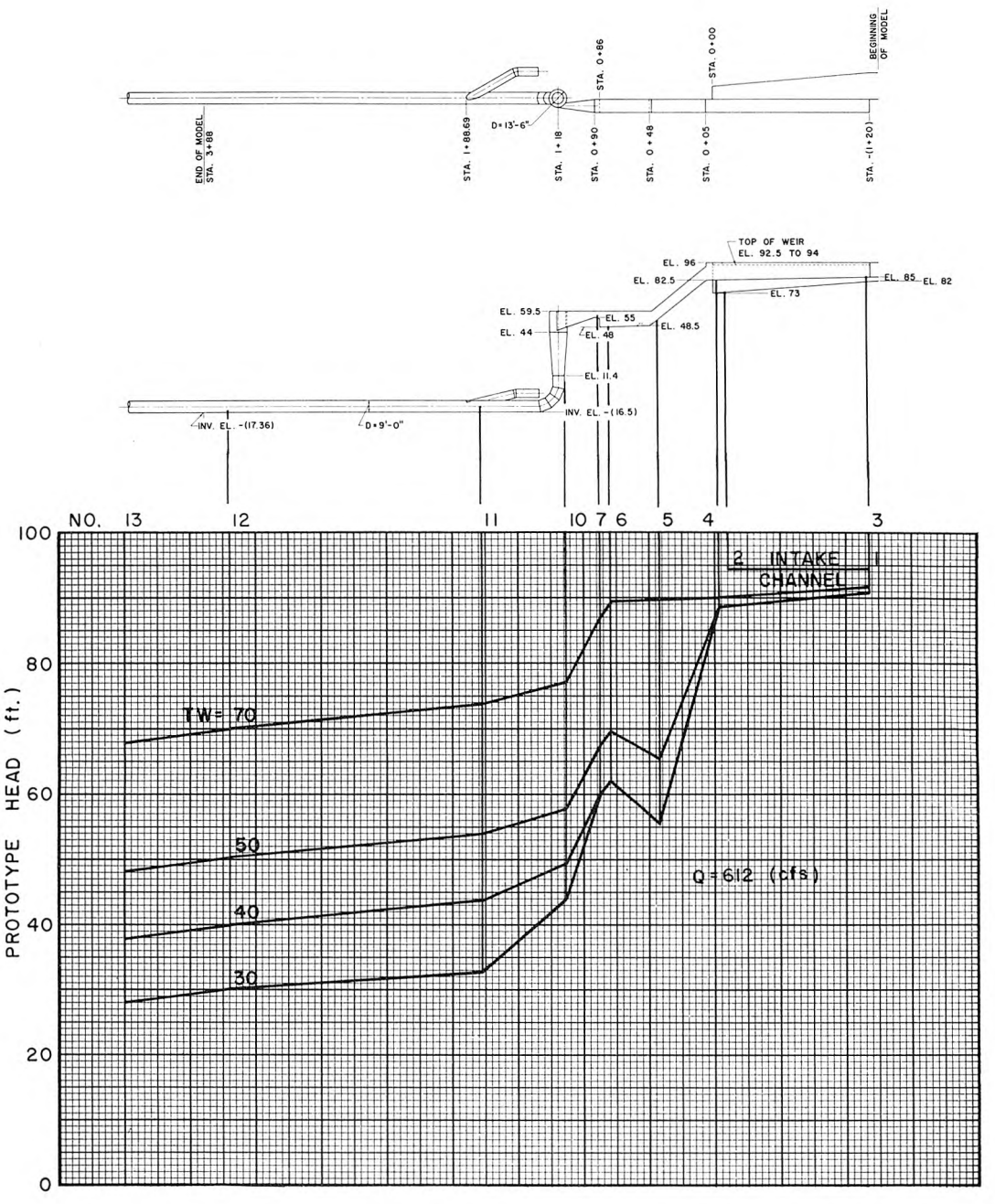


Fig. 39a. Piezometric head distribution for final model, 1LM-3, $Q_p$ = 612 cfs.

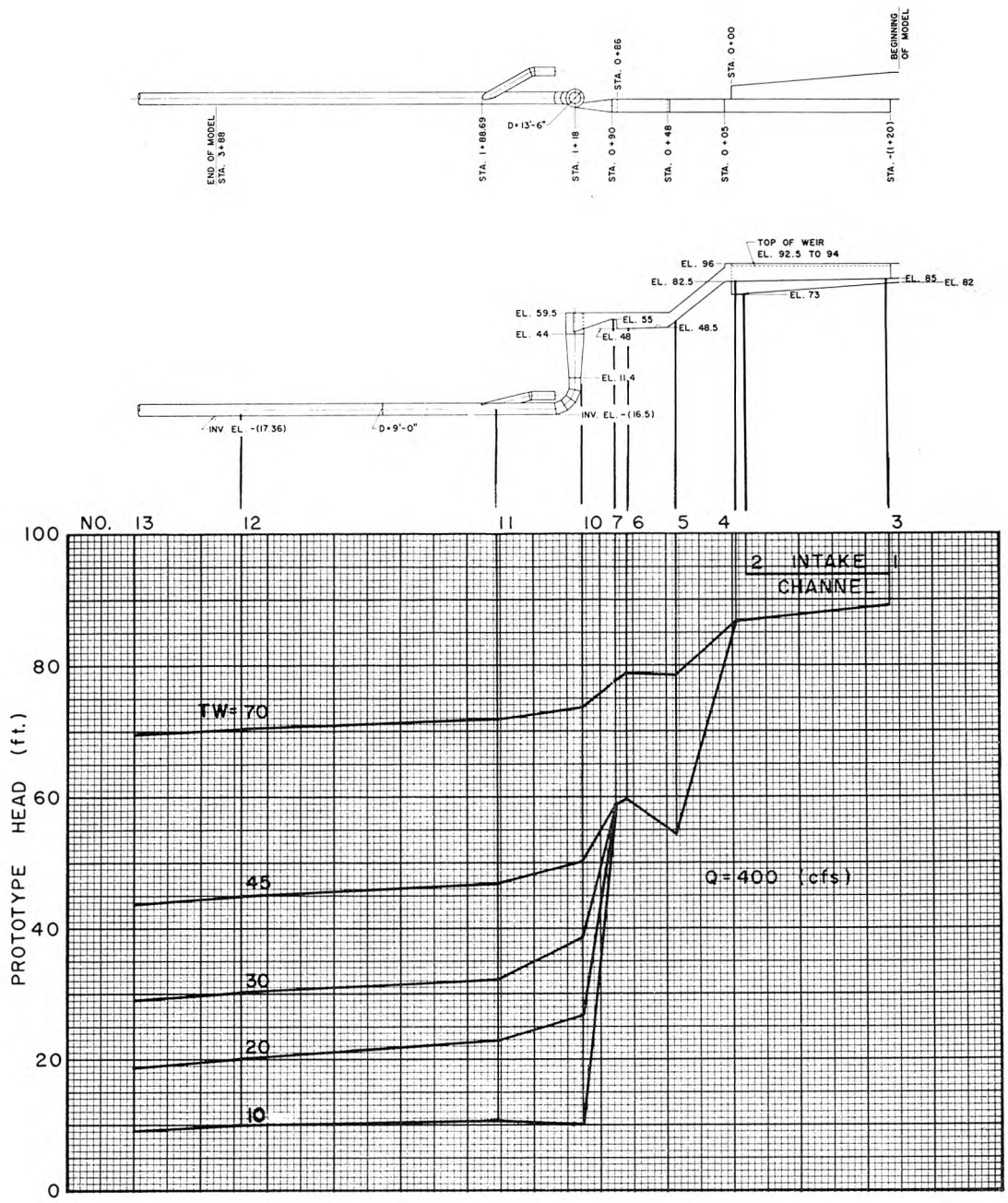


Fig. 39b. Piezometric head distribution for final model, 1LM-3, $Q_p$ = 400 cfs.

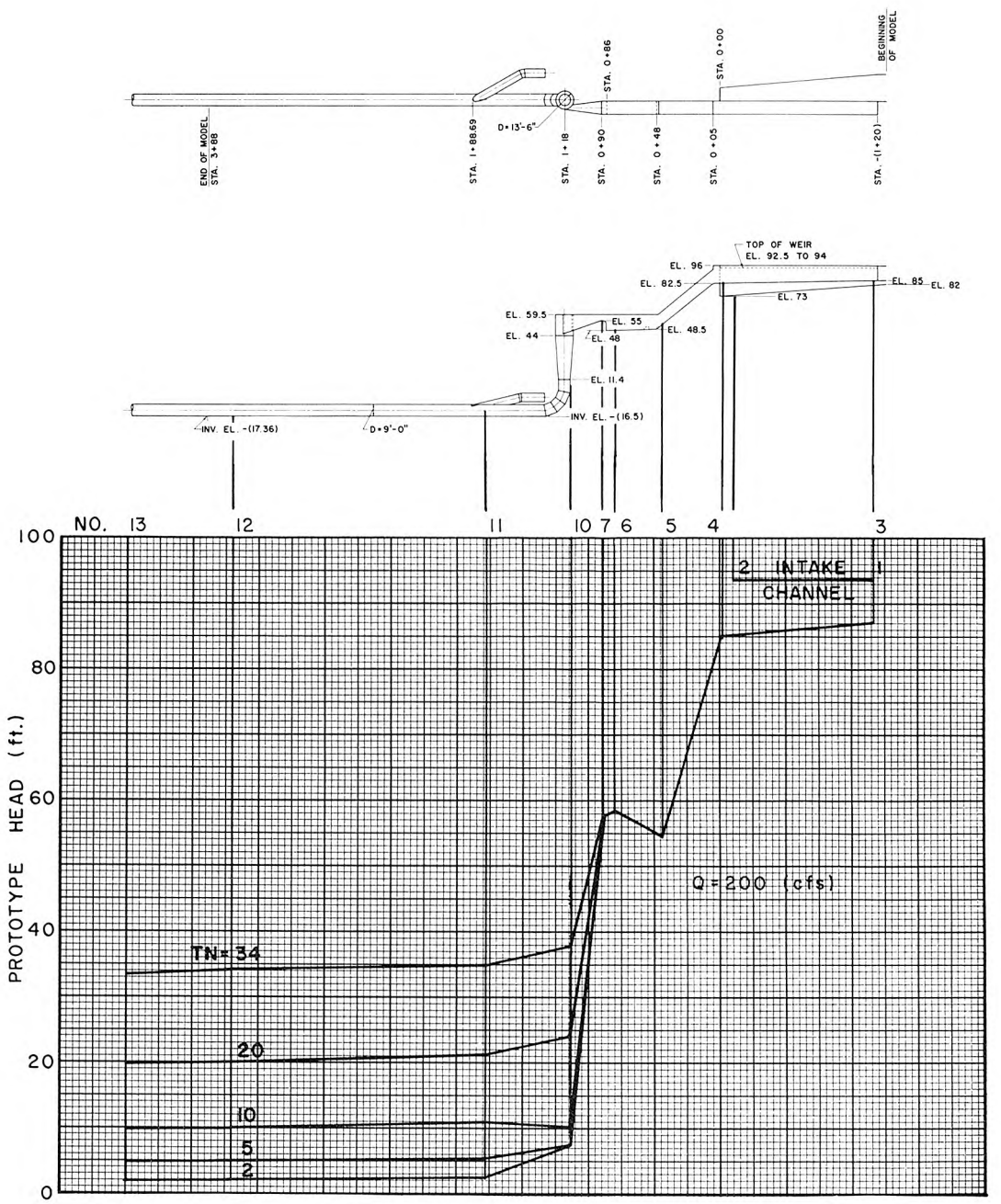


Fig. 39c. Piezometric head distribution for final model, 1LM-3, $Q_p$ = 200 cfs.

TABLE 4

ENERGY LOSS IN VORTEX TUBE AND PIPE
UNDER SUBMERGED CONDITION

| Flow | $\frac{V^2}{2g}$ | (Piezo. head at 6) -(Piezo. head at 12) | Energy loss $\Delta E$ | $\Delta E / \frac{V^2}{2g}$ |
|---|---|---|---|---|
| cfs | ft | ft | ft | |
| 612 | 1.43 | 19.5 | 18.5 | 13.0 |
| 500 | 0.96 | 13.2 | 12.5 | 13.0 |
| 400 | 0.61 | 8.6 | 8.2 | 13.4 |
| | | | Ave. | 13.1 |

large additional head loss must be due to the swirl and the induced counter-flow in the core of the pipe.

# CHAPTER 5
# DISCUSSION OF RESULTS

## 5.01 Limitation on Results and Sources of Errors

The results of any model test give no absolute assurance that the prototype will perform exactly as predicted from the model, because of some secondary factors in the prototype which cannot be successfully modeled. In the present study (as in many Froude models) viscous effects in the model were undoubtedly more pronounced than in the prototype in spite of the fact that the friction factor for the smooth lucite model outfall is approximately equal to that of the concrete prototype pipe. One way in which viscosity affects the flow is the dissipation of the swirling motion in the pipe downstream from the vortex drop structure. In the model, with its smaller Reynolds number, the decay may be expected to be more rapid; this in turn may have an effect on the strength of the counterflow in the core of the outfall pipe, which is a helpful factor in rejecting air. A similar reverse flow is expected to exist in the prototype, but if it is much weaker, more net air entrainment should be expected. This is called a scale effect.

Another scale effect is the difference in behavior of air bubbles. In the prototype the size of the air bubbles will probably be only slightly bigger. The bubbles cannot increase in size in proportion to the length scale because the surface tension would be insufficient to make them stable, i.e., prevent them from breaking into smaller bubbles. Recognizing that accelerations and pressure gradients are equal in prototype and model according to Froude's Law, and assuming that the bubbles are approximately the same size, one may conclude that the relative velocity between bubble and fluid (i.e., the rate of "rise," or motion toward the eye of the vortex) would be identical in model and prototype. On the other hand, flow field velocities will be scaled up to the prototype by the factor $\sqrt{18} = 4.24$ from the large model, so that

for similarity a similar increase in relative bubble velocity is required*. Consequently, if the bubbles are no larger in the prototype, the escape of entrained air will not be nearly as rapid. This is the principal reason for allowing such a substantial scaling factor for air entrainment, namely 10, in this model study. However, offsetting the above considerations is the fact that the bubbles may well be somewhat larger in the prototype than in the model. Also, as a cloud of air bubbles "rises" through long columns of water, there will be more coalescences, which will improve the removal efficiency, just as flocculation does in the settling of particles as the settling tank gets deeper.

Since the amounts of air recirculated through the vent pipes from the 7-foot pipe and the top of the vortex structure are so large (Figs. 37 and 38) in comparison to the air entrainment in the outfall (Fig. 35), one might well inquire into the adequacy of the scaling factor of 10 set for the small amount entrained in the outfall. For these large vented quantities the factor 5 appears reasonably safe (see Sec. 3.03); thus, the indicated prototype air demand in the chute for flows greater than 300 cfs would be 15 per cent by volume (5 times sum of values in Figs. 35, 37, and 38), and 5 per cent at the base of the vortex tube for flows of 100 or 200 cfs (for which stilling basin does not seal). To achieve 1 per cent maximum net entrainment in the outfall then requires $\frac{15-1}{15}$ = 93 per cent removal of the total air entering the structure for the flows of 300 cfs or more (compared to model value of 99.7 per cent), and only $\frac{5-1}{5}$ = 80 per cent removal for the 100 and 200 cfs flows (compared with minimum model value of 97 per cent). It does not seem likely that the efficiency of air removal by the vents could suffer by greater amounts than indicated as allowable by these calculations.

The flow patterns in the stilling basin and in the vortex tube are not strongly influenced by viscous forces, and the reproduction in the prototype

---

* It should be noted that the rise velocity, w, of air bubbles in water is not a simple function of the effective bubble diameter, d, because of the flattening of the bubble as d increases. Results of experiments in tap water (Haberman and Morton, 1956; W. F. Navin, 1960) indicate a steady rise of w with increasing d (up to about d = 1 mm for which w = 21 cm/sec), followed by very slow change as bubbles become flatter (up to d = 5 mm (0.2 in.) for which w = 25 cm/sec) and then further gradual increase in w with effective diameter.

may be expected to be very good. However, there may be some difficulty in interpretation of the tailwater head between model and prototype. For the prototype the possible tailwater levels were calculated on the basis of simple pipe friction, not taking into account any additional energy loss in the pipe due to the swirling motion. In the model it is easily seen that some of the energy dissipation caused by the vortex structure actually takes place in the downstream sections of pipe rather than in the structure itself; since the model of necessity is truncated at Sta. 3+88, or 270 feet (prototype) downstream of the vortex tube, some of the further extra loss due to the swirl may also have been truncated. In other words, in the model the piezometric head at the wall at Sta. 3+70 was assumed to represent the tailwater level, whereas, in fact, had the model pipe been very long, the head at this point may have been found to be still above the normal hydraulic grade line projected back at a uniform slope from reaches of the pipe free from the swirl. This is exactly the same problem encountered in determination of head loss due to pipe bends; the loss is not all in the bend itself, but is partly manifested as an additional loss in a reach of pipe downstream in which the velocity distribution is disturbed.

It was because of the coupling between the vortex structure and the pipe downstream that the large model was built with nearly three times as much of the downstream pipe as in the small models. It now appears that even if two or three times again as much pipe had been included in the large model, the swirl would still be detectible at the downstream end. Even so, it is believed that the effects of the swirl in generating additional head loss in the pipe are most pronounced near the drop structure. Furthermore, if the model results underestimate this loss, then the water level in the vortex tube will rise higher than predicted, a factor which will improve its performance. A slight reduction in peak flow capacity of 612 cfs may occur if the assumed conservative value of Manning's n of 0.017 for the outfall pipe actually occurs, because Table 4 already predicts a loss of 18.5 ft for fully submerged flow in the drop structure at 612 cfs; addition of 18.5 ft to the maximum computed tailwater of 78 ft (Fig. 5) gives 96.5 ft, or about 2.5 ft in excess of available. (It may be noted that the designated

peak, 612 cfs, is itself a rather conservative figure, and it is not likely to be ever reached with shore facilities presently planned.)

The measured values of the air entrainment and air discharge from the vents are the only quantitative measurements subject to errors of any significance. (Flow rate, for example is in error not more than 1 per cent and probably not more than 0.5 per cent.) Considering the natural fluctuations in the flow of air, the efficiency of the air collectors, slight deviations from atmospheric pressure in the volumetric measuring column, and other minor sources of error, the investigators believe that the air measurements are subject to errors of $\pm$ 20 per cent, with a minimum error of $\pm$ 20 ppm assigned to all measurements of less than 100 ppm. In view of the uncertainties of the scaling factor for prototype values, however, these measurement errors in the model are easily tolerable, and further improvements in technique were not warranted.

## 5.02 Prototype Testing

Because of the unusual nature of the recommended structure, it is vital to the profession that the model predictions be compared with actual prototype behavior to determine scale effects, especially for air entrainment. Therefore, a comprehensive program of prototype testing is highly recommended and minor features (such as piezometers) to accomplish this should be included in the initial construction.

A testing program should include the following, if at all possible:

1. Measurement of discharge.
2. Measurement of piezometric heads at selected points, corresponding if possible to those in the model.
3. Visual observations of flow type in the vortex tube (through a hatch in the top).
4. Measurement of the air discharge in each of the two vent pipes.
5. Measurement of inflow of fresh air into the enclosed weir overflow structure; if there are no air leaks, this quantity will equal the net air entrainment into the ocean outfall.

6. Visual observation of foaming, any instabilities, or other phenomena not observed in the model.
7. Inspection for any cavitation damage (none expected) or excessive erosion.

It is recognized, of course, that such a program is rather difficult because of the location of the structure and the fact that it is completely enclosed. Nonetheless, the potential value to the City of San Diego and the engineering profession will justify the cost of any carefully conceived testing programs.

Although it was anticipated that some information on scaling effects would be obtained by comparison of the small (27 : 1) and large (18 : 1) models, they were obscured by effects of changes in the configuration of the structure. The scope of the model investigation did not permit exact duplication of models on different scales.

## 5.03 Vortex Flow Pattern

The strength or circulation of the vortex in the vortex tube is an important flow characteristic which was varied during the investigation by changes in the diameter of the vortex tube at the top and the geometry of the flow inlet. The circulation $\Gamma$ is defined as the line integral of the velocity around a closed path C enclosing the center of the vortex, i.e.,

$$\Gamma = \oint_C \overline{v} \cdot d\overline{\Gamma}$$

where $\overline{v}$ is the velocity vector and $d\overline{\Gamma}$ is the element of the curve, C, which will be considered to be in a plane normal to the axis of the vortex, and the dot denotes scalar product. For irrotational flow $\Gamma$ is constant for any curve C enclosing the vortex singularity, but in the present case $\Gamma$ will be variable on account of internal shear and vorticity. If the paths C are considered to be circles, then $\Gamma$ becomes a function of the radius r,

$$\Gamma(r) = \int_0^{2\pi} v_\theta r d\theta$$

where $v_\theta$ is the velocity component around the circle (i.e., in $\theta$-direction).

Assuming $v_\theta$ is independent of $\theta$,

$$\Gamma(r) = 2\pi r v_\theta(r) \tag{5-1}$$

For an ideal fluid, $\Gamma$ would be constant for any position along the vortex tube (including elbow and pipe downstream) by Kelvin's Theorem, considering r = R = radius of the tube wall. On account of viscous stresses, it may be expected, however, that the circulation $\Gamma$ will decrease downstream, and thus be a maximum at the top of the vortex tube where the flow enters. Actually, the boundary layer on the wall will make $\Gamma$ equal to zero right at the wall, but it may be expected to be a maximum very close to the wall.

The maximum circulation $\Gamma_m$ may be estimated from

$$\Gamma_m = 2\pi R_i V_i, \tag{5-2}$$

where $V_i$ = inlet velocity (tangential component), and

$R_i$ = displacement of centerline of inlet channel from centerline of vortex tube*.

The significance of the numerical value of $\Gamma_m$ may be made clearer by making it dimensionless by dividing by $2\pi R V_{zo}$ where R = radius of outfall pipe, and $V_{zo}$ = mean axial velocity in outfall. Denoting this ratio by $\Gamma_*$, which is the same in model and prototype,

$$\Gamma_* = \frac{\Gamma_m}{2\pi R V_{zo}} = \frac{R_i V_i}{R_o V_{zo}} \tag{5-3}$$

Now for ideal fluid flow, $\Gamma(r) = \Gamma_m$ = constant, and the value of $\Gamma$ at the top of the vortex tube would be the same as in the outfall pipe downstream from the elbow. For this ideal case then, with $V_{\theta w}$ = tangential velocity at wall,

$$\Gamma_* = \frac{R_o V_{\theta w}}{R_o V_{zo}} = \frac{V_{\theta w}}{V_{zo}} = \tan \phi_*. \tag{5-4}$$

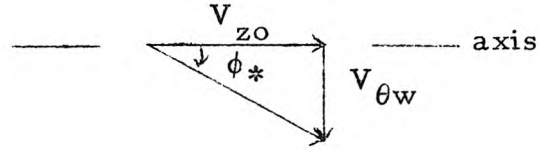


* Slight adjustment for effect of guide vane is neglected, as it cannot be specifically computed.

In other words, for ideal fluid flow $\Gamma_*$ would be just the tangent of $\phi_*$, the angle which the streamline at the wall makes with the axis of the pipe. The stronger the circulation, the bigger is $\phi_*$, and the flatter are the helixes for the streamlines. The ideal values ($\phi_*$) may be computed and compared with the corresponding actual values ($\phi$) measured with dye streaks in the model (Fig. 33).

For Model 1LM-3, the computation of $\Gamma_*$ (prototype dimensions) is as follows by eq. (5-3):

$$R_i = 5.58 \text{ ft}$$

$$V_i = Q/A_i = \frac{Q}{3.33y_i} \quad \text{where } y_i \text{ is the depth at inlet}$$

$$R_o = 4.50 \text{ ft}$$

$$V_{zo} = Q/\pi R_o^2 = Q/63.6 \text{ ft}^2$$

$$\Gamma_* = \frac{R_i V_i}{R_o V_{zo}} = \frac{5.58\ (63.6)}{(4.50)\ 3.33y_i} = \frac{23.7 \text{ ft}}{y_i}$$

The result shows a dependence on the depth at the inlet. For full flow at the inlet (Type AS), $y_i = 12.34$ ft, $\Gamma_* = 1.94$ and $\phi_* = \tan^{-1}(1.94) = 63°$. This compares favorably with measured values of $\phi = 50\text{-}55°$ (Fig. 33) for Type AS flows, allowing for some expected decay of the circulation and boundary layer effects.

For lower flows the value of $\phi_*$ increases; for example, from Fig. 28b for Q = 400 cfs, TW = 30 ft, it may be estimated that $y_i \approx \frac{1}{2}(12.34) \approx 6$ ft, giving $\Gamma_* \approx 4$, and $\phi_* = 76°$. The measured value of $\phi$ was 55°. The measured angle $\phi$ follows the expected trend toward higher values at lower flows and tailwaters, although the difference between $\phi_*$ and $\phi$ widens, owing to increased viscous effects, as water spirals down the walls of the vortex tube at high velocity in a thin sheet for low tailwaters (cf. Type B flow, Fig. 30).

In the pipe downstream from the elbow the flow in the central core has a reverse axial flow component. (See Sec. 4.03.5 and Fig. 32.) A hypothesis for the cause of it is as follows. As the helical flow progresses downstream, the strength of the circulation decreases gradually. The piezometric head is always less in the center of the pipe than at the wall; but

going downstream this difference decreases and ultimately becomes zero when the vortex is completely dissipated. If this differential (wall to center) decreases more rapidly than does the head at the wall going downstream, then the pressure in the central region actually increases for some distance going downstream. The adverse pressure gradient thus formed could be the driving force for the reverse axial flow.

Reverse flow in the core of a swirling flow was first reported qualitatively by J. B. Nuttall (1953) for flow in a short efflux pipe. For flow through a convergent nozzle under conditions of high swirl and low head, A. M. Binnie and J. D. Teare (1956) reported a zone of reverse flow, not at the core, but rather in an annulus at intermediate radii. Under special conditions several such annular zones were observed. Later, Binnie, G. A. Hookings, and M. Y. M. Kamel (1957) reported similar effects in a convergent-divergent nozzle, including a measured velocity distribution showing zero or slight reverse flow for radii between 0.7 and 0.85 inches in a section of the convergent nozzle where the radius of the wall was 1.5 inches. Earlier experimental work by Binnie and Hookings (1948) on whirlpools did not specifically identify any reverse flow, but air entrainment was noted when the vortex became feeble.

Another device utilizing reverse flow in a swirling flow is the Ranque-Hilsch tube, used for separating gases of different density (usually hot and cold). With flow introduced tangentially at the center of a tube, it has been found that the discharge from one end is hotter than the other. A. J. Reynolds (1962) has recently made detailed velocity measurements in this device, and shows again reverse flow (of lighter gas in this case) in the core of a swirling flow.

## 5.04 Suggestions for Future Research

The swirling flow phenomena encountered in this limited model investigation should be further investigated in a basic research project. It is suggested that swirling flow be studied in long uniform pipes to determine:

1. The effect of the swirl on the overall energy dissipation in the flow,
2. The distribution of velocity (time average) and vorticity

in the cross section, and shear stress on the wall.

3. The turbulence and diffusion characteristics.
4. The rate of decay of the circulation with distance.
5. The conditions under which there are zones of reverse flow and their extent.

These research results might indicate that swirling flow is an effective means of dissipating excess energy in a pipeline. Previous discrepancies in results of ordinary pipe friction tests might be explained by small amounts of swirl present, but unnoticed. Pumps with rotating impellers undoubtedly produce some swirling motion in the flow in the discharge pipes, but the effects have not been adequately assessed.

In open channel flow there is evidence that even very weak secondary currents have a marked effect on sediment transport and configurations of sand bottoms. Meanders induce secondary currents, and vice versa. However, these currents are so weak that they are difficult to study. Thus, it may be quite useful to study the swirling flow in a pipe first because of the simpler geometry and the possibility of generating much stronger swirls.

The basic mechanics of generation of air bubbles in water should be better understood in order to make more reliable models and predictions of air entrainment in hydraulic structures. Basic research on this subject could be done with a simple idealized setup, such as a jet impinging on a free surface in a tank of water, in order to avoid the geometric complexities of an actual structure such as the one modeled in this investigation.

# CHAPTER 6
# SUMMARY OF RESULTS AND CONCLUSIONS

The basic objective of this investigation was to develop and test a suitable hydraulic drop structure for conveying sewage effluent at maximum flow of 612 cfs from the sewage treatment plant at elevation 94 feet into a closed ocean outfall pipe with a variable hydraulic grade line level. The dissipation of energy has to be accomplished in a reasonably compact structure without troublesome air entrainment. The principal results and conclusions based on a survey of the technical literature and tests on six small models (scale 28.5 or 27 to 1) and one final large model (18 to 1) are summarized below.

1. Because of the topography at the site and other engineering considerations, a two-part drop structure was selected, consisting of essentially a chute and hydraulic jump stilling basin for the upper part, and a vortex chamber with tangential flow inlet for the lower part.

2. It was decided that the air entrainment rate in the prototype outfall should not exceed 1 per cent of the discharge by volume at atmospheric pressure. At least 1 per cent can be expected to be taken into solution because of the increasing hydrostatic head in the outfall as it follows the ocean bottom to depths over 200 feet. Larger amounts could cause difficulty by collecting in large pockets and blowing back, or discharging visibly into the ocean.

3. A review of the literature indicated that the prototype air entrainment concentration would be considerably more than indicated by the model, which has to be operated in accordance with Froude's Law. It was decided that a scaling factor of 10 would be safe. Thus, the model had to meet a limit of 0.1 per cent or 1000 ppm by volume of air discharge in the outfall.

4. The basic components of the drop structure shown in Fig. 1 were used in the model tests from the beginning, but the geometry was changed between successive models (see Fig. 11). For the final recommended geometry shown in Figs. 1 and 12 (Model 1LM-3), the flow characteristics in all components were satisfactory within the operating range of head and discharge (Fig. 5).

5. The flow pattern in the vortex chamber was especially sensitive to the geometry of its inlet channel and guide vanes, whose purpose was to introduce the flow tangentially into the vortex chamber to produce a vortex free of surges and waves. For the final recommended configuration instabilities were held to tolerable limits, the maximum observed surge being 1.1 feet at a 2+ sec period (prototype).

6. The flow in the vortex chamber has been classified into four types: A, full vortex; AS, full vortex partially sealed at top; C, sheet flow at wall down to a hydraulic jump; and B, sheet flow along wall down into a pool at the bottom (see Fig. 25). Fig. 26 gives flow type as a function of flow and tailwater head over the operating range; in general with decreasing tailwater level the sequence was AS, A, C, to B.

7. The flow in the outfall pipe downstream of the vortex chamber was strongly swirling except at very low tailwater heads. At the center of the pipe there was a core of fluid flowing backward with respect to the main flow. Since the entrained air collects in the center of the pipe by centripetal action, this reverse flow core is very effective in pushing the air back to the free surface for release. The reverse flow phenomenon has been reported recently by other investigators (see Sec. 5.03).

8. In the final model, 1LM-3, the maximum observed rate of air entrainment in the outfall flow within the operating range was 206 ppm by volume, well within the 1000 ppm limit set for the model (to correspond to 10,000 ppm = 1 per cent in prototype). (See Fig. 35 for results for full range of operating conditions.)

9. Comparison of air entrainment data for the various models tested (Fig. 36 and Appendix B) shows unquestionably the merit of the vortex concept for reducing air entrainment. Furthermore, reductions by factors of 10 to 1000 in air entrainment were achieved by successive geometric adjustments of the models. For example, for prototype discharge of 350 cfs and tailwater head of 24 feet, the ratio of air to water discharge in the outfall was as follows (Fig. 36):

| Model | Type | Ratio of Air to Water (ppm by volume) |
|---|---|---|
| 5S | Simple pipe, no vortex | 16,500 |
| 1SI | First trial, vortex type | 5,970 (vent closed)<br>4,350 (vent open) |
| 1LM-3 | Final recommendation, vortex type | 6 |

10. Allowance must be made in the prototype for venting air from the top of the vortex structure and from the 7-foot diameter pipe at a point downstream from the closed butterfly valve (this is in the alternative flow circuit). (See Fig. 23.) Model tests showed that the maximum release from the top of the vortex structure in the operating range was 33,100 ppm and through the 7-foot pipe 6880 ppm within the operating range (but up to 70,900 ppm just 3.5 feet below minimum operating tailwater head at 300 cfs). (See Figs. 37 and 38.)

11. Assuming a scaling factor of 5 for vented air, the vent piping from each of the two points described in (10) above must have a capacity of 100 cfs air with a pressure rise of not more than 1 to 2 feet of water in the structure being vented. A common pipeline for both points is permissible because the large venting requirements cannot be simultaneous. It is essential to the safe operation of the entire vortex drop structure that these vents always be open and not obstructed by valves or accumulated grease or other solids. If the vortex chamber is not vented, the air pressure will build up, thereby depressing the water level in the vortex chamber, increasing air entrainment into the outfall, and forcing the hydraulic jump back up the chute.

12. Even under full flow conditions in the vortex chamber, the loss of head flow through the chamber and the downstream piping in the model was found to be 13 velocity heads, whereas only 2 or 3 would be expected (Table 4). It is therefore concluded (with limited evidence) that swirling flow in a pipe greatly increases hydraulic resistance, especially considering the reverse flow in the core. Further research on this topic would be worthwhile.

## ACKNOWLEDGEMENTS

The authors would like to express their appreciation to Professor Vito A. Vanoni for his assistance and valuable criticism, offered generously throughout the course of this investigation.

The writers wish to acknowledge with sincere thanks the indispensable and capable assistance of the following members of the laboratory staff: Mr. Elton F. Daly for constructing the various models and offering innumerable practical suggestions; Mr. Robert L. Greenway for assisting in the construction of the models and performing much of the photographic work; Mr. Arthur N. Schmitt for assisting in the detailed designing of the models, running tests, and preparing many of the figures for the report; Mr. Carl Eastvedt for still and motion-picture photography of the final large model; Mr. Ronald Parman for preparing some of the figures for the report; and finally Mrs. Shirley Graham for handling all secretarial work, including typing the manuscript and coordinating its publication during absences of the authors following completion of the work.

# APPENDIX A

## VELOCITY DISTRIBUTION IN SWIRLING FLOW IN PIPE

# APPENDIX A
# VELOCITY DISTRIBUTION IN SWIRLING FLOW IN PIPE

The limited scope of the model study did not permit detailed exploration of the characteristics of the interesting flow pattern in the model outfall pipe. (See Secs. 4.03.5 and 5.03.) However, after completion of the sponsored investigation, two students enrolled in a laboratory course measured the angle of the velocity vector to the pipe axis and the total and static head along a radius of the pipe at prototype Sta. 2+89 for $Q$ = 312 cfs (0.226 cfs model), TW = 40 ft. This flow condition was chosen because there were no visible air bubbles or filament along the center of the vortex to interfere with the measurements. The direction of flow was first measured with a very small null-reading directional pitot tube, and then small total head and static head probes were set in turn at the predetermined angles at various radii. The piezometer at the wall at Sta. 3+70 was used for a reference head for making pressure readings with a Statham differential pressure transducer and a suitable bridge circuit. In this way rapid measurements were possible without being disturbed by slight fluctuations in the system pressure.

In Fig. 40 the lower three curves show the basic measurements of angle and head, from which the upper three curves were derived for the distribution of total velocity and its axial and tangential components. Although these data represent only one condition, it is believed reasonably typical on the basis of visual observations of many other flows.

It may be noted that as r increases, the tangential velocity does not decrease as fast as $\frac{1}{r}$, which would be expected for a free vortex. Therefore, the circulation $\Gamma$ increases with increasing r, the changes being very rapid for r<0.05 ft, and gradual for r>0.05 ft. This is a stable velocity distribution according to Taylor's criterion. At r = 0.22 ft, $\Gamma$ reaches a maximum value of 2.18 $ft^2/sec$, and then because of boundary friction, the circulation decreases as r approaches the radius of the wall.

The zone of reverse axial flow ($\phi$>90° or V cos$\phi$<0) is clearly seen to be r<0.05 ft, about 1/5 of the pipe radius. It should be noted that within this zone the head and velocity measurements may not be considered highly accurate because: (a) the radius is no longer large compared to the length

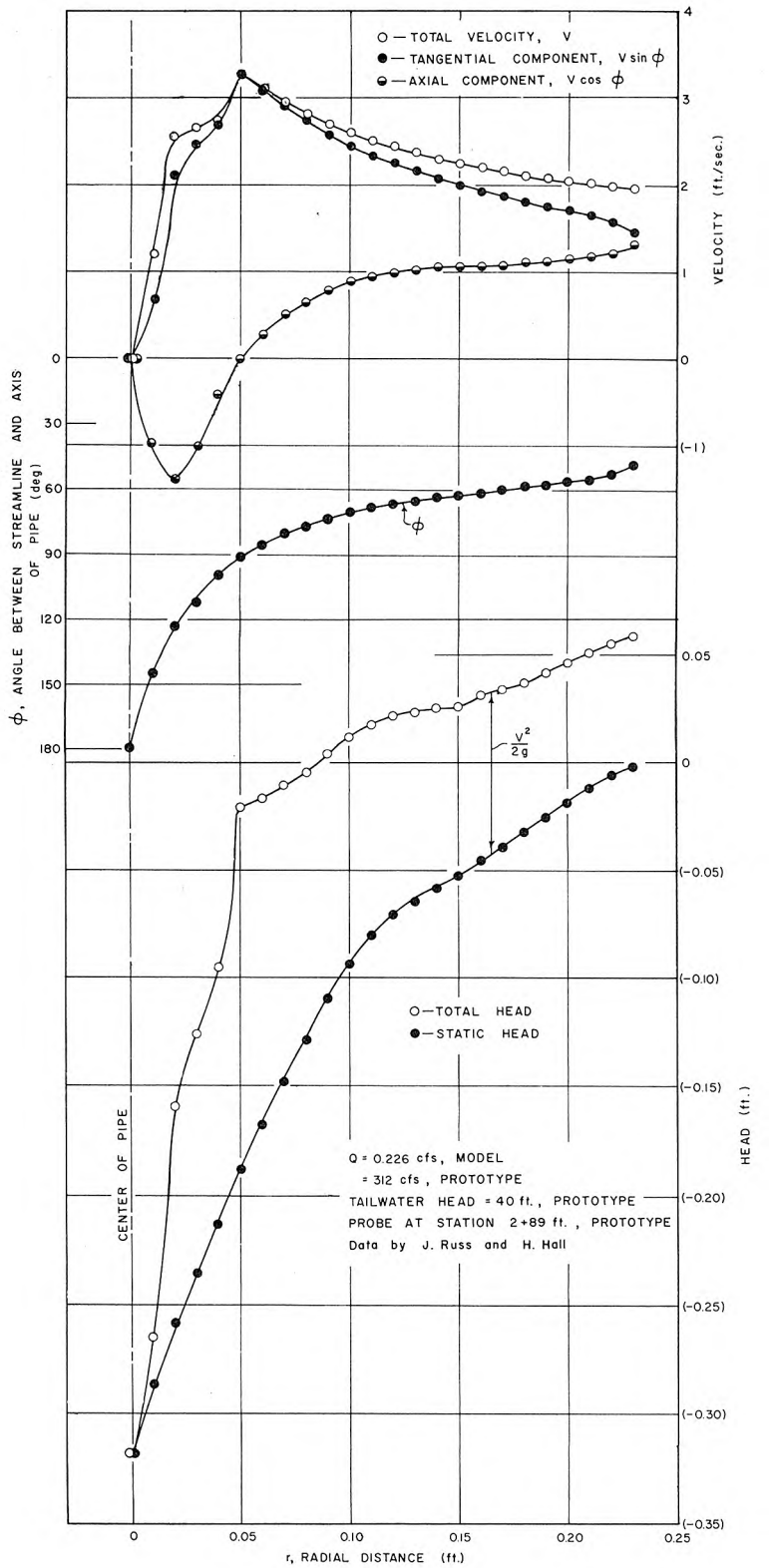


Fig. 40. Measurements of velocity and head in swirling flow in 6-in. pipe about 9 ft downstream of vortex tube and elbow. Note reverse axial flow ($\phi > 90°$ and $V \cos\phi < 0$ in zone $r < 0.05$ ft).

of the probe (about 0.02 ft); (b) the eye of the vortex fluctuates a few 0.01 ft in position; and (c) turbulent fluctuations become large compared with mean velocities making measurement of the mean difficult.

If the radial velocities are assumed negligible, then the distribution of static head (h) should be directly related to the tangential component ($v_t$) of the velocity by the equation

$$g\frac{dh}{dr} = \frac{v_t^2}{r}$$

Integration of this equation confirmed the values of h (lowest curve on Fig. 40) within 0.01 ft for $r \geq 0.08$ ft. However, for $r < 0.08$ ft the computed values of h were significantly lower than those measured, indicating that in this zone either there is some radial flow or that the measurement of the tangential velocity was not accurate — both likely possibilities.

Since the velocity measurements were all made along just one radius (from the center to the top of the pipe), there is no assurance of axial symmetry; in fact, considering the bend upstream, it would be surprising if there were symmetry. Integration of the axial velocity over the area presuming symmetry gives a discharge of 0.196 cfs or 13 per cent less than that measured with a calibrated venturi meter. It is believed that this discrepancy is indicative of some asymmetry of the velocity distribution.

To explain how energy is dissipated in a swirling flow, further measurements are needed at various positions along the pipe to show changes with distance and along several radii to check symmetry. However, with the reverse flow in the core in addition to the swirling motion, one may presume that the turbulent shear stresses and resultant energy dissipation must be much larger than the normal case without circulation.

# APPENDIX B

## AIR ENTRAINMENT DATA
## AND
## GEOMETRY FOR PRELIMINARY MODELS

# APPENDIX B
# AIR ENTRAINMENT DATA AND GEOMETRY FOR PRELIMINARY MODELS

Although the observed air entrainments and air vent discharges shown in Figs. 35, 37, and 38 for the final model configuration (1LM-3) are of the most immediate interest, the following graphs (Figs. 41-51) are also presented to summarize air entrainment data for the other, preliminary models. The air entrainment graphs for 5S and 1LM-3 are included in this group for ease of comparison. The general decrease in air entrainment progressing in sequence through 1S, 1SI, 2S, 3S, 3SI, 4S, 6S, 6SM, 1L, and 1LM-3 shows how each step in the testing program contributed to knowledge of factors affecting air entrainment.

A big improvement occurred between 2S and 3S when the tapered vortex tube was first introduced. This allowed a stronger vortex to be generated by the inflow at the top, and the convergence smoothly accelerated the tangential velocity as the flow moved down toward the elbow. However, because the vortex appeared too strong, the taper was reduced again later in the final model (1L) by making the diameter of the top 13.5 feet rather than 18 feet (nominal) as in Models 3S, 4S, 6S, and 6SM (compared to bottom diameter of 9 feet or 9.5 feet).

Minor decreases in air entrainment also occurred as the inlet was improved to avoid flow interference between the entering flow and the flow already swirling in the vortex tube (for example, compare 6S and 6SM and see also Sec. 4.03.3 on guide vanes).

Another important factor was the elevation of the outfall pipe and elbow. When it was raised from -14.6 feet (or -14.7 feet), (pipe centerlines for 1S, 1SI, 2S, 3S, and 3SI) to -8.0 feet for Model 4S at the request of the design engineers (see Fig. 11), the air entrainment rates became too high at the lowest tailwater conditions as large amounts of air started to be swept down into the elbow. Therefore, it was lowered slightly to -9.4 feet for Models 6S and 6SM and still further to -12.0 feet for the final model (1L and 1LM-3) to avoid heavy entrainment at very low tailwater heads in the operating range. Fig. 38 shows clearly how the discharge of air through the vent

on the 7-foot pipe suddenly increases just below the curve for minimum tailwater head; had the structure been a few feet higher, these points would have fallen within the possible operating range, and might have represented troublesome conditions in the prototype.

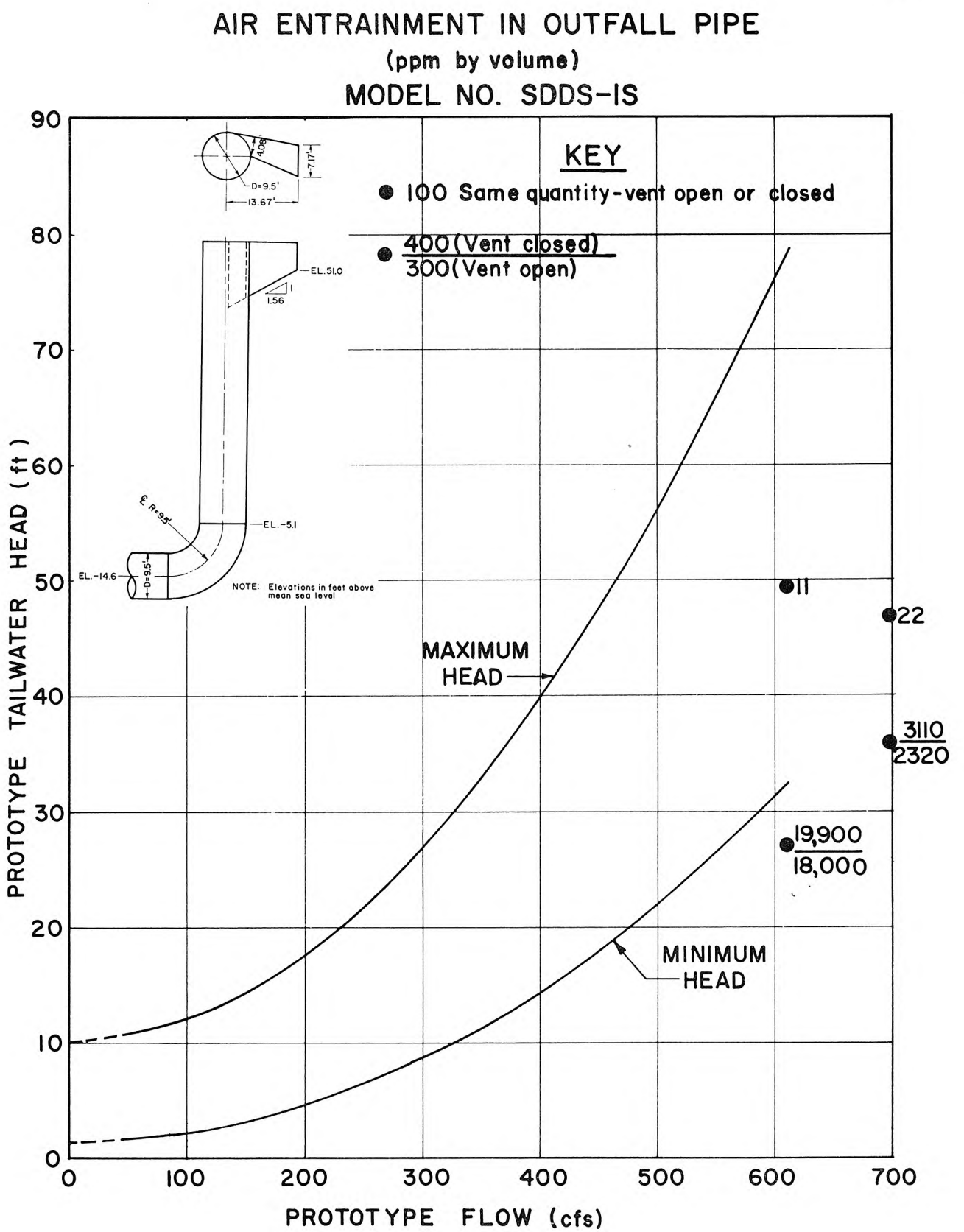


Fig. 41. Air entrainment in outfall pipe as function of flow condition for Model 1S.

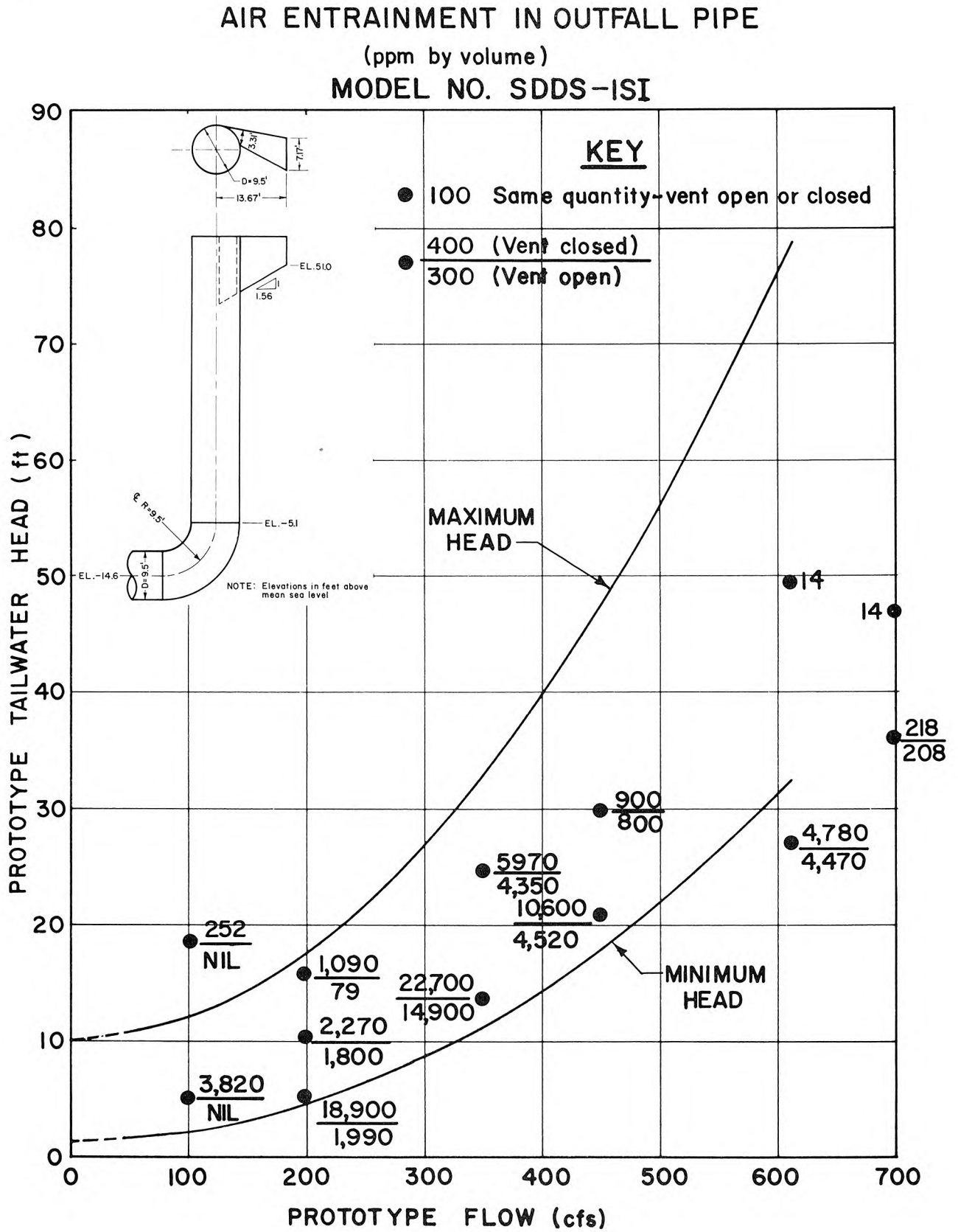


Fig. 42. Air entrainment in outfall pipe as function of flow condition for Model 1SI.

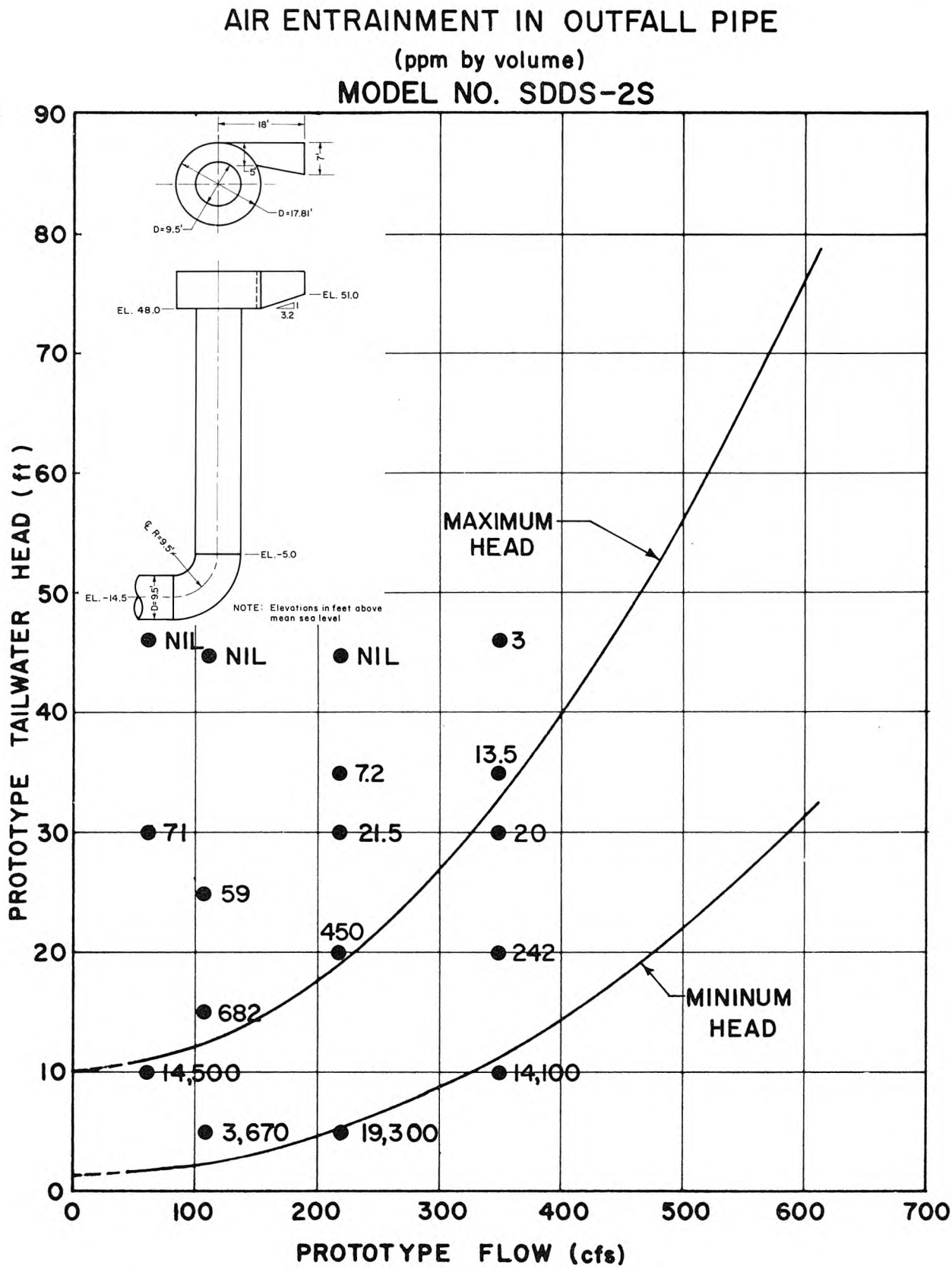


Fig. 43. Air entrainment in outfall pipe as function of flow condition for Model 2S.

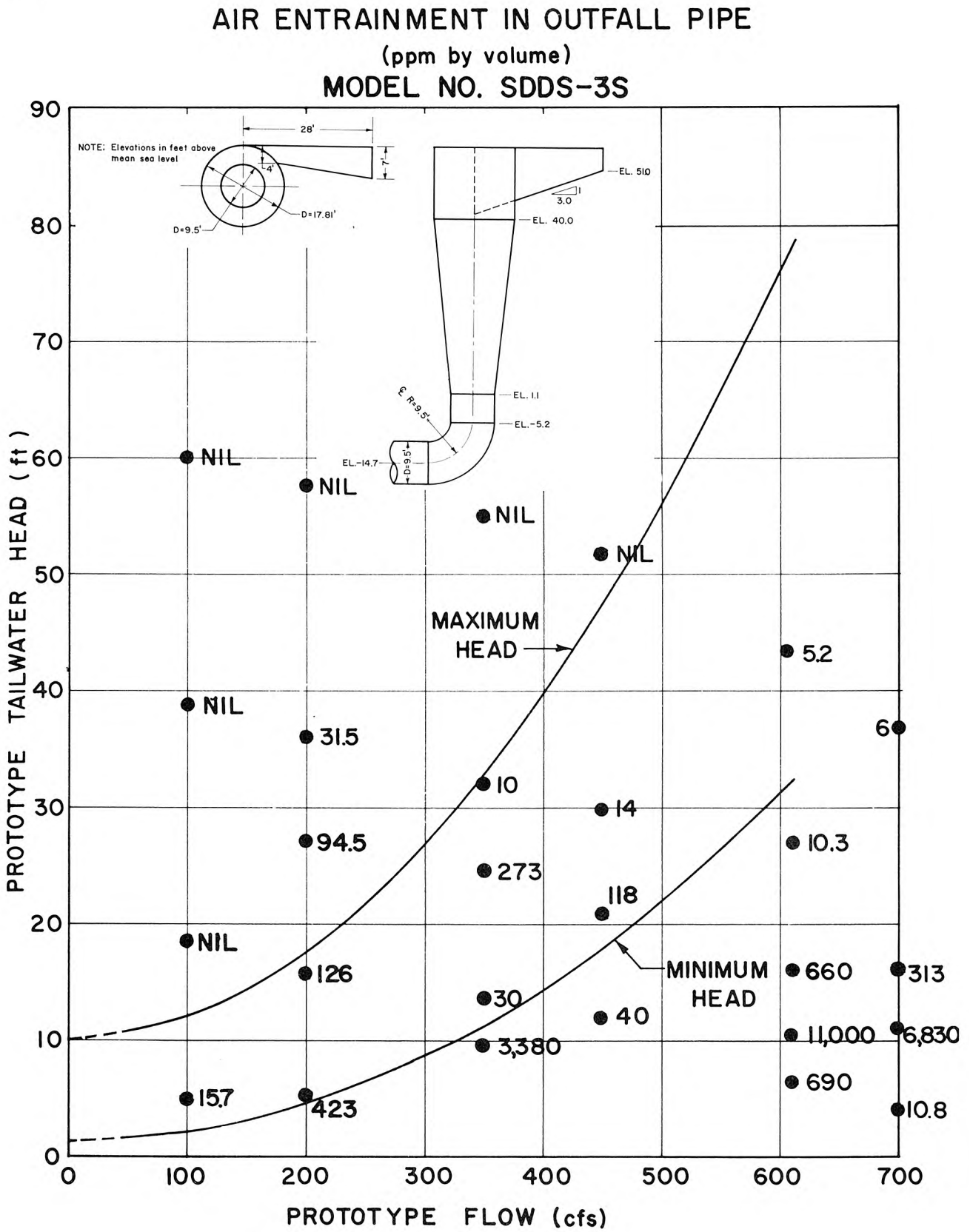


Fig. 44. Air entrainment in outfall pipe as function of flow condition for Model 3S.

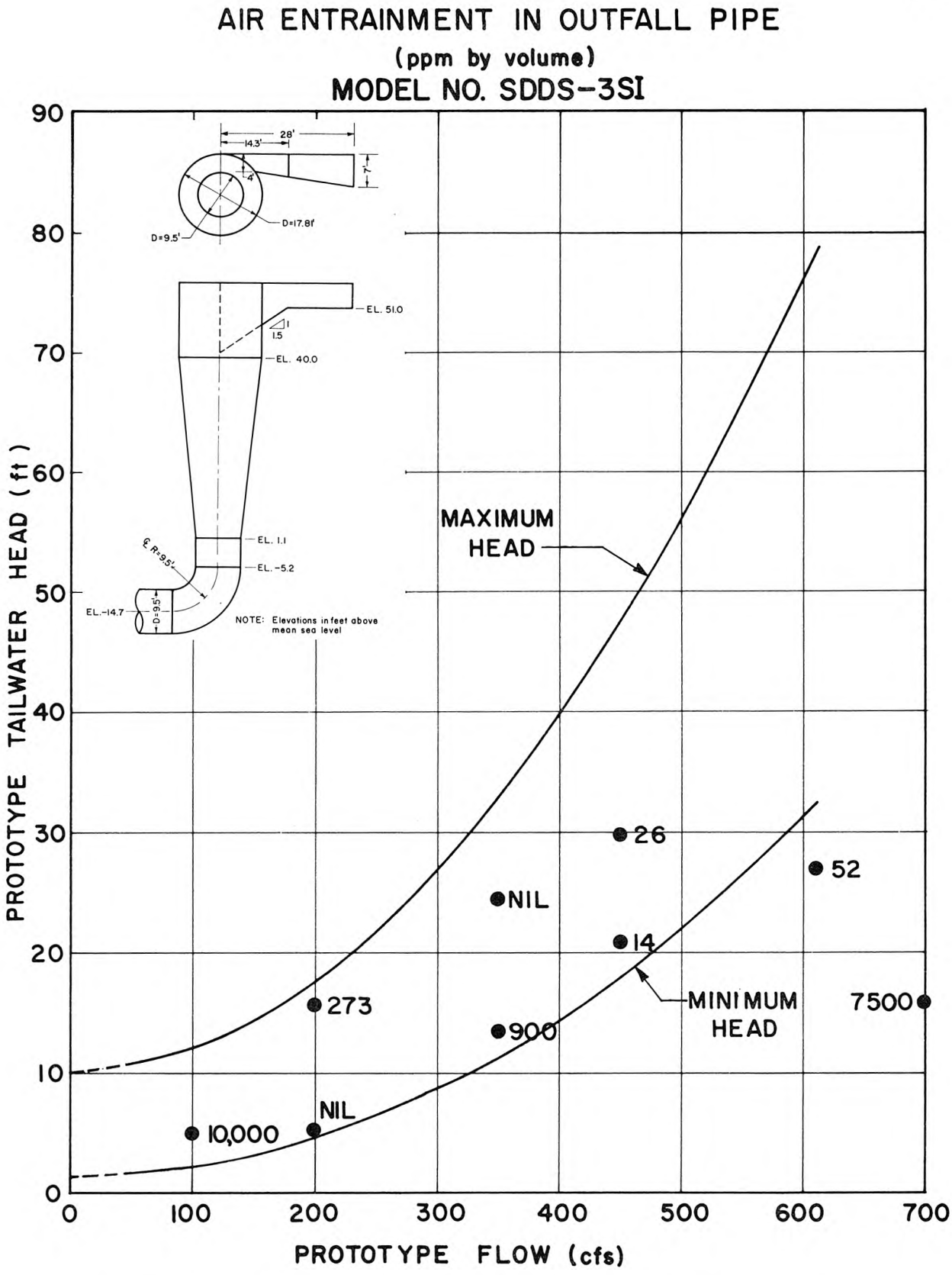


Fig. 45. Air entrainment in outfall pipe as function of flow condition for Model 3SI.

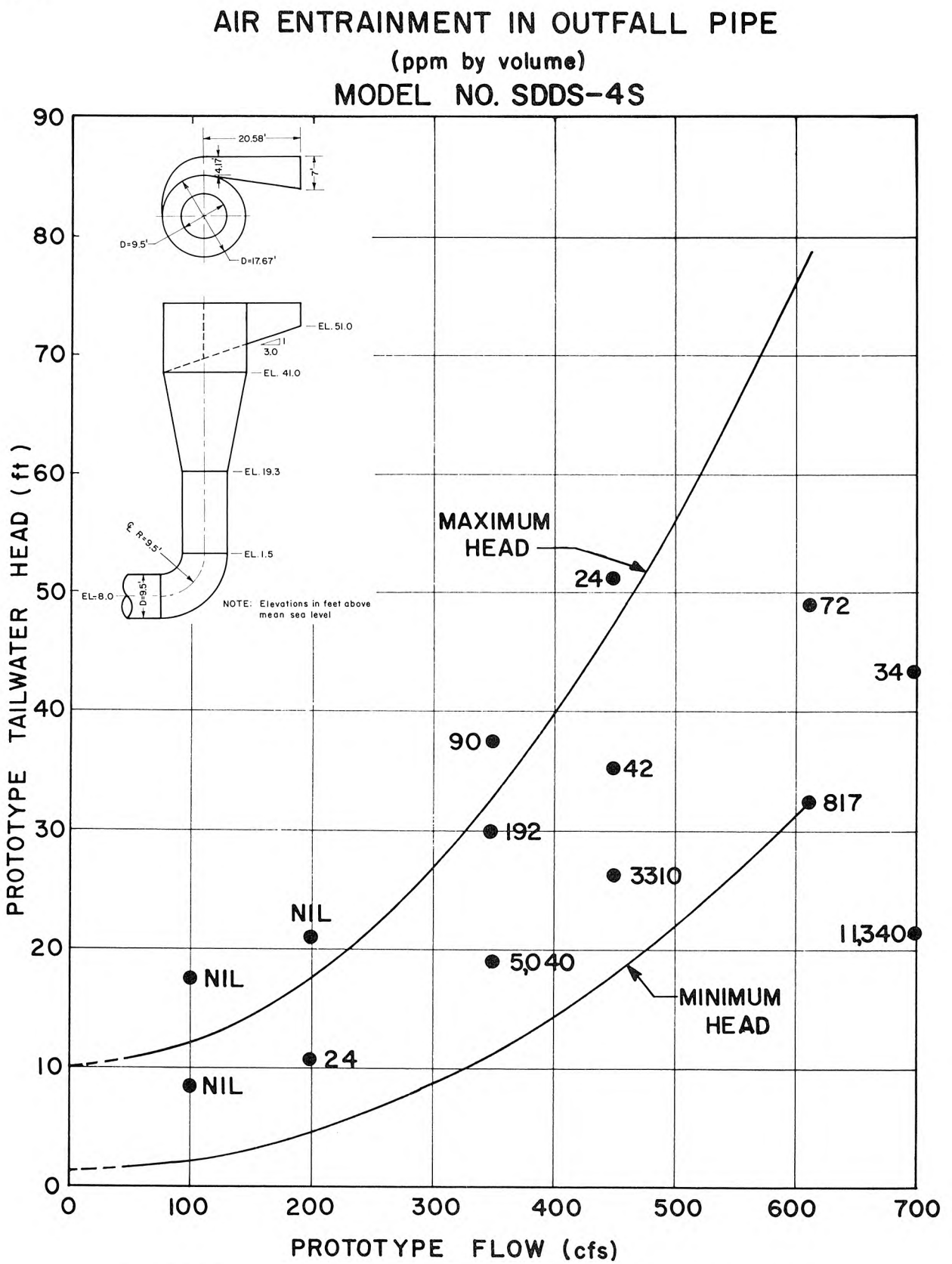


Fig. 46. Air entrainment in outfall pipe as function of flow condition for Model 4S.

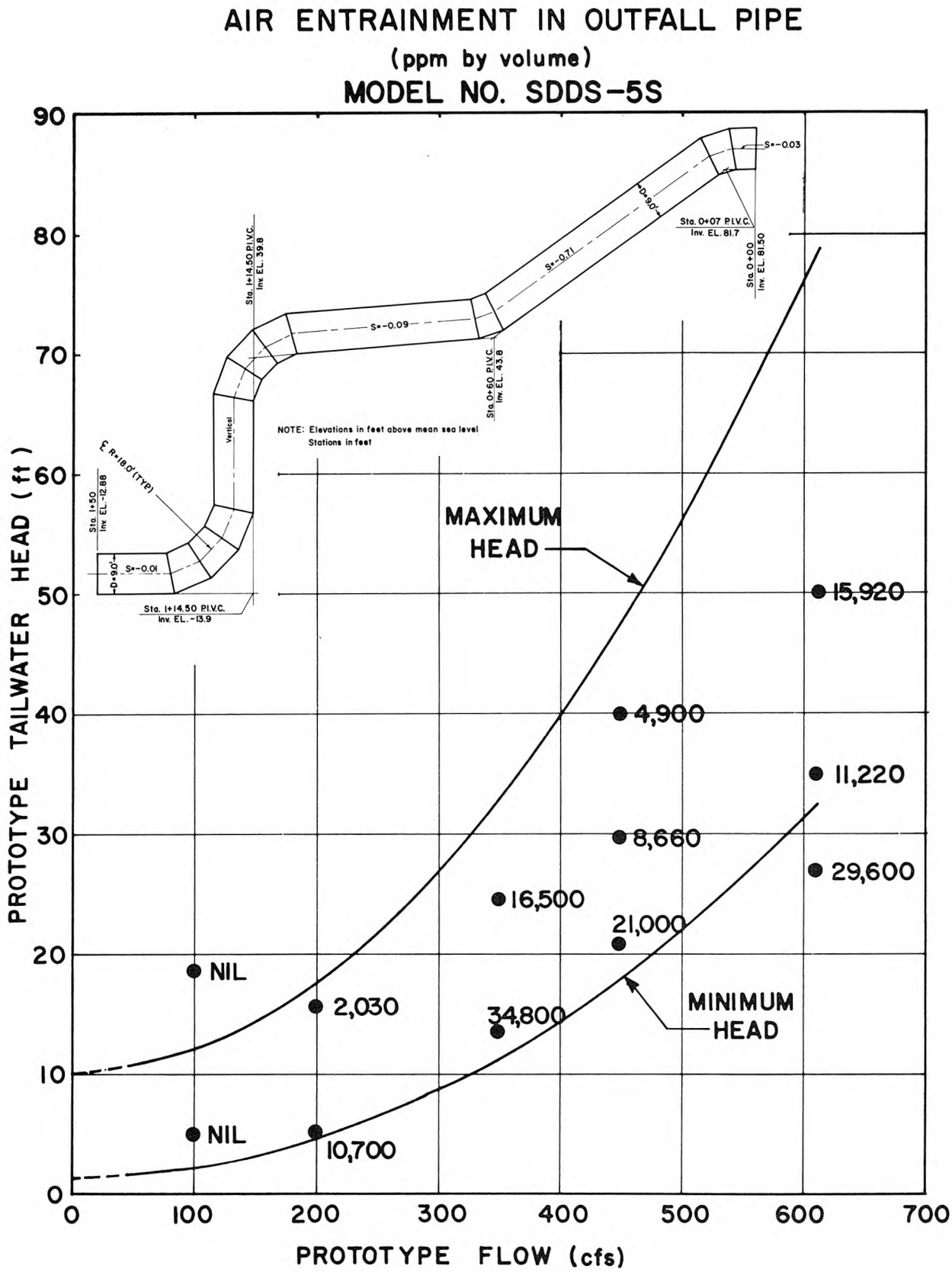


Fig. 47. Air entrainment in outfall pipe as function of flow condition for Model 5S.

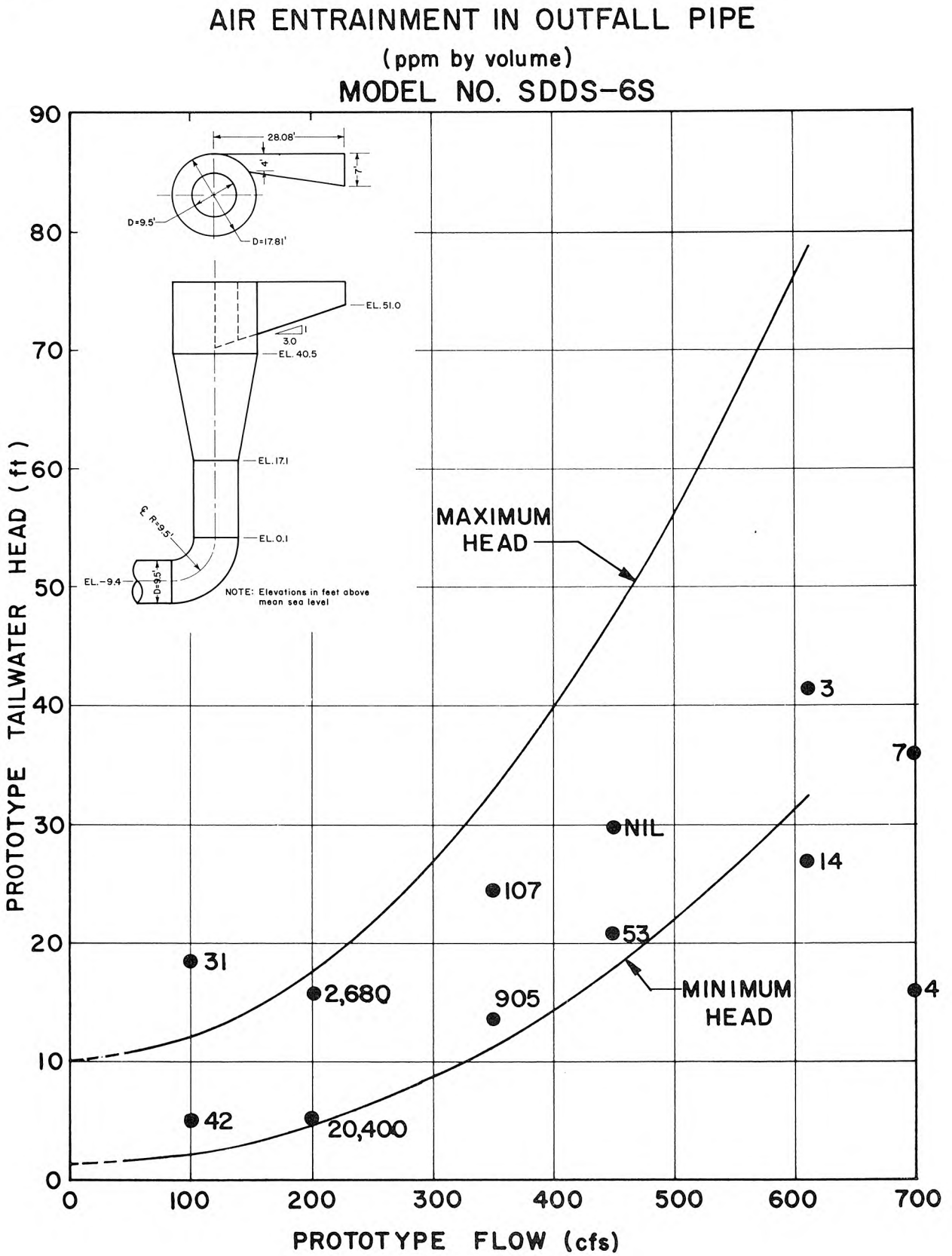


Fig. 48. Air entrainment in outfall pipe as function of flow condition for Model 6S.

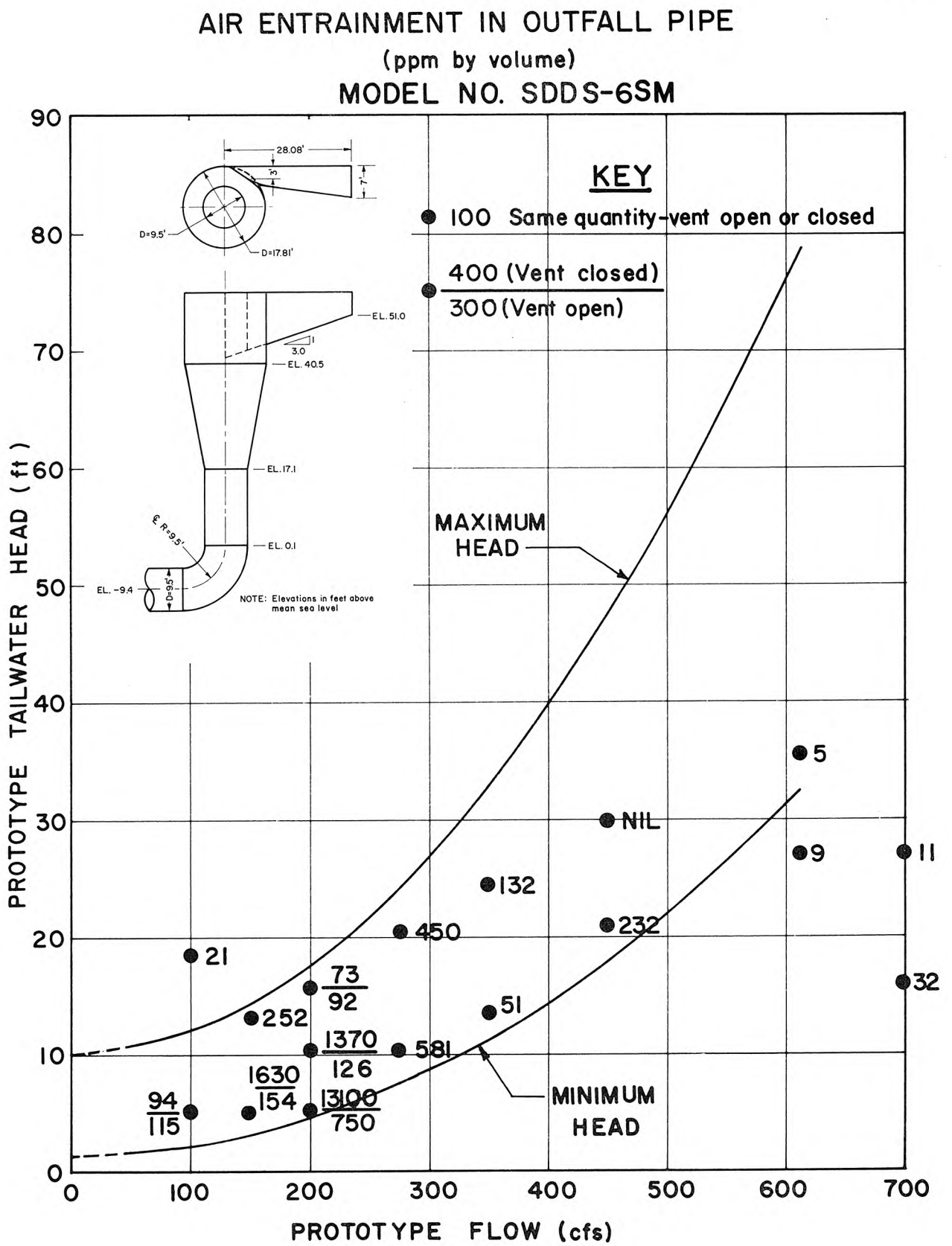


Fig. 49. Air entrainment in outfall pipe as function of flow condition for Model 6SM.

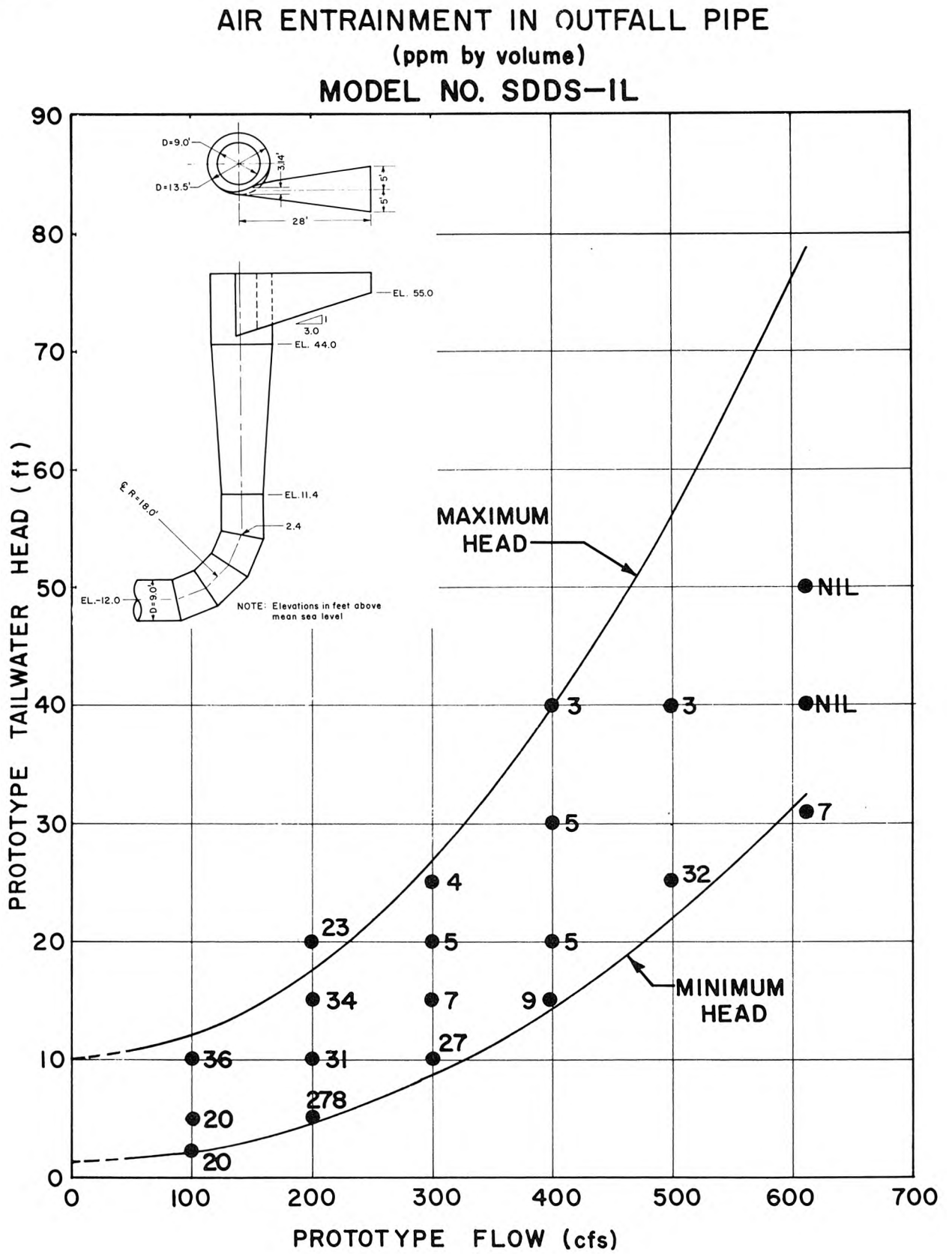


Fig. 50. Air entrainment in outfall pipe as function of flow condition for Model 1L.

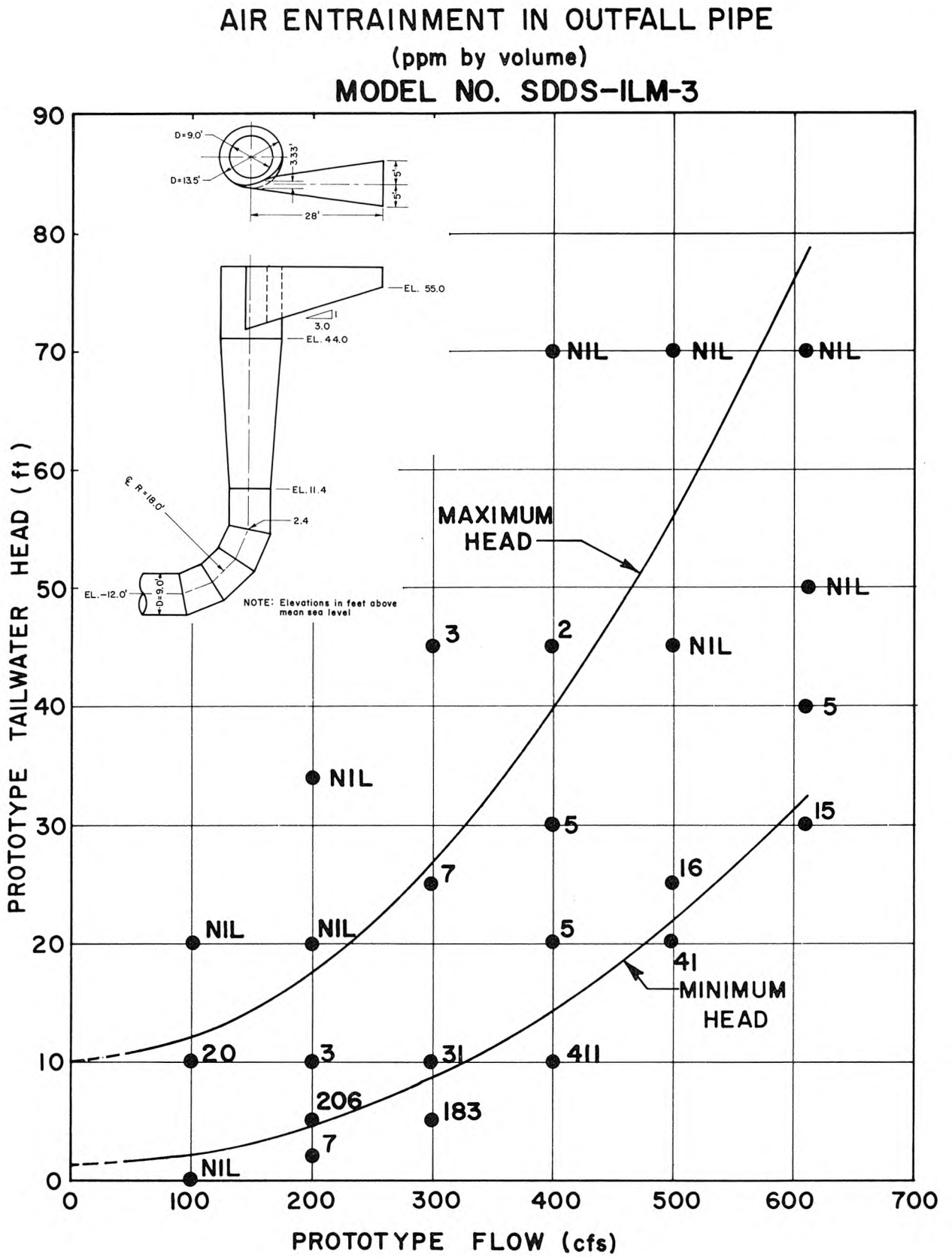


Fig. 51. Air entrainment in outfall pipe as function of flow condition for Model 1LM-3.

# REFERENCES

Anderson, Sigurd H. (1961), "Model Studies of Storm-Sewer Drop Shafts," St. Anthony Falls Hydraulic Laboratory, Technical Paper No. 35, Series B, Univ. of Minn., Minneapolis, Minn., Dec. 1961.

A.S.C.E. (1961), "Aerated Flow in Open Channels," Progress Report of Task Committee on Air Entrainment in Open Channels, J. Hyd. Div., Proc. ASCE, v. 87, HY 3, May 1961, pp. 73-86.

Binnie, A. M., and Hookings, G. A. (1948), "Laboratory Experiments on Whirlpools," Proc. Royal Society of London, Series A, v. 194, pp. 398-415, 1948.

Binnie, A. M., Hookings, G. A., and Kamel, M. Y. M. (1957), "The Flow of Swirling Water through a Convergent-Divergent Nozzle," J. Fluid Mechanics, v. 3, pp. 261-274, 1957.

Binnie, A. M., and Teare, J. D. (1956), "Experiments on the Flow of Swirling Water through a Pressure Nozzle and an Open Trumpet," Proc. Royal Soc., A., v. 235, pp. 78-89, 1956.

Boughton, N. O. (1959), "Laboratory Studies on the Use of Siphons and Vortex Chambers for the Exclusion of Air at Secondary Intakes," Proc. 8th Congress, Internat. Assoc. for Hyd. Res., Montreal, Canada, 1959, Paper 5-D.

Boughton, N. O. (1960), "Tooma-Tumut Project, Tooma-Tumut Tunnel, Intermediate Shaft Intakes, Vortex Chamber Model Studies," Fluid Mechanics Report No. S.H. 24, Snowy Mountains Hydro-Electric Authority, New South Wales, Australia, Oct. 1960.

Bradley, J. N., and Peterka, A. J. (1957), "Hydraulic Design of Stilling Basins," (a series of six papers), J. Hyd. Div., Proc. ASCE, v. 83, HY 5, Oct. 1957, Papers 1401-1406.

Brooks, N. H., and Blackmer, W. H. (1962), "Preliminary Final Report on the Studies of Energy Dissipator for Sewage Flowing into the Ocean Outfall for San Diego," W. M. Keck Laboratory of Hydraulics and Water Resources, California Institute of Technology, Tech. Memo 62-3, Pasadena, Calif., 30 March 1962.

Brooks, N. H., and Kennedy, John F. (1961), "Report on Hydraulic Model Study of Overflow Channel to Ocean Outfall, San Diego Sewerage Project," Pasadena, Calif., July 1961 (on file at W. M. Keck Laboratory of Hydraulics and Water Res., Calif. Inst. of Tech., Tech. Memo 61-4).

Campbell, F. B., and Guyton, B. (1953), "Air Demand in Gated Outlet Works," Proc. Minnesota Internat. Hyd. Conv., Internat. Assoc. for Hyd. Res., 1953, pp. 529-533.

Cotillon, J. (1959), "Supply Shafts for Power Tunnels and the Problem of Air Entrainment," Proc. 8th Cong., Internat. Assoc. of Hyd. Res., Montreal, Aug. 1959, Paper 17-D.

Eastwood, W., Taylor, G. A., and Allen, J. (1953), "Scale Model Experiments in High Head Siphons and Vortex Chambers Connected Thereto," Proc. Inst. Civ. Eng., v. 2, pt. 1, pp. 556-584, Sept. 1953.

Haberman, W. L., and Morton, R. K. (1956), "An Experimental Study of Bubbles Moving in Liquids," Trans. ASCE, v. 121, 1956, p. 227.

Holmes and Narver-Montgomery (1958), "Basic Plan for the Collection, Treatment and Disposal of Sewage for the Metropolitan Area, San Diego, California," Los Angeles, California, Nov. 1958.

Hsu, Hsieh-Ching (1947), "Vortex over Outlet," M.S. thesis, Univ. of Iowa, Ames, Iowa, June 1947.

Jevdjevich, V. and Levin, L. (1953), "Entrainment of Air in Flowing Water and Technical Problems Connected with It," Proc. Minnesota Internat. Hyd. Convention, Internat. Assoc. for Hyd. Res., 1953, pp. 439-453.

Kalinske, A. A. (1941), "Hydraulics of Vertical Drains and Overflow Pipes," Univ. of Iowa Studies in Engineering, Bull. 26, Dec. 1941, pp. 26-40.

Kalinske, A. A., and Robertson, J. M. (1943), "Air Entrainment in Closed Conduit Flow," Trans. ASCE, v. 108, pp. 1435-1516.

Kolf, R. C. (1956), "Vortex Flow from Horizontal Thin-Plate Orifices," Ph. D. thesis, Univ. of Wisconsin, Madison, Wisconsin, 1956.

Kolf, R. C., and Zielinski, P. B. (1959), "The Vortex Chamber as an Automatic Flow-Control Device," J. Hyd. Div., Proc. ASCE, v. 85, No. HY 12, Dec. 1959, pp. 1-8.

Laboon, J. F. (1960), "Development and Design Features of the Pittsburgh Sewerage Project," Public Works, v. 91, No. 10, Oct. 1960, pp. 106-114.

Laboon, J. F. (1961), "Construction and Operation of the Pittsburgh Project," J. Water Pollution Control Federation, v. 33, No. 7, July 1961, pp. 758-782 (see p. 766).

Lamb, Owen P. (1949), "Air Entrainment in Flowing Water – A Summary and Bibliography of Literature," St. Anthony Falls Hydraulic Lab., Univ. of Minn., Project Report No. 19, Minneapolis, Minn., Aug. 1949.

Laushey, Louis M. (1952), "Flow in Vertical Shafts," Carnegie Inst. of Technology, Dept. of Civil Engineering Research Report, Pittsburgh, Pa., Aug. 1952.

Laushey, L. M., and Mavis, F. T. (1953), "Air Entrained by Water Flowing down Vertical Shafts," Proc. Minnesota Internat. Hyd. Conv., Internat. Assoc. for Hyd. Res., 1953, pp. 483-487.

Marquenet, G. (1953), "Entrainement d'Air par un Écoulement en Conduite Verticale Application aux Puits d'Adductions Secondaires," Proc. Minnesota Internat. Hyd. Conv., Internat. Assoc. for Hyd. Res., 1953, pp. 489-506.

Navin, W. F. (1960), "Rise Velocity of Bubbles and Drops in De-aeration Chambers," Fluid Mechanics Report No. S.H. 26, Snowy Mountains Hydro-Electric Authority, New South Wales, Australia, Nov. 1960.

Nuttall, J. B. (1953), "Axial Flow in Vortex," Nature, London, v. 172, pp. 582-3, Sept. 26, 1953.

Peterka, A. J. (1954), "Spillway Tests Confirm Model-Prototype Conformance," Technical Monograph No. 16, U. S. Bureau of Reclamation, Oct. 1954, Denver, Colo.

Peterka, A. J. (1956), "Morning-Glory Shaft Spillways: Performance Tests on Prototype and Model," Trans. ASCE, v. 121, 1956, pp. 385-409.

Reynolds, A. J. (1962), "A Note on Vortex Tube Flows," J. Fluid Mechanics, v. 14, pp. 18-20, Sept. 1962.

Stevens, J. C., and Kolf, R. C. (1959), "Vortex Flow through Horizontal Orifices," Trans. ASCE, v. 124, 1959, pp. 871-893.

U. S. Bureau of Reclamation (1960), "Design of Small Dams," Denver, Colorado (or U. S. Govt. Printing Office, Washington, D. C.).

U. S. Corps of Engineers (1961), "Air Demand – Regulated Outlet Works," Sheet and Chart 050-1 of Hydraulic Design Criteria, 11th Revision, 1961 (also in all issues since 1952), Waterways Experiment Sta., Vicksburg, Miss.

Viparelli, M. (1961), "Air and Water Currents in Vertical Shafts," La Houille Blanche, v. 16, pp. 857-869, Dec. 1961.